TRANSPORTATION RESEARCH RECORD

497

Formerly issued as Highway Research Record

Soil Properties

10 reports prepared for the 53rd Annual Meeting of the Highway Research Board

subject areas

61 exploration-classification (soils)
62 foundations (soils)
63 mechanics (earth mass)
64 soil science

TRB

TRANSPORTATION RESEARCH BOARD

NATIONAL RESEARCH COUNCIL

Washington, D. C., 1974

NOTICE

These papers report research work of the authors that was done at institutions named by the authors. The papers were offered to the Transportation Research Board of the National Research Council for publication and are published here in the interest of the dissemination of information from research, one of the major functions of the Transportation Research Board.

Before publication, each paper was reviewed by members of the TRB committee named as its sponsor and accepted as objective, useful, and suitable for publication by the National Research Council. The members of the review committee were chosen for recognized scholarly competence and with due consideration for the balance of disciplines appropriate to the subject concerned.

Responsibility for the publication of these reports rests with the sponsoring committee. However, the opinions and conclusions expressed in the reports are those of the individual authors and not necessarily those of the sponsoring committee, the Transportation Research Board, or the National Research Council.

Each report is reviewed and processed according to the procedures established and monitored by the Report Review Committee of the National Academy of Sciences. Distribution of the report is approved by the President of the Academy upon satisfactory completion of the review process.

The National Research Council is the principal operating agency of the National Academy of Sciences and the National Academy of Engineering, serving government and other organizations. The Transportation Research Board evolved from the 54-year-old Highway Research Board. The TRB incorporates all former HRB activities but also performs additional functions under a broader scope involving all modes of transportation and the interactions of transportation with society.

TRR 497
ISBN 0-309-02287-8
LC Cat. Card No. 74-16830
Price: $4.80

CONTENTS

FOREWORD

This RECORD points up the variety and range of subjects that make a soil engineer's life so interesting. From the frosty provinces of Canada to the soil-forming heat and humidity of Ghana, research results are presented that should make the respective soil problems more understandable at the least. Between these extremes the subjects of deflection, drainage, consistency limits, and dilatancy receive due attention.

Pagen and Khosla, Argue and Denyes, and Laba all treat some phase of low-temperature effects: on the rheological characteristics of a compacted subgrade, on resultant frost penetration, and on "frost-grip" or adfreezing of granular soils.

Cumberledge et al. describe the deflection response of a pavement surface as dependent on subgrade moisture and pavement surface temperature. Moynahan and Sternberg relate base course drainage to the fines content of the aggregate, finding little difference between horizontal and vertical permeability.

Kandiah and Arulanandan examine the effects of initial water content on the critical shear stress as related to erosion. Gadallah, Russell, and Yoder present data to indicate that moisture tension tests can be used on a routine basis to determine the consistency limits. Kumapley and Inkabi investigated means of obtaining the liquid limit for micaceous or silty soils of low plasticity and found that roughening the cup would produce better and more consistent results. George and Shah found that shape, surface texture, and size of individual grains, in that order, govern dilatancy characteristics of granular media.

Gidigasu reviews the problems of identifying unsuitable or troublesome laterite materials. He points out that despite much study there still is no reliable means of accurately predicting the field behavior of all lateritic soils.

EFFECT OF FREEZE-THAW ON RHEOLOGICAL CHARACTERISTICS OF A COMPACTED CLAY

Charles A. Pagen, Mobil Research and Development Corportation, Paulsboro, New Jersey; and
Vijay K. Khosla, Herron Testing Laboratories, Cleveland*

This research quantitatively evaluates the effect of freeze-thaw cycles on the rheological characteristics of a compacted subgrade. Kaolin clay samples compacted by drop hammer with 25, 40, and 80 total blows were tested over a wide range of moisture contents and densities. Unconfined compression and creep tests were performed. The failure and rheological parameters investigated to relate soil strength are unconfined compressive strength, modulus of elasticity, creep modulus, and complex modulus. Preliminary tests conducted to find the critical number of freeze-thaw cycles after which further conditioning will not have any significant effect on the soil strength parameters indicated that the limit of such conditioning cycles is nine. Therefore, all the samples were subjected to nine freeze-thaw cycles before testing. The experimental results indicated that moisture content does not seem to be a suitable parameter to determine the effect of compaction energy on the failure or rheological parameters of a compacted soil subjected to freeze-thaw cycles. Degree of saturation, on the other hand, provides meaningful results as to the variation of strength parameters. The research also indicated that in-service conditions should be controlled to limit the saturations to less than 85 to 90 percent (lower limit corresponding to compaction energy of 25 blows and upper limit to 40 and 80 blows). At saturation above these limits, the soil loses a major portion of its strength and approaches a minimum.

•PROBABLY no other engineering structures are subjected to such wide variations in loading and climatic conditions as airport and highway pavement structures. A highway that must be designed for frost is at a disadvantage in that both its superstructure and substructure are exposed to extreme and changing climatic influences. The various factors taken into consideration while designing the highway pavement can be grouped into two broad categories: (a) type and amount of traffic and (b) climatic conditions and their effects. However, our present concern is to evaluate the effect of climatic conditions and in particular the effect of freeze and thaw on the strength characteristics of the cohesive soils.

During the cold periods of winter when the temperature goes below the freezing point, the moisture in the soil freezes, accompanied by an increase in volume. This increase in volume can produce cracks and result in loss of strength. To meet the requirements of traffic in such environments, highway subgrades may require greater compaction (depending on the extent of freezing anticipated in that area) than that necessitated by the usual weather conditions. Of much more importance to the construction and maintenance of highways and airfields is the loss of soil strength upon thawing because many base courses and subgrades lose a major portion of their strength during the spring thaw and cause pavement failure. The main factors that influence the frost action in

Publication of this paper sponsored by Committee on Frost Action.

*The research was conducted by the authors as former faculty members at Ohio State University.

soil during winter and the reaction during spring thaw are the soil type, compacted state of the soil, temperature of the soil and its surroundings, and supply of water (7).

This paper deals with the situations where the surface and underground drainage systems are adequate so that no appreciable changes occur in the moisture content of the subgrade because of extreme climatic conditions expected during any year. In such cases the damage done to the strength of the soil will depend on the as-compacted moisture content and the compaction energy imparted to the soil at the time of laying a highway. The present case, which corresponds to the field conditions where freezing and thawing can occur periodically because of seasonal changes in temperature and where the water table is well below the ground surface so that the migration of water in the subgrade is not possible either by capillary action or because of pressure drop due to temperature gradient or by any other means (such as rain), will be designated a closed system.

OBJECTIVE AND SCOPE

All civil engineering structures derive their ultimate support from soils and rock materials, which are required to support different magnitudes and types of loads under a variety of environmental conditions. In highway construction projects, compacted soil is used as a subgrade material and is required to support loads of the overlying pavement system and traffic.

The soil compaction process effects a variety of properties that can be broadly categorized into two interrelated types: physical and engineering properties. The physical properties, i.e., the moisture and density, can be used to analyze the efficiency of a compaction process. However, engineers are not only interested in the density per se but rather in its effect on the engineering properties describing the soil support conditions.

Physical properties of soils such as moisture and density can be duplicated in the laboratory and can also be used in the field for quality-control measures. But they bear the limitation that they cannot be directly incorporated in the pavement design methods. It has been demonstrated (13, 14, 15) that the achievement of a compaction level—i.e., density—at the dry side of optimum may result in a different soil property from that at the wet side of optimum. Also, the compaction of a soil at the dry side of optimum leads, regardless of compaction method, to similar flocculated structure and therefore to similar strength deformation characteristics. At the wet side of optimum, however, different methods of compaction develop different levels of shear strain, resulting in different soil structure and engineering properties. In general, static compaction methods produce little shear strain as compared to kneading compaction methods, which induce large shear strain and subsequently result in dispersed soil structure. This indicates that soils compacted to a given density and moisture content may exhibit different engineering properties depending on the method of compaction utilized. Therefore, if the physical properties cannot fully satisfy the requirements of pavement design and performance evaluation, what other limiting engineering properties need to be selected?

In general pavement design theories, the materials constituting the several load-distributing layers of the structure are considered as ideal elastic material so that the stresses and strains in the different layers may be determined (4, 5). However, it is well known that no pavement material is perfectly elastic, and the compacted soil of a highway subgrade is no exception. All materials have time-dependent stress-strain characteristics. Therefore, in defining the stress-strain time-dependent characteristics of a compacted subgrade, the compacted soil may be more rationally treated as a linear viscoelastic material under specified conditions. Soil, being a natural material, is not an ideally linear viscoelastic material, just as there is no perfectly elastic Newtonian or plastic material (6, 12). But within a certain stress-strain range the mechanical behavior of soils, as an engineering approximation, can be treated like that of a linear viscoelastic material (most traffic loads fall within the linear viscoelastic range of subgrade materials). By establishing the linear viscoelastic nature of soils, the viscoelastic constants of the material can be evaluated by any of the rheological tests,

which are all interrelated by the viscoelastic theory (1, 2). In the search for suitable engineering properties to be used in evaluation of laboratory- and field-compacted specimens, the approach of testing soils as linear viscoelastic materials was emphasized by Pagen and Jagannath (9, 10). The same approach was followed in the present study.

Thus, the objective of this study was to find the optimum initial compaction energy and molding moisture content or degree of saturation for a given soil on the phenomenological level—using fundamental rheological strength parameters such as the linear viscoelastic moduli—for which the loss of strength will be minimum when subjected to freezing and thawing.

Failure and rheological strength parameters used are the unconfined compressive strength σ_c', modulus of elasticity E, creep modulus E_c, and complex elastic modulus $/E^*/$. $/E^*/$ may be obtained by either of two types of tests: a series of dynamic tests performed at different frequencies or a single static test extending over a large range of time. In the present study static creep test was performed to find this parameter and creep modulus E_c. A brief review of the theoretical concepts concerning the conversion from time to frequency domain and subsequent evaluation of complex elastic modulus are discussed in the next section. The unconfined compressive strength test was used to find compressive strength and modulus of elasticity.

Preliminary tests were also conducted to find the optimum number of freeze and thaw cycles after which further application of such conditioning cycles will not affect the compacted state and thus reduce the soil strength. Once found, all soil samples were subjected to this critical number of cycles and then tested to evaluate the failure and the rheological strength parameters.

COMPLEX ELASTIC MODULUS

The concept of the complex elastic modulus or creep modulus applied in the study to define the viscoelastic response of materials on a fundamental level is based on the fact that, when an alternating stress of a given frequency varying sinusoidally with time is applied to a material, the response of the material will be a sinusoidal strain of the same frequency but that lags the stress by a phase angle ϕ (11). Thus, mathematically, the complex elastic modulus relates the axial sinusoidal stress applied to a linear viscoelastic material to the resulting axial strain. In such a case, the strain is related to the stress by a complex number that is a function of frequency and that may be called the complex elastic modulus of the material.

To illustrate these concepts, let an alternating stress $\sigma = \sigma_o \sin \omega t$ be applied to a linear viscoelastic material whose complex modulus is denoted by E^*. The steady-state response of the material will be an alternating strain $\epsilon = \epsilon_o \sin(\omega t - \phi)$ with the same frequency as the stress and amplitude ϵ_o. If $E'(\omega)$ and $E''(\omega)$ are the real and imaginary parts of E^* and j is the imaginary unit, then by definition

$$/E^*/ = \frac{\sigma_o}{\epsilon_o} \tag{1}$$

$$E' = /E^*/ \cos \phi \tag{2}$$

$$E'' = /E^*/ \sin \phi \tag{3}$$

$$\phi = \tan^{-1} \frac{E''}{E'} \tag{4}$$

$$/E^*/ = [E'^2 + E''^2]^{1/2} \tag{5}$$

$$E^* = E' + jE'' \tag{6}$$

Let $\sigma(t)$ be a given stress in periodic waveform such that $\sigma(t + T) \equiv \sigma(t)$ where T is the period. Then the exponential form of the Fourier series expansion of $\sigma(t)$ is given by

$$\sigma(t) = \sum_{n=-\infty}^{\infty} \sigma_n \exp(jn\omega t) \tag{7}$$

where $\omega = 2\pi/T$ and σ_n represents the complex Fourier coefficient such that

$$\sigma_n = \frac{1}{T} \int_{-T/2}^{T/2} \sigma(t) \exp(-jn\omega t)_{dt} \tag{8}$$

For any nonperiodic stress, Fourier methods may be extended by regarding the stress as being a single wave of infinite period. In such a case, the Fourier series is replaced by a Fourier integral that expresses a nonperiodic function as the superimposition of steady-state sinusoids of all frequencies, each of which endures from $t = -\infty$ to $t = \infty$. Let $\sigma(t)$ be a nonperiodic stress. Then we may write

$$\sigma(t) = \lim_{T\to\infty} \sum_{n=-\infty}^{\infty} \sigma_n \exp(jn\omega t) = \lim_{T\to\infty} \sum_{n=-\infty}^{\infty} \frac{\sigma_n}{\Delta f} \exp(jn\omega t)\, \Delta f \tag{9}$$

where $\Delta f = 1/T$. Then, in the limit,

$$\sigma(t) = \frac{1}{2\pi} \int_{-\infty}^{\infty} \sigma(j\omega) \exp(j\omega t)\, d\omega \tag{10}$$

where

$$\sigma(j\omega) = \lim_{T\to\infty} \frac{\sigma_n}{\Delta f} = \lim_{T\to\infty} \int_{-T/2}^{T/2} \sigma(t) \exp(-jn\omega t)\, dt \tag{11}$$

Hence

$$\sigma(j\omega) = \int_{-\infty}^{\infty} \sigma(t) \exp(-j\omega t)\, dt \tag{12}$$

if the given function be the strain $\epsilon(t)$. Then we may write

$$\dot{\epsilon}(j\omega) = \int_{0}^{\infty} \dot{\epsilon}(t) \exp(-j\omega t)\, dt \tag{13}$$

where it has been assumed that the strain, and hence the rate of strain, is zero for $t < 0$. Integrating by parts, the expression takes the form

$$\epsilon(j\omega) = [\epsilon(t) \exp(-j\omega t)]_0^{\infty} + j\omega \int_{0}^{\infty} \epsilon(t) \exp(-j\omega t)\, dt \tag{14}$$

Unfortunately, as it stands, this expression does not converge at the upper limit unless $\epsilon(t) \to 0$ as $t \to \infty$, which is not here assumed to be the case. To overcome this difficulty, we transform the related function $\dot{\epsilon}(t) \exp(-\alpha t)$, where α is a positive constant, to obtain

$$\dot{\epsilon}(\alpha + j\omega) = \int_0^\infty \dot{\epsilon}(t) \exp(-\alpha + j\omega t)\, dt \tag{15}$$

Integrating by parts, as before, the expression becomes

$$\epsilon(a + j\omega) = [\epsilon(t) \exp -(\alpha + j\omega)]_0^\infty + (\alpha + j\omega) \int_0^\infty \epsilon(t) \exp -(\alpha + j\omega)\, dt \tag{16}$$

Now this expression will converge to zero at the upper limit for any positive value of α, no matter how small, provided $\epsilon(t)$ does not grow large as rapidly as an exponential function such as t becomes infinite. Defining $\epsilon(i\omega)$ as the upper limit of the transform $\epsilon(\alpha + i\omega)$ while α approaches zero, we get

$$\dot{\epsilon}(j\omega) = -\epsilon(0) + i\omega\epsilon(i\omega) \tag{17}$$

As mentioned before, the complex elastic modulus may be obtained in analytical form by recording the axial response of the material to an axial stress and transforming both stress and strain to frequency domain. In obtaining the Fourier transform of the response, it is convenient to obtain the transform of the rate of strain instead of the strain and then go back to find the transform of the strain, in order to achieve a better accuracy, which comes about as the result of approximating the differentiated function $\dot{\epsilon}(t)$ rather than the original curve $\epsilon(t)$. Thus, in transforming the response from the time domain to the frequency domain, the curve representing the axial strain as a function of time is first differentiated graphically to obtain the curve of rate of axial strain as a function of time. This curve is then approximated by a series of exponentials. The steps for such an approximation are as follows:

1. The steady-state rate of strain (stage of constant increase in strain with time) is subtracted throughout from the total rate of strain $\epsilon(t)$.
2. The resulting curve is plotted on semilog paper, with the rate of strain on the vertical log scale and the lowest portion of the curve approximated by a straight line.
3. The difference in rate of strain between the curve and the straight line is calculated as a function of time, and the result is plotted on semilog paper.
4. The lower portion of this curve is again approximated by a straight line, and the second difference is calculated.
5. The process is repeated until the remaining difference can be completely represented by a straight line.
6. Exponentials representing each of the straight lines are determined and added to the constant rate to obtain a fairly good approximation of the original $\dot{\epsilon}(t)$ curve. The rate of strain as a function of time is then expressed in the form

$$\dot{\epsilon}(t) = A_1 \exp(-k_1 t) + A_2 \exp(-k_2 t) + \cdots + A_n \exp(-k_n t) + \dot{\epsilon}_{ss} \tag{18}$$

where $A_1 \exp(-k_i t)$ is the equation of the ith straight line and $\dot{\epsilon}_{ss}$ is the constant rate of strain. Using Eq. 12, we get

$$\dot{\epsilon}(i\omega) = \frac{A_1}{k_1 + j\omega} + \frac{A_2}{k_2 + j\omega} + \cdots + \frac{A_n}{k_n + j\omega} + \frac{\dot{\epsilon}_{ss}}{j\omega} \tag{19}$$

and using Eq. 17

$$\epsilon(i\omega) = \frac{1}{j\omega}\left[\frac{A_1}{k_1 + j\omega} + \frac{A_2}{k_2 + j\omega} + \cdots + \frac{A_n}{k_n + j\omega} + \frac{\dot{\epsilon}_{ss}}{j\omega} + \epsilon(0)\right] \tag{20}$$

If $\sigma(t) = \sigma_0$ for $t > 0$ and $= 0$ for $t < 0$, then for fundamentals

$$\sigma(i\omega) = \frac{\sigma_0}{j\omega} \quad \text{and} \quad E^* = \frac{\sigma(i\omega)}{\epsilon(j\omega)}$$

one obtains

$$E^*(j\omega) = \frac{1}{\frac{1}{\frac{k_1\sigma_0}{A_1} + \frac{j\omega\sigma_0}{A_1}} + \frac{1}{\frac{k_2\sigma_0}{A_2} + \frac{j\omega\sigma_0}{A_2}} + \cdots \frac{1}{\frac{k_n\sigma_0}{A_n} + \frac{j\omega\sigma_0}{A_n}} + \frac{1}{\frac{j\omega\sigma_0}{\dot{\epsilon}_{ss}}} + \frac{1}{\frac{\sigma_0}{\epsilon(0)}}}$$

which is the fundamental relation sought.

MATERIALS AND SAMPLE PREPARATION

Material

A mined and processed soil, Kaolin, was selected for the investigation of effect of environmental conditions on the rheological characteristics of soils. The Kaolin (EPK) was obtained from the Edgar Minerals Corporation, Gainesville, Florida. The clay is a relatively uniform soil with no thixotropic effects (8, 16) and low-level swelling characteristics. Other advantages are its white color, convenient powdered form, lack of odor, and ease with which the samples can be trimmed. Particle size distribution and other properties of kaolinite clay are shown in Figure 1.

Figure 1. Particle size distribution and classification of kaolinite clay.

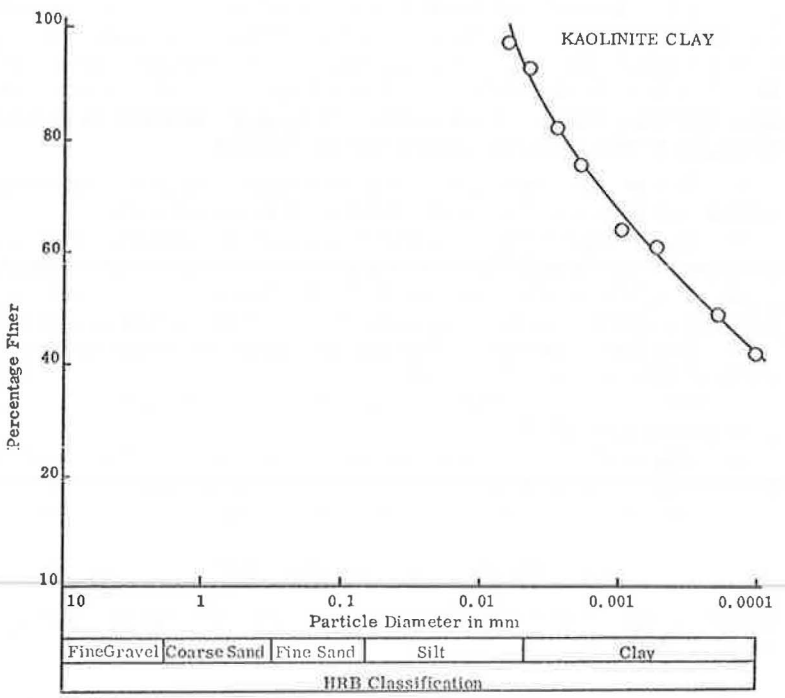

Atterberg Limits			Specific Gravity	Soil Classification		
L · L%	P · L%	P · I%		Unified Soil Classification	AASHO Classification	F. A. A. Classification
58	36	22	2.60	M H	A-7-5 (16)	E-8

Sample Preparation

The soil passing the U.S. No. 12 sieve was first oven-dried and mixed with the required amount of distilled water following the mixing procedure specified in ASTM method D-698-64T. The mixed soil was then stored in a sealed plastic container in a humid room for a minimum of 12 hours to allow the molding water to be distributed uniformly throughout the soil.

Soil samples $1\frac{5}{16}$ in. (3.33 cm) in diameter and 2.816 in. (7.15 cm) in height were prepared using the Ohio State University standard drop hammer compaction (8). The apparatus has a 3.62-lb (1.642 kg) hammer, which is picked up by a special link in the drive chain that catches on a movable ring to release the weight. The ring is held in the pick-up position by a cone mounted on top of a spring in the hammer head. The metal head is held 10 in. (25.4 cm) from the top of the sample, ensuring the correct height of the hammer fall. All the samples were prepared by compacting the soil (applying the desired number of blows) in the mold using five layers of equal soil weight. The input of compaction energy in this case can be calculated in work units (for example, 40 total blows per sample with 8 blows per layer equals 54,480 ft-lb/ft^3 (26 kJ/m^3), which corresponds closely to the modified AASHO compaction energy of 56,300 ft-lb/ft^3 (27 kJ/m^3). After extruding the sample from the mold, the test specimen was weighed, wrapped in a plastic bag, and completely coated with wax. The sample was then stored in a humid room for several days in order to develop a homogeneous distribution of moisture throughout the sample. After this, the samples were taken from the humid room for conditioning. The samples, before being tested either in the creep test or the unconfined compression test, were subjected to the critical number of freeze and thaw cycles determined in the preliminary studies. Each freeze cycle consisted of 7 hours in the freezer having a constant temperature of -20 F (-29 C). After the freeze cycle, the samples were taken from the freezer and kept in the humid room during the night for the thaw cycle. In every case, the last thaw cycle before the creep testing was at least 2 days long.

EXPERIMENTAL PROCEDURE

To obtain the complete information about the viscoelastic properties, i.e., the rheological strength parameters, it is necessary to obtain stress and strain measurements over a wide range of the time or frequency scale. As already discussed, for the material and conditions employed, the rheological creep test was found to be the most suitable experiment. Because the unconfined compression test serves as a single means of measuring the undrained shear strength and is quick and simple to perform, it was also selected to correlate the strength characteristics of the various specimens.

Creep Test

The creep test is a nondestructive type of test. A typical frame used to perform the creep test consists of a Clockhouse triaxial cell, loading apparatus, and LVDT to measure the axial strain. The LVDT was connected to a Sanborn Model 321 recorder to obtain a continuous recording of the axial strain. Accurate loading or unloading was performed by an oil-pressure loading device. Based on the linearity tests conducted on the soil, it was decided to use 8.0 psi (55 kPa) as the axial stress.

It was found that the deformation of the sample under the load in the first loading cycle is larger than that observed in the subsequent loading and unloading cycles. However, the response of the soil reaches a steady-state condition after two cycles (8). The response under the steady-state load cycle is a typical representation of the soil behavior under the repeated loadings encountered in highway conditions. Thus, in order to condition the samples under the load, the creep test procedure consisted of cycling the axial load twice through the load and unload cycles. The third cycle, used to obtain the experimental data, consisted of 30 minutes of loading and 30 minutes of creep recovery in the unloaded state. After the sample had been tested, it was wrapped in a plastic bag, coated with wax, and stored in the humid room until the unconfined compression test was performed.

The axial strain data, as a function of time, were used to calculate the creep modulus E_c and to evaluate the complex elastic modulus $/E^*/$ by transforming the experimental results from time domain to the frequency domain. A typical calculation of the magnitude of the complex elastic modulus from such creep data can be found in the literature (12). In the analysis of the data, $/E^*/$ corresponding to a frequency of w = 0.1 radians per second was used. This frequency corresponds to the very low vehicle speed of 0.065 mph (0.1 km/hour) and was selected based on investigations carried out by Baker (3), who showed that subgrade materials loaded by low-speed traffic will exhibit greater deformations. Traffic just starting or stopped corresponds to the low-speed situations; hence, parking areas may be expected to develop greater ruts and fail earlier than high-speed roadway sections of equal design under the same load magnitude and frequency of application. Once the strength of subgrade is defined in terms of viscoelastic strength parameter $/E^*/$, the allowable distribution of the stresses and the structural design of pavements can be more rationally studied by the use of material science design procedures now being investigated (3, 5).

Unconfined Compression Test

The unconfined compression test is a destructive type of test. The apparatus consists of a Genor triaxial cell and Instron Model TTBML universal testing machine. In this test, a continuous relation between stress and strain is obtained by continuously and axially straining the sample at a constant rate of strain until failure. The tests were performed following ASTM specification D-2166-63-T at a strain rate of 2.82 percent per minute [0.2 cm per minute for samples 2.816 in. (7.15 cm) in height]. Unconfined compressive strength and modulus of elasticity were found with the help of this test.

PRELIMINARY STUDIES

As discussed, one of the most important factors affecting the pavement performance is climate. Frost action includes both frost heave and loss of subgrade support during the frost-melt period. The structural damage to pavements during the spring thaw may result in very high maintenance costs and in some cases may be of such magnitude as to require posting the road and prohibiting the use of heavy loads during the critical period (19). Damage to the pavement may still be greater if the seasonal variations in the temperature are such that they result in periodic freezing and thawing. The results of the research conducted by Walker et al. (17, 18) also confirm this fact. However, it is expected that, after a certain limit, subjecting the soil to additional periodic freezing and thawing will not result in any appreciable loss of subgrade strength.

The object of the preliminary studies was to find the critical number of freeze-thaw cycles so that any additional cycles do not indicate any significant changes in the failure and rheological strength parameters of unconfined compressive strength, modulus of elasticity, creep modulus, and complex elastic modulus.

For this purpose, soil samples of Kaolin clay with initial molding moisture content of 28.34 percent and 40 blows compaction energy were subjected to 0, 3, 6, 9, 12, and 24 freeze-thaw cycles. The samples were then tested under creep and for unconfined compressive strength.

Figure 2 is a typical plot indicating the variation in creep modulus with the number of freeze-thaw cycles. It indicates that for practical purposes it can be assumed that the rheological strength parameter E_c does not change appreciably after eight cycles. The same trend was found to be true for $/E^*/$, E, and σ_c'. It was thus decided that all soil samples will be subjected to nine freeze-thaw cycles before testing.

DISCUSSION OF EXPERIMENTAL RESULTS

It is known that the widely used soil parameters of dry density, unconfined compressive strength, penetration needle resistance, California bearing ratio, etc., although convenient, do not exactly reflect the true stress-strain characteristics of the compacted soil in service because the characteristics are greatly influenced by the environ-

Figure 2. Creep modulus versus number of freeze-thaw cycles.

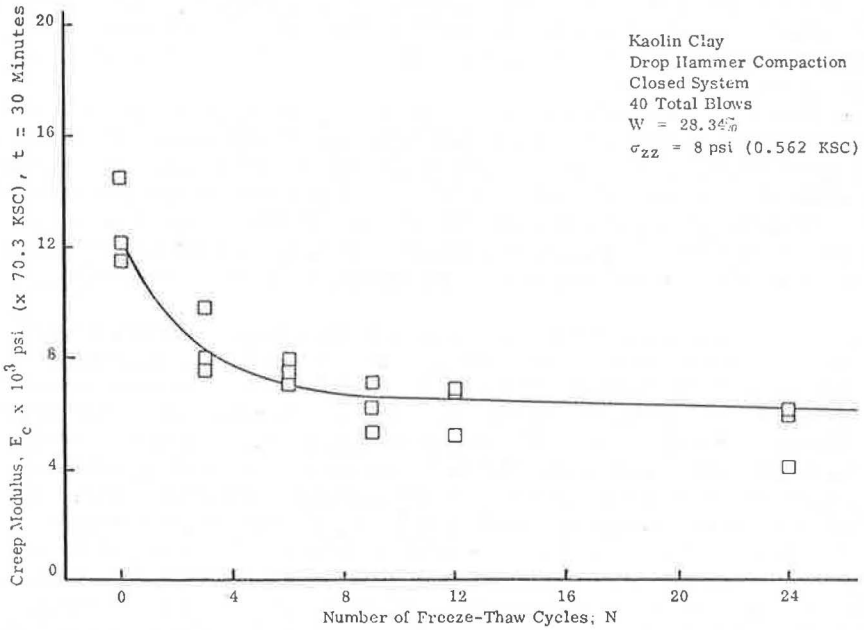

Figure 3. Dry unit weight versus moisture content for drop hammer compaction.

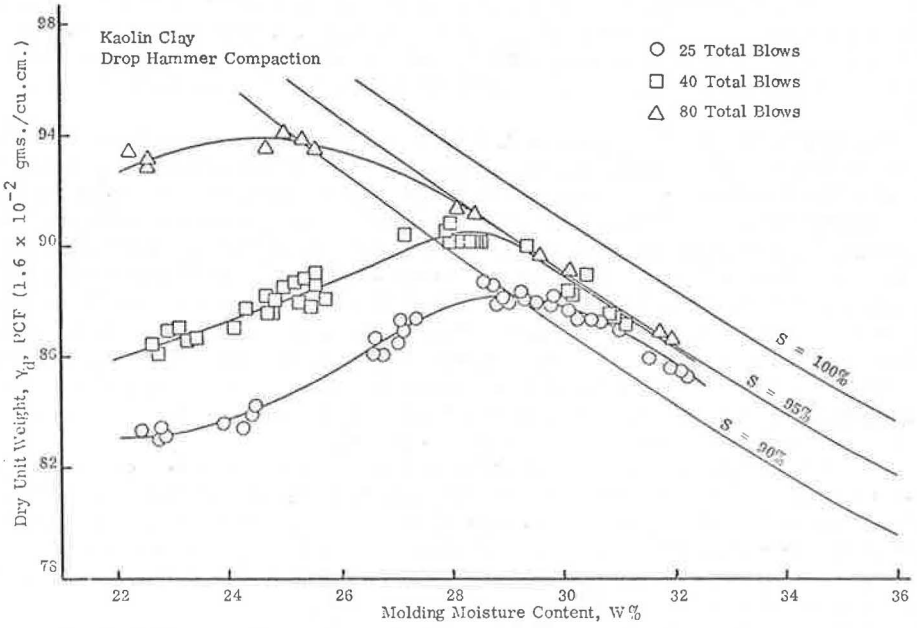

mental and loading conditions experienced by highway embankments. These parameters are not directly or fundamentally related to the strength and deflection parameters used in the structural design of rigid or flexible pavements. However, rheological parameters seem to describe the characteristics of highway subgrade more rationally than many parameters presently in vogue.

For any compactive effort, the variation in the selected parameter can be studied either at a constant moisture content or at a constant degree of saturation. Kaolin soil samples were prepared using three energy levels of 25, 40, and 80 blows. The moisture contents ranged from 22 to 32 percent: 22, 25, 29, and 32 percent for samples with 25 and 80 blows of compaction energy and 22, 25, 27, 29, and 32 percent molding water contents for samples with 40 blows compaction energy. Figure 3 shows the plot of dry unit weight versus percentage of molding moisture content at different levels of compaction energy.

Figures 4, 5, 6, and 7 are the plots of creep modulus E_c, complex elastic modulus $/E^*/$, modulus of elasticity E, and unconfined compressive strength σ_c' respectively versus initial molding moisture content. These plots show that for the investigated compaction energies the rheological and failure parameters increase with an increase in the moisture content on the dry side of the moisture-density curve up to a certain level of maximum value. After this stage, further increase in the molding moisture content results in a decrease in the value of these parameters. However, for any one parameter, somewhere between moisture content of 27 and 28 percent, the effect of compactive effort seems to vanish and moisture content remains the principal factor controlling the soil strength. Any increment in moisture content over 27 to 28 percent reverses the phenomena. The reason for the reversal is not known. This warrants further investigation to evaluate the soil structure produced during compaction and after freeze-thaw cycles and its influence on the engineering properties of the soils. For higher moisture contents of 32 percent and over, these parameters drop in value significantly and the effect of compaction energy once again becomes negligible.

Figure 7 shows that the behavior of failure parameter σ_c' differs slightly from that of the rheological parameters. For the soil specimens having moisture contents on the extreme dry side of the moisture-density curve, while σ_c' shows a rapid increase with increase in the compactive effort, other rheological parameters do not seem to differ appreciably.

For any compaction level it is apparent that a change in moisture content from 22 to about 26 percent causes only a small change in E_c, $/E^*/$, E, and σ_c' and all the variations can be accommodated within a very narrow band. But for any increase in moisture over 26 percent, these parameters drop significantly, indicating an appreciable effect of the moisture content. These plots also demonstrate that increasing the compactive effort from 40 to 80 blows does not bring about much change in E_c, $/E^*/$, or E and all the difference appears within the compactive efforts of 25 and 40 blows. However, the same conclusion does not seem to hold for the unconfined compressive strength data because, at all moisture contents, compaction energy affects considerably the failure parameter σ_c'. Only near 27.5 percent water content (which was previously indicated as the point where the phenomena of the variations in rheological parameters with water content reverse), the compactive effort does not seem to affect σ_c'.

It is clear from these plots that, except for very low and very high molding moisture contents corresponding to the two extremes of the moisture-density curves, the effect of the moisture content on the rheological parameters seems to be more pronounced for the soil specimens with higher compaction energies than for the specimens with low compaction energies because of the greater proportionate variations in these parameters with any changes in the moisture content.

Until now the effect of compaction on the failure and rheological parameters was studied at constant moisture content. However, because the optimum moisture content has different magnitudes for various amounts of compaction energies, a given moisture content may be on the dry side of optimum for low levels of compaction and on the wet side of optimum for high levels of compaction energy. By studying the response of the soils at constant degree of saturation, this drawback can be avoided. Therefore, the variation of the selected soil parameters due to a range of compaction energy inputs

Figure 4. Creep modulus versus initial molding moisture content.

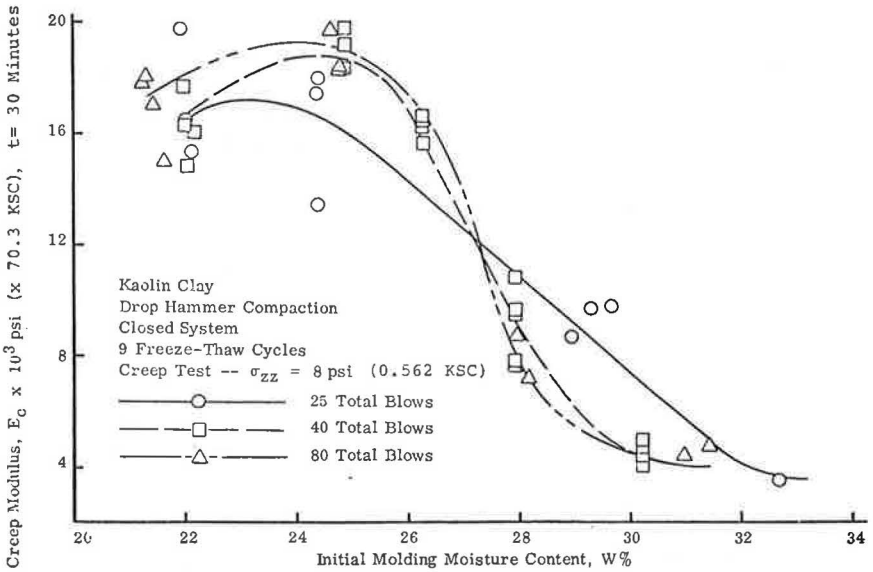

Figure 5. Magnitude of complex elastic modulus versus initial molding moisture content.

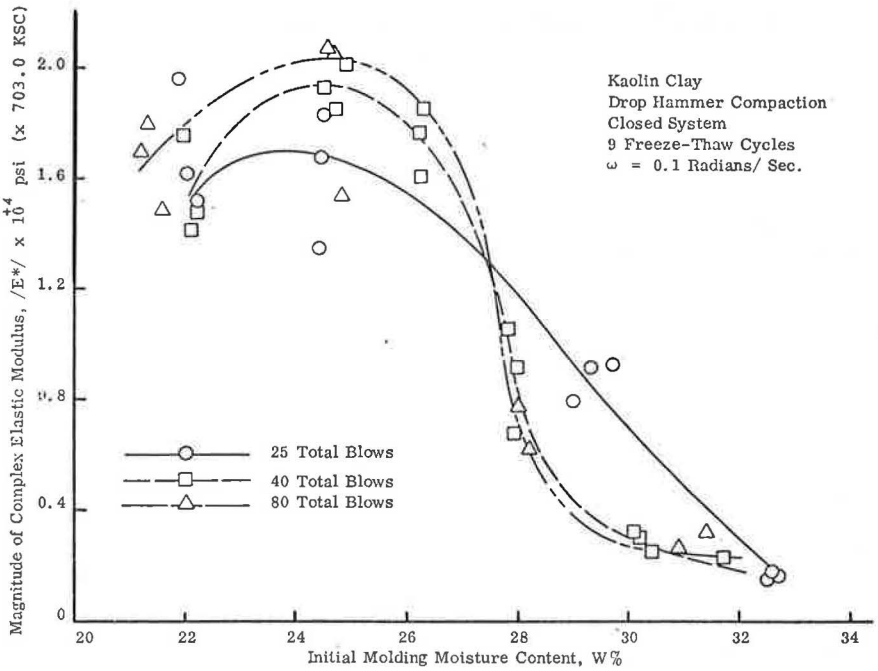

Figure 6. Modulus of elasticity versus initial molding moisture content.

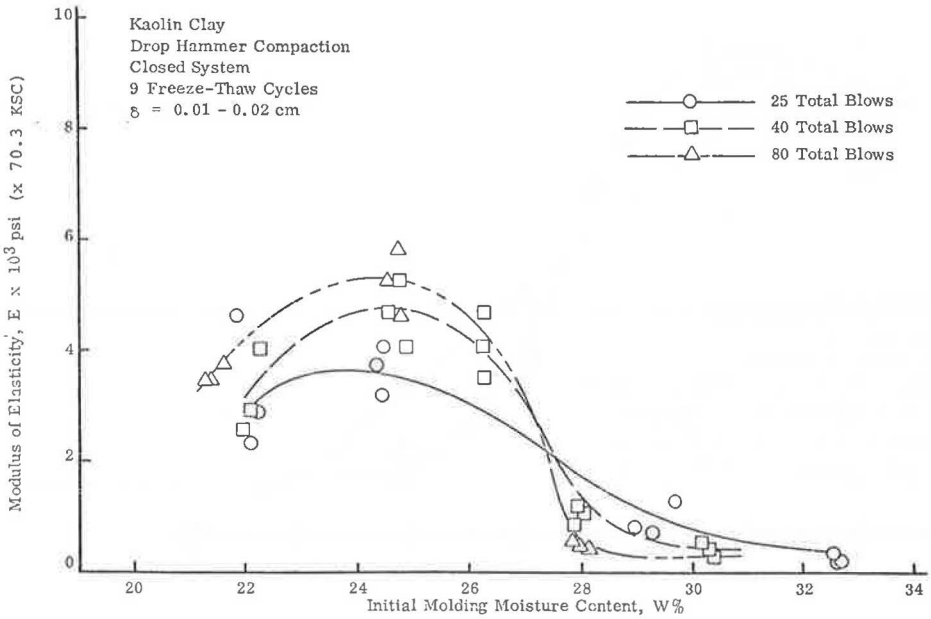

Figure 7. Unconfined compressive strength versus initial molding moisture content.

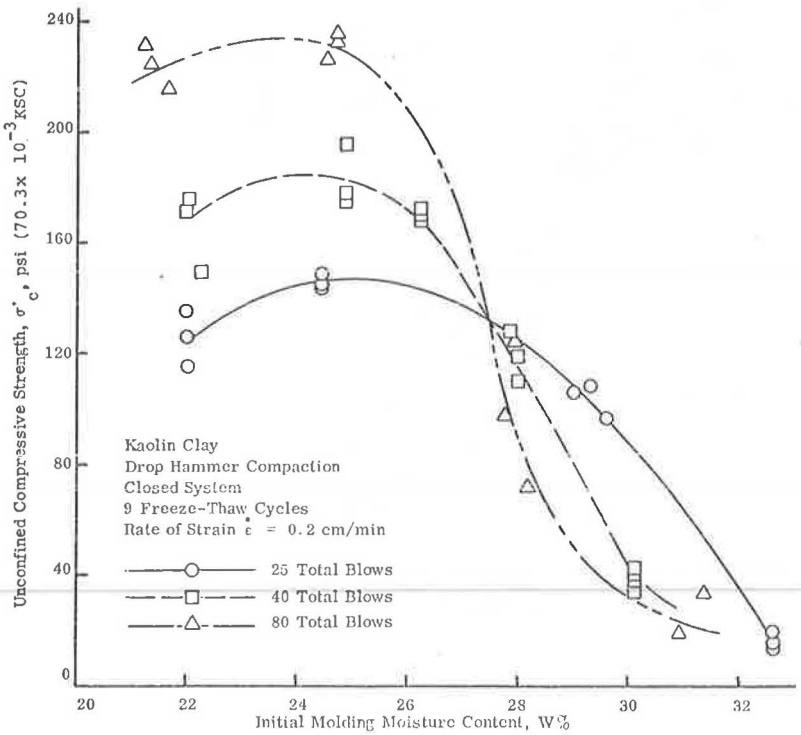

was also studied at a constant degree of saturation. The effect of saturation on rheological and strength parameters of Kaolin is shown in Figures 8, 9, 10, and 11. As in the case of the effect of moisture content on these parameters, for each compaction energy level the values of E_c, $/E^*/$, E, and σ_c' increase with an increase in saturation up to a certain point of maximum value. The location of this point depends on the compaction energy imparted to the specimen. Saturations at which strength parameters reach their maximum value increase with an increase in the energy input. Further increase in saturation results in a decrease in the value of the selected parameter. Up to about 80 percent for specimens with 25 blows and 85 percent for specimens with 40 and 80 blows initial degree of saturation does not seem to affect E_c, $/E^*/$, E, and σ_c' significantly. However, after these critical values of saturations, the soil strength in terms of the selected parameters starts decreasing rapidly with any small increase in saturation. For all practical purposes, it can be said that with any further increase in saturation from about 80 to 90 percent (lower limit corresponding to compaction energy of 25 blows and upper limit to compaction energies of 40 and 80 blows), the soil loses a major portion of its strength and subsequently approaches a minimum value. For subgrades where the seasonal changes in temperature are such that freezing and thawing can occur without an increase in the initial saturation, the data suggest that the soils should be compacted with saturations corresponding to the dry side of the moisture-density curve. In any case, the initial saturation should not be more than approximately 85 percent because, after this point, the soil strength starts decreasing rapidly and thus will render the pavement unsuitable to sustain heavy loads.

For the design of either rigid or flexible pavements, the modulus of elasticity or the complex elastic modulus are the critical factors because these parameters control serviceability, deformation characteristics, and the design thickness of the different components of the pavements. As such, the variation of these parameters with saturation should be critically investigated for any soil to be used as a subgrade material. If we look at the variation of these parameters with saturation, it is apparent that within a range of about 70 to 90 percent, for any particular saturation, these parameters are significantly controlled by the compaction energy. For a given saturation, an appreciable increase in the rheological parameters can be achieved by increasing the compaction energy from 25 to 40 blows. However, further increase in the compaction energy does not bring about any appreciable change in the rheological parameters of E_c, $/E^*/$, and E. At low saturations, below 70 percent, and higher saturations, above 90 percent, these parameters do not seem to be influenced by the compactive efforts investigated in the present study but at normal subgrade saturations encountered under highway pavements these parameters are greatly affected by the amount of compaction energy.

The variations in the values of unconfined compressive strength with saturation do not exactly follow the same trends as indicated by E_c, $/E^*/$, or E. Within 70 to 80 percent initial saturation, any increase in the compaction energy results in a proportionate increase in σ_c', after which compressive strength starts dropping suddenly and reaches its minimum between saturations of 90 and 95 percent.

The results of this study thus indicate that the effects of freeze and thaw cycles are more severe for higher moisture contents or saturations because, for such values, all the rheological strength parameters practically reach their minimum and render the highway or airport pavement useless for supporting the normal traffic loads. Attention should be directed toward compacting the subgrades with low degrees of saturation and designing better drainage systems so that any appreciable increase in the moisture content from the as-compacted state can be avoided. If only the compressive or shear strength failure are the criteria, then the subgrade, where the soil has properties comparable to those of Kaolin and the method of compaction produces a soil structure close to the one obtained from the drop hammer, should be compacted with high energy levels. This is based on the fact that the parameter of unconfined compressive strength is very sensitive to the compactive effort and increases rapidly with an increase in number of drop hammer blows for the moisture contents on the dry side of optimum. What compaction energy should be used for this purpose will depend on the traffic loads the highway is designed for. However, if serviceability and deformation characteristics are

Figure 8. Creep modulus versus initial degree of saturation.

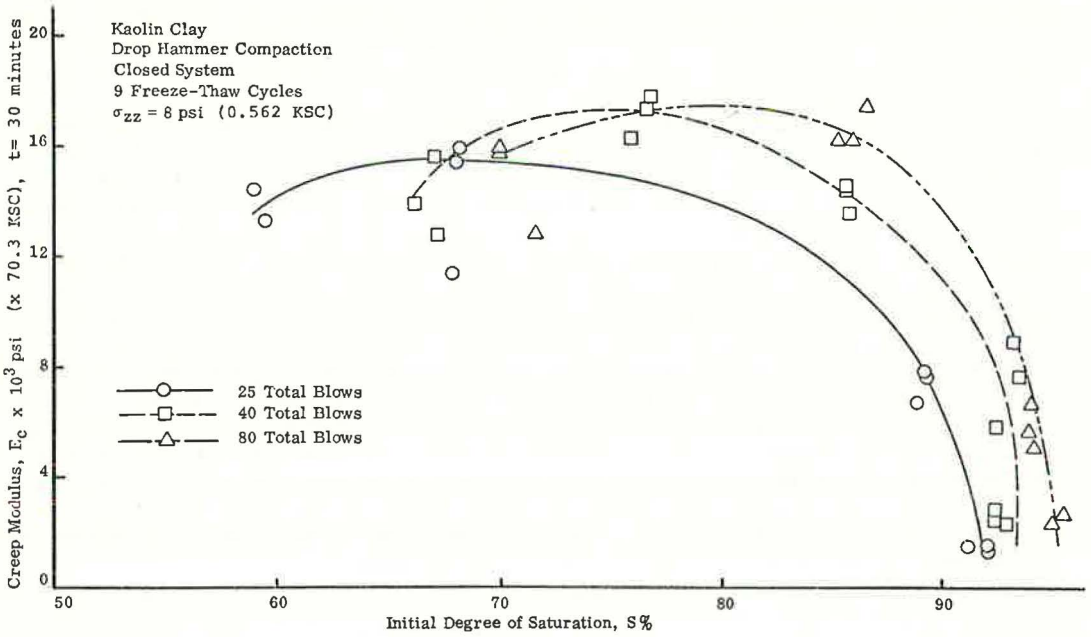

Figure 9. Magnitude of complex elastic modulus versus initial degree of saturation.

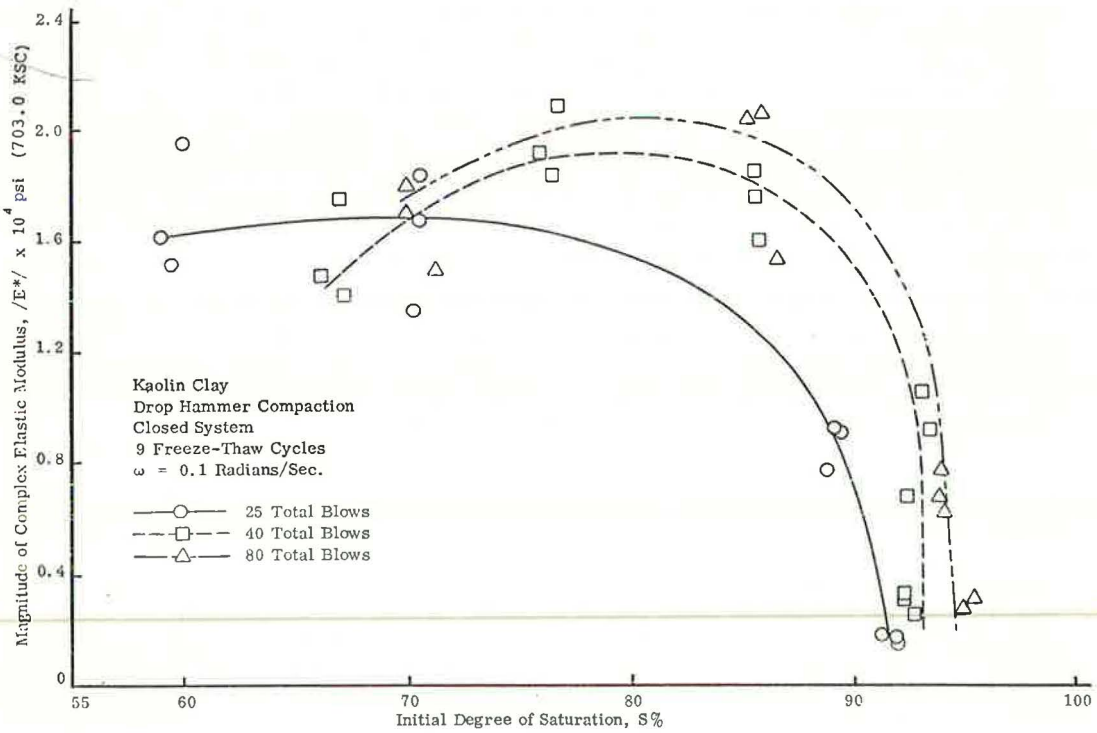

Figure 10. Modulus of elasticity versus initial degree of saturation.

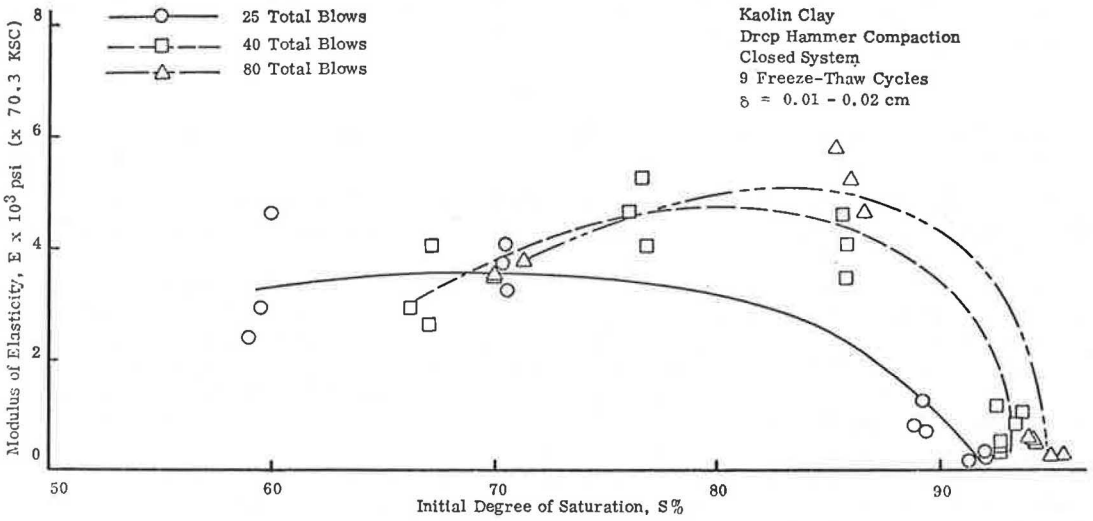

Figure 11. Unconfined compressive strength versus initial degree of saturation.

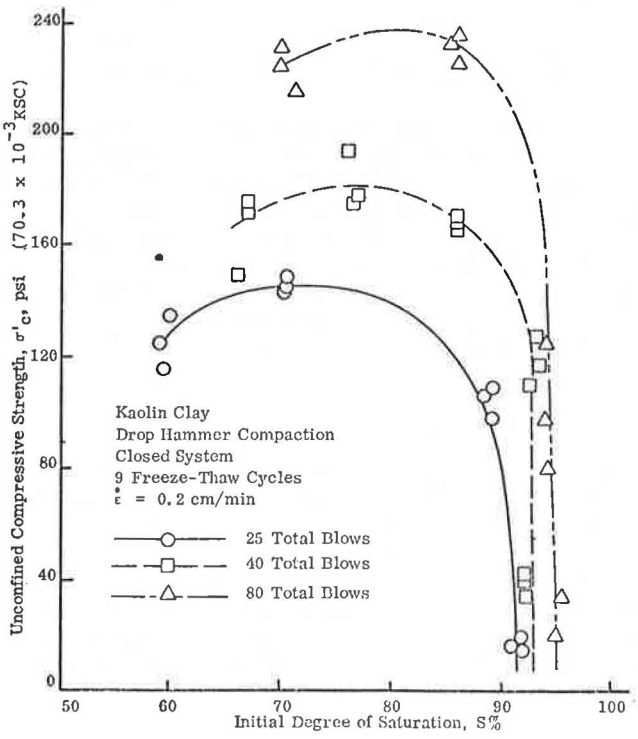

the main considerations in the design, then compaction with 40 drop hammer blows will serve the purpose as long as the saturations can be controlled to correspond to the dry side of the moisture-density curve.

CONCLUSIONS

For the materials and conditions investigated, the following are the major conclusions of this research:

1. Preliminary tests indicated that the critical number of freeze-thaw cycles was nine. Additional such cycles will not bring about any appreciable change in the rheological or standard strength parameters.
2. Moisture content does not seem to be a suitable parameter to determine the effect of compaction energy on the rheological or failure parameters of a compacted soil subjected to freeze-thaw cycles. This is so because two different trends were found over the full range of moisture contents utilized for the present study. Although these parameters showed an increase with an increase in the compactive effort up to a moisture content of about 27.5 percent, further increase in the moisture content had the effect of reversing the phenomena completely.
3. Reversal of phenomena as indicated for the variation with respect to moisture content was, however, absent when the changes in the selected parameters were related to saturation. Saturation has very little effect on E_c, $/E^*/$, E and σ_c' up to about 80 percent for specimens with 25 blows and 85 percent for the soil specimens prepared with 40 and 80 blows of compaction energy. However, after these critical saturations, the parameter values decrease rapidly with any further increase in saturation. For all practical purposes, it seems that for any increase in saturation over 85 to 90 percent (lower limit corresponding to compaction energy of 25 blows and the upper limit to 40 and 80 blows), the soil loses a major portion of its strength and approaches a minimum value of the selected parameter.
4. If only the failures in compression or shear strength are the criteria, then the subgrades should be compacted with high energy levels because the results have shown that any increase in compaction energy brings about a proportionate increase in σ_c'. However, if serviceability and deformation characteristics are the main considerations in design, then the compaction energy of 40 blows will serve the purpose, because further increase in the compaction energy does not bring about any appreciable change in the rheological parameters of E_c, $/E^*/$, or E. This is true for the conditions when the saturations can be controlled to approximately correspond to the dry side of the moisture-density curve and the method of compaction produces a soil structure close to the one obtained from the drop hammer.

ACKNOWLEDGMENTS

The material in this paper was partially obtained from the Ohio State University Research Report EES-248-4, written by the authors while at the Transportation Engineering Center, Department of Civil Engineering, Ohio State University. The research work was conducted by the authors at OSU and was sponsored by the Ohio Department of Transportation in cooperation with the U.S. Department of Transportation, Federal Highway Administration. The interest and cooperation of these agencies are gratefully acknowledged. The opinions, findings, and conclusions are those of the authors and not necessarily those of the Ohio Department of Transportation or the Federal Highway Administration.

REFERENCES

1. The AASHO Road Test—Pavement Research, Report No. 5. HRB Spec. Rept. 61E, 1962.
2. Alfrey, T. Mechanical Behavior of High Polymers. International Publishers, New York, 1948.
3. Baker, R. F. Pavement Design Using Rheological Concepts. Proc., International Conf. on Structural Design of Asphalt Pavements, Univ. of Michigan, 1962.

4. Bastiani, A. The Explicit Solution of the Equation of the Elastic Deformations for a Stratified Road Under Given Stresses in the Dynamic Case. Proc., International Conf. on Structural Design of Asphalt Pavements, Univ. of Michigan, 1962.
5. Coffman, B. S., Kraft, D. C., and Tamayo, J. A Comparison of Calculated and Measured Deflections for AASHO Test Road. Proc., Association of Asphalt Paving Technologists, Vol. 33, 1964, pp. 54-90.
6. Freudenthal, A. M. The Inelastic Behavior of Engineering Materials and Structure. John Wiley and Sons, New York, 1950.
7. Jumikis, A. R. Frost Penetration Problems in Highway Engineering. Rutgers Univ. Press, New Brunswick, New Jersey, 1955.
8. Pagen, C. A., and Jagannath, B. N. Fundamentals of Soil Compaction. Engineering Experiment Station, Ohio State Univ., Rept. EES 248-1, July 1966.
9. Pagen, C. A., and Jagannath, B. N. Evaluation of Soil Compaction by Rheological Techniques. Highway Research Record 177, 1967, pp. 22-43.
10. Pagen, C. A., and Jagannath, B. N. Mechanical Properties of Compacted Soils. Highway Research Record 235, 1968, pp. 13-26.
11. Papazian, H. S. Response of Linear Viscoelastic Materials in the Frequency Domain. Engineering Experiment Station, Ohio State Univ., Bull. 192, July 1962.
12. Reiner, M. Building Materials, Their Elasticity and Inelasticity. North Holland Publishing, Amsterdam, 1954.
13. Seed, H. B., Mitchell, J. K., and Chan, C. K. The Strength of Compacted Cohesive Soils. Proc., ASCE Research Conf. on Shear Strength of Cohesive Soils, 1960, pp. 877-964.
14. Seed, H. B., and Chan, C. K. Structure and Strength Characteristics of Compacted Clays. Jour., Soil Mechanics and Foundations Division, American Society of Civil Engineers, Oct. 1959.
15. Seed, H. B., Chan, C. K., and Lee, C. E. Resilience Characteristics of Subgrade Soils and Their Relation to Fatigue Failures in Asphalt Pavements. Proc., International Conf. on Structural Design of Asphalt Pavements, Univ. of Michigan, 1962, pp. 611-636.
16. Skempton, A. W., and Northey, R. D. The Sensitivity of Clays. Geotechnique, Vol. 3, No. 1, March 1952.
17. Walker, R. D., and Kavabulut, C. Effect of Freezing and Thawing on Unconfined Compressive Strength of Lime-Stabilized Soils. Highway Research Record 92, 1965, pp. 1-11.
18. Walker, R. D., Erkan, E., and Krebs, R. D. Strength Loss in Lime-Stabilized Clay Soils When Moistened and Exposed to Freezing and Thawing. Highway Research Record 198, 1967, pp. 1-8.
19. Yoder, E. J. Principles of Pavement Design. John Wiley, New York, 1959.

ESTIMATING THE DEPTH OF PAVEMENT FROST AND THAW PENETRATIONS

G. H. Argue and B. B. Denyes, Construction Engineering and Architectural Branch, Canadian Air Transportation Administration, Ottawa

The design of foundations and pavements is affected by the depth to which frost penetrates during the winter or, in the case of permafrost areas, the depth reached by summer thaw. This report contains information on the depth of these penetrations as recorded at a number of Canadian airports. Correlations are developed between site air freezing index and the maximum depth of frost penetration beneath both asphalt and portland cement concrete pavements kept clear of snow during the winter. The standard error of these correlations is approximately 16 and 12 in. (41 and 30 cm) respectively. The maximum frost penetration that might be expected in undisturbed snow-covered areas is related also to site air freezing index. Similarily, for permafrost areas, relationships are developed between thaw penetration and site thawing index. More accurate estimates of frost penetration may be calculated if detailed soils information is available. Air freezing indices normally available for a site must be corrected to a pavement surface freezing index when making these calculations. The measurements recorded in the frost depth study indicate that the ratio of pavement surface/air freezing index decreases as site air freezing index decreases.

•THE design of many structures is influenced by ground frost conditions. The depth of seasonal frost penetration dictates thickness requirements for frost-protected pavements and is also an important factor to be considered when deciding on burial depths for building foundations and facilities such as water and sewer lines. Similarly, in permafrost regions, the depth of the active layer has a major influence on pavement thickness requirements and on the depth of pile embedment for building foundations.

Both types of ground frost conditions are encountered in Canada. In the southern part of the country the ground is normally unfrozen, and subfreezing temperatures penetrate the surface layers only during the winter months. In Arctic regions the ground is permanently frozen, with surface thaw occurring in the summer. The depth of these seasonal frost and thaw penetrations varies extensively throughout the country due to a wide range of climatic factors and soil conditions.

From 1964 to 1971, seasonal frost and thaw penetrations were recorded at a number of Canadian airports by the Construction Engineering and Architectural Branch of the Ministry of Transport. The information resulting from this survey is useful in estimating the maximum depth of frost and thaw penetrations at sites where actual measurements are not available.

THE FROST AND THAW DEPTH SURVEY

Frost Depth Indicator

The depths of frost and thaw penetrations were recorded at airports instrumented with frost depth indicators of the type devised by Gandahl (1). This instrument, with slight modifications incorporated by the Ministry of Transport, is shown in Figure 1.

Publication of this paper sponsored by Committee on Frost Action.

The instrument consists of a transparent acrylic plastic tube inside a heavier plastic casing. The tube and casing are inserted into a vertically bored hole to a depth exceeding the expected frost or thaw penetration. The inner acrylic tube contains a 0.05 percent solution of xylene cyanol. Normally a blue color, this solution turns colorless upon freezing. The depth of frost penetration is measured by simply extracting the inner acrylic tube from its casing and recording the depth of colorless solution. In the case of thaw, the depth of blue solution is measured.

Unlike thermocouple installations, which record actual soil temperatures, the frost depth indicator identifies only frozen and unfrozen zones. The frost depth indicator has certain advantages compared to thermocouples, provided that the only point of interest is the location of the ground frost line. The device is inexpensive, and a large number of installations for a comprehensive survey can be made without the necessity of complex recording devices at each site. Moreover, the simplicity of the instrument is such that it can be readily understood and used by inexperienced personnel. Instrument malfunctions can usually be easily identified.

In general, the Gandahl frost depth indicator performed satisfactorily during the frost survey program. Occasional difficulties arose when the indicator was frozen in and extraction of the instrument was either damaging or impossible.

Sites Instrumented

In 1964 frost depth indicators were installed at 30 airports in Canada. An additional 25 airports were instrumented in 1967, and some of the previous installations were then deleted from the program. The location of the instrumented airports is shown in Figure 2 in relation to the approximate boundaries of the continuous and discontinuous permafrost zones in Canada. Forty-two of these airports are situated in the southern part of the country, which experiences seasonal frost, and the depth of frost penetration during the winter was recorded at these sites. The eight airports located in the discontinuous permafrost zone have mean annual temperatures below 32 F (0 C), but the frost depth indicators recorded a seasonal frost penetration at these airports rather than permafrost. Thaw penetrations during the summer were recorded at five sites founded on permafrost (Cambridge Bay, Churchill, Frobisher, Inuvik, and Resolute).

Two or three frost depth indicators were usually installed at each airport. One indicator was located in a paved area surfaced with either asphaltic concrete or portland cement concrete kept relatively free of snow during the winter. Another indicator was located in an unpaved area with typical organic cover where snow was allowed to accumulate undisturbed.

Frost and Thaw Penetration Records

Frost and thaw penetration depths were recorded at weekly intervals throughout the season of interest by maintenance personnel or meteorological observers stationed at each airport. Table 1 gives the average maximum depth of frost penetration measured at each airport under pavement surfaces only. Table 2 gives the average maximum depth of thaw penetration recorded at permafrost sites. Site freezing or thawing indices are also given in these tables.

The freezing index is a measure of the severity of subfreezing temperatures experienced at a site, and it is the most influential climatic factor in predicting the depth of frost penetration. The freezing index is recorded in degree-days and is computed by accumulating from day to day during the freezing season the differences between 32 F (0 C), and the mean daily temperature. The freezing index begins to accumulate in the fall when the mean daily temperature falls below 32 F (0 C) and it reaches a maximum in the spring prior to thaw. The thawing index, which is of use in predicting the depth of summer thaw in permafrost regions, is similar to the freezing index except that it measures the above-freezing temperatures experienced during the summer.

For each set of frost or thaw penetration records, the corresponding freezing or thawing indices were computed from air temperatures recorded approximately 4 ft (1.2 m) above ground level by the Meteorological Branch of the Ministry of Transport. Show depth data were obtained during the winter months for those indicators located

Figure 1. Gandahl-type frost depth indicator (DOT pattern).

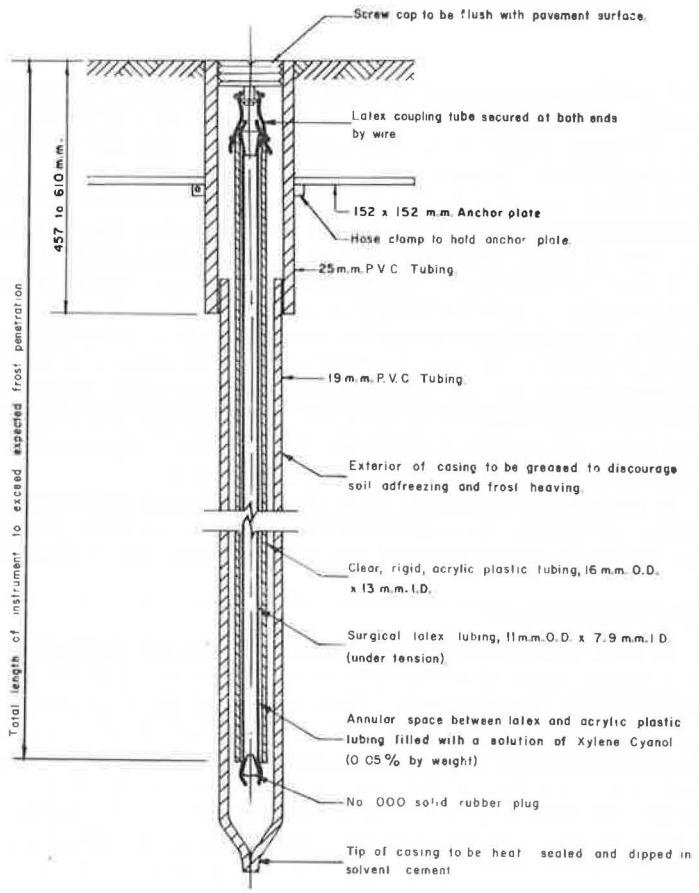

Figure 2. Airports instrumented in frost depth survey.

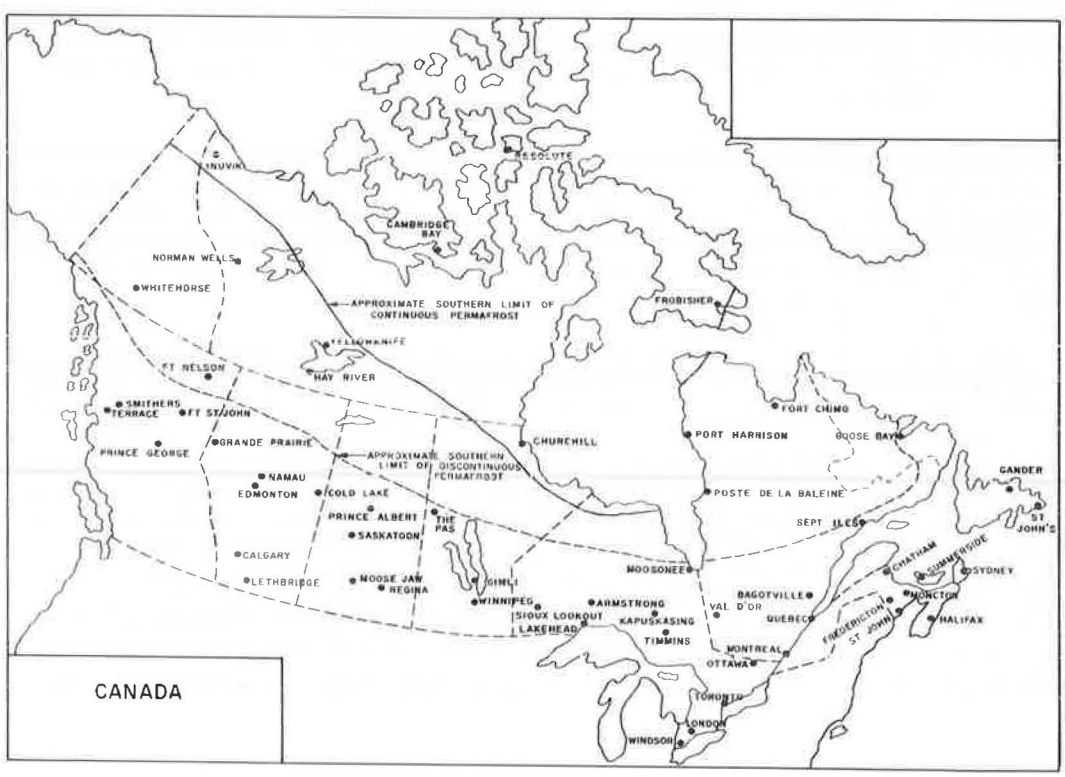

Table 1. Average frost penetrations, 1964-1971.

Seasonal Frost Sites	Number of Years Observed	Average Freezing Index (F degree-days)	Average Frost Penetration (in.)	
			Asphalt-Surfaced Pavements	PCC-Surfaced Pavements
Bagotville, Que.	4	2,840		84
Calgary, Alta.	5	2,067	76	
Chatham, N.B.	1	1,892		78
Cold Lake, Alta.	3	3,549		108
Edmonton, Alta.	6	3,301		87
Fort Nelson, B.C.	7	4,852	129	
Fort St. John, B.C.	1	2,603	112	
Fredericton, N.B.	3	1,573		68
Gander, Nfld.	4	1,092		55
Gimli, Man.	3	3,438	118	
Grande Prairie, Alta.	4	3,545	80	
Halifax, N.S.	4	941		45
Hay River, N.W.T.	2	5,641	140	
Lakehead, Ont.	4	2,833	59	
Lethbridge, Alta.	3	1,511	46	
London, Ont.	1	988	34	
Moncton, N.B.	3	1,366	49	
Montreal, Que.	3	1,730	56	
Moose Jaw, Sask.	4	2,820	102	
Namao, Alta.	3	3,097		106
Ottawa, Ont.	3	1,662	62	
Prince Albert, Sask.	4	4,328	99	
	3	4,139		119
Prince George, B.C.	4	1,757	64	
Quebec, Que.	3	2,290	51	
Regina, Sask.	7	3,488	80	
St. John, N.B.	4	1,401		62
St. John's, Nfld.	4	611	28	
Saskatoon, Sask.	2	3,372	69	
Sept-Iles, Que.	2	2,270	70	
Smithers, B.C.	3	1,780	60	
Summerside, P.E.I.	4	1,209		49
Sydney, N.S.	4	875	36	
Terrace, B.C.	1	1,002	60	
The Pas, Man.	5	4,620	119	
Toronto, Ont.	3	1,022	36	
Val d'Or, Que.	3	3,127	84	
Whitehorse, N.W.T.	7	4,022		127
Winnipeg, Man.	3	3,596	73	
	4	3,762		84
Yellowknife, N.W.T.	2	7,559	169	

Table 2. Average thaw penetrations, 1965-1971.

Permafrost Sites	Number of Years Observed	Average Thawing Index (F degree-days)	Average Thaw Penetrations (in.)		
			Asphalt-Surfaced Pavements	Gravel Surfaces	Undisturbed Natural Surfaces
Cambridge Bay, N.W.T.	3	1,087		57	
Frobisher, N.W.T.	2	1,292	78		
Inuvik, N.W.T.	4	2,053		89	
	5	2,181			53
Resolute, N.W.T.	2	473		26	

in areas with undisturbed snow cover. At the time of installation, bore holes were drilled for soil-sampling purposes. The thicknesses of distinct soil layers were measured and samples were taken for mechanical analysis and determination of moisture content. No density measurements were made.

MAXIMUM PENETRATIONS RELATED TO CLIMATIC INDICES

Frost Penetration in Snow-Cleared Pavements

The depth of frost penetration depends on both climatic factors and soil conditions. However, rough estimates of maximum frost penetration, which are sufficient for some purposes, can be predicted with a knowledge of the air freezing index only. From the data collected at Canadian airports, Figures 3 and 4 show the relationship between these variables for snow-cleared pavements surfaced with asphaltic concrete and portland cement concrete respectively. If the maximum frost penetration in inches is denoted by X and the maximum air freezing index by F (F degree-days), the regression relationships are approximately

Pavement Surface	Equation	Standard Error
Asphalt	$X = -24 + 2.0\sqrt{F}$	15.8 in. (40.1 cm)
Concrete	$X = -10 + 1.9\sqrt{F}$	12.2 in. (31.0 cm)

The negative values at low freezing indices indicate that the air freezing index must reach certain minimum values before frost penetration is experienced. This effect occurs because average pavement surface temperatures are slightly higher than the corresponding air temperatures measured approximately 4 ft (1.2 m) above the ground surface and the freezing index at the pavement surface will lag behind the air freezing index. Due to the black color of asphalt, slight differences also occur in the average temperature of asphalt and portland cement concrete surfaces, which leads to a lesser depth of frost penetration in asphalt pavements than in portland cement concrete pavements for the same air freezing index.

In Figures 3 and 4, a distinction is made between observations in pavements having cohesive subgrades and those having predominantly granular subgrades. Normally, with other factors equal, one would expect deeper penetrations in granular subgrades, but this trend is not noticeable in Figures 3 and 4. Most likely, the influence of subgrade type is not noticeable in Figures 3 and 4 because dense pavement layers are generally thicker on cohesive subgrades than on granular subgrades and because the substantial thicknesses of airport pavements in general tend to attenuate the effects of subgrade type.

Frost Penetration in Undisturbed Snow-Covered Areas

Figure 5 shows the maximum frost penetrations observed in undisturbed snow-covered areas plotted against the maximum air freezing index. Because of differences in the depth of snow cover, these observations are much more variable than those for snow-cleared pavements. However, for design purposes, an upper limit representing the maximum frost penetration that might be expected can be established from Figure 5. The equation, $X = 1.7\sqrt{F}$, describes this upper boundary. The maximum expected penetration occurs when little or no snow cover is present during the freezing season. A comparison of Figure 5 with Figures 3 and 4 shows that the average depth of frost penetration in undisturbed snow-covered areas amounts to approximately one-half the penetration that occurs under snow-cleared paved areas.

The insulating effects of snow cover are shown in Figure 6, where the ratio $X/\sqrt{F}$ is plotted against average depth of snow cover. The points are dispersed because the insulation effect depends not only on the average depth of snow but also on the time of season it is in place and on the snow density. A trend, however, is quite noticeable in Figure 6. Beginning at approximately 1.2, for no snow cover, the proportionality constant between depth of frost penetration and square root of the freezing index decreases with increasing depth of cover to a value of about 0.4 for 2 ft (61 cm) of snow.

Figure 3. Maximum frost penetrations in asphalt-surfaced pavements.

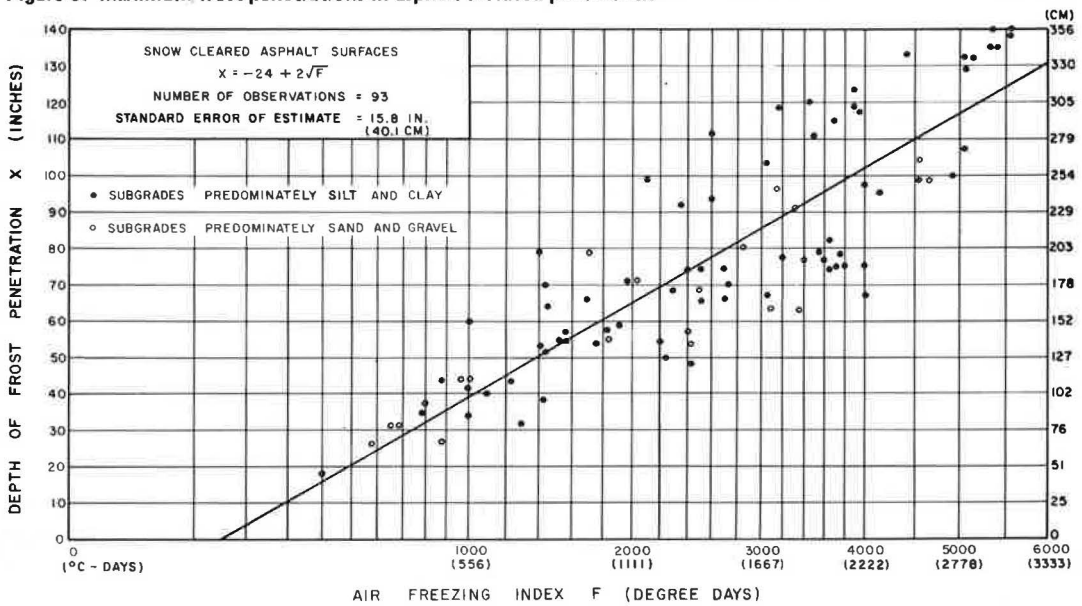

Figure 4. Maximum frost penetrations in PCC-surfaced pavements.

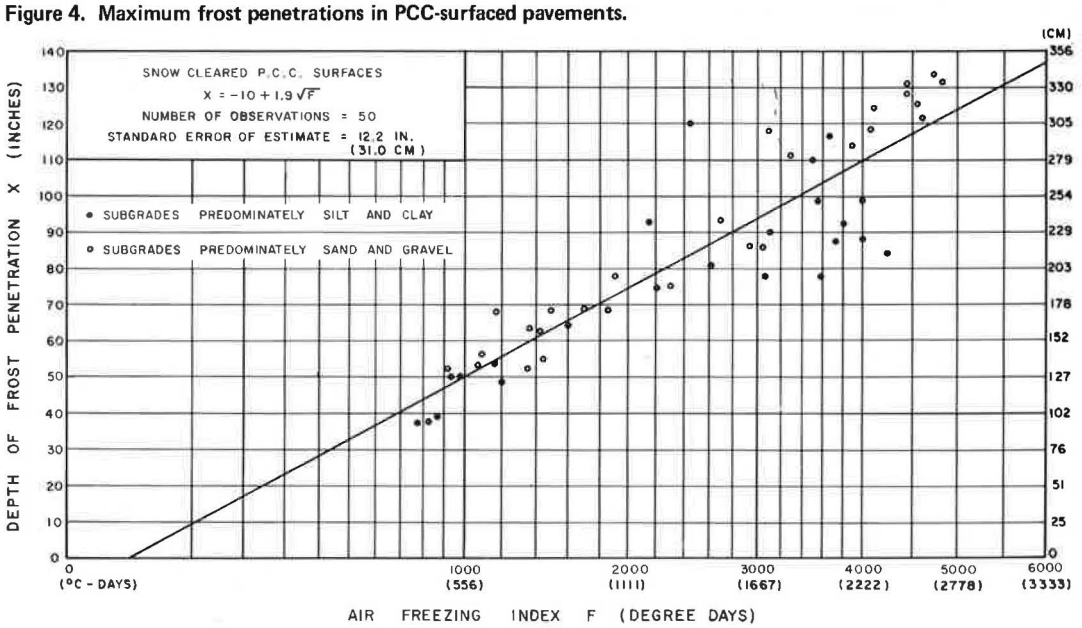

Figure 5. Maximum frost penetrations in undisturbed snow-covered areas.

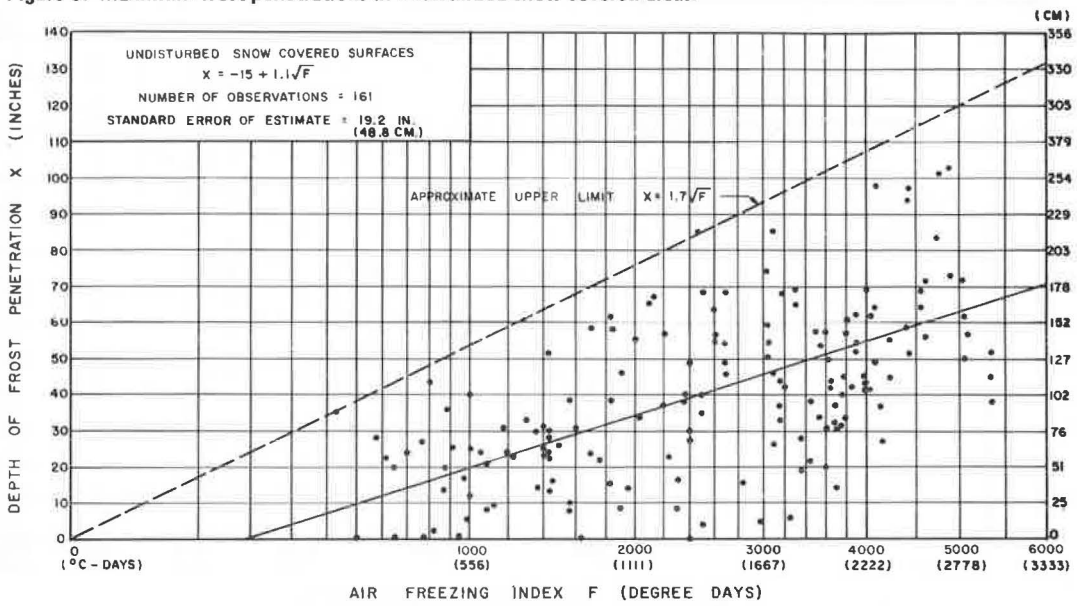

Figure 6. Ratio of $X/\sqrt{F}$ versus average snow cover.

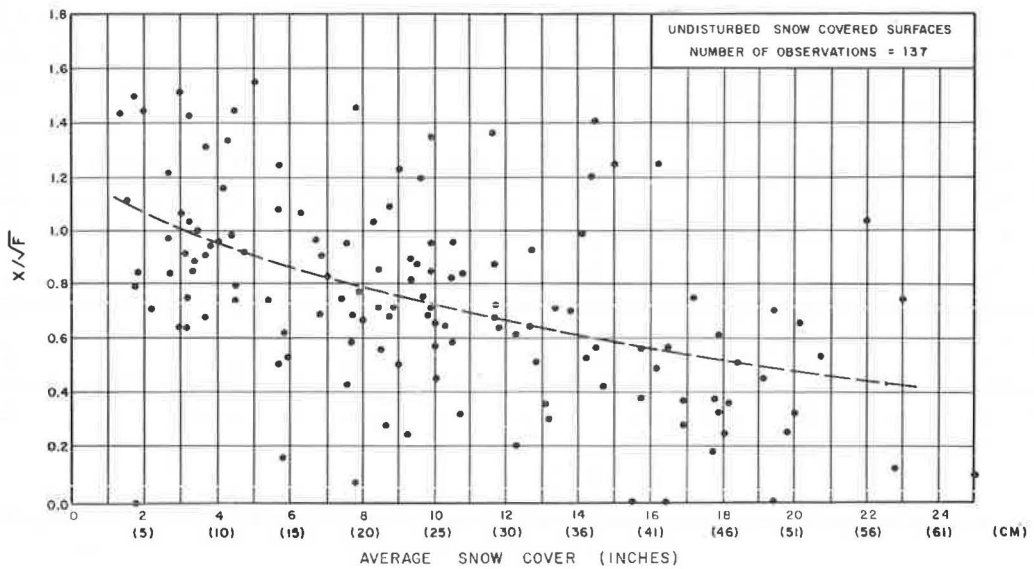

Thaw Penetration in Permafrost

The data obtained from the study on the maximum depth of summer thaw in both asphalt and gravel-surfaced pavements founded on permafrost are limited by the few sites instrumented. The observations recorded for gravel surfaces are plotted in Figure 7 against maximum thawing index on a square-root scale. Figure 7 provides a very approximate indication only of the maximum thaw penetration that might be expected; more measurements are needed to adequately define the relationship.

Figure 8 shows some measurements of maximum thaw depths recorded in undisturbed natural ground areas. Most of these measurements were obtained during a previously conducted program in which maximum thaw depths at a number of northern permafrost sites were established by soundings. Although the thaw depths are quite variable because of variations in soil condition and depth of organic cover, an upper boundary can be established from Figure 8. If the site thawing index is denoted by I, the maximum active layer depth in inches that might be expected at the site is in the order of $1.85\sqrt{I}$.

CALCULATION OF FROST PENETRATION IN PAVEMENTS

Modified Berggren Equation

The theoretical calculation of frost penetration depths is commonly based on the modified Berggren equation (2, 3, 4, 5). The equation may be written in the following form for layered soil systems such as pavements (6, 7):

$$\Delta F_n = \frac{L_n \Delta X_n}{24\,\lambda^2} \left\{ \sum_{i=1}^{(n-1)} R_i + \frac{R_n}{2} \right\}$$

where

ΔF_n = the partial pavement surface freezing index required to freeze the nth layer (F degree-days);
ΔX_n = thickness of the nth layer (ft);
L_n = latent heat of fusion of the nth layer (Btu/ft^3);
λ = correction coefficient based on site soil and climatic factors;
R_i = thermal resistance of the ith layer = $\Delta X_i / K_i$; and
K_i = thermal conductivity of the ith layer (Btu/ft/hour/deg F).

As Figure 9 shows, the total pavement surface freezing index required to freeze n layers in the pavement structure is determined by summing the partial freezing indices, ΔF_n, required to freeze each layer.

Soil Thermal Properties

For use in the modified Berggren equation, the coefficient of thermal conductivity K, latent heat of fusion L, and correction coefficient λ may be estimated from Figure 10. The thermal conductivity values given in Figure 10 were established by Kersten (8). Latent heat of fusion depends on the amount of water in the soil and may be calculated as 1.434 γd Wn, where γd is the dry density of the soil in pounds per cubic foot and Wn is the moisture content in percent. As given by Aldrich (5), the correction coefficient λ is a function of the mean annual temperature experienced at a site, the average freezing temperature, and the soil moisture content. In Figure 10, which gives approximate values for λ, the variables of mean annual temperature and average freezing temperature have been replaced by the site air freezing index by using empirical correlations between these statistics.

Freezing Index Surface/Air Correction Factors

An additional factor entering frost depth calculations is the relationship between pavement surface freezing index and air freezing index. Calculations with the modified

Figure 7. Maximum thaw penetrations in gravel-surfaced runways on permafrost.

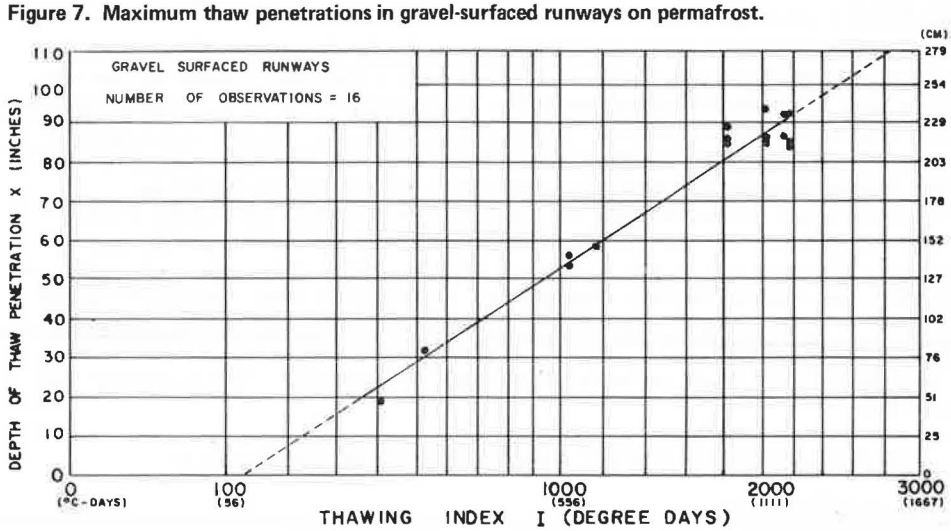

Figure 8. Maximum thaw penetrations in undisturbed permafrost areas.

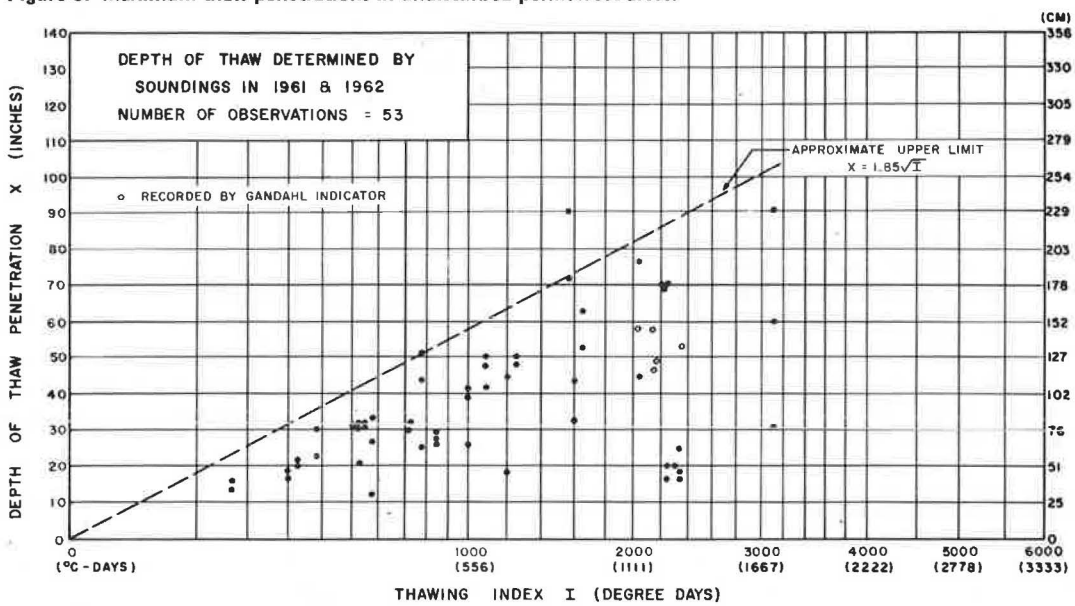

Figure 9. Layered soil system.

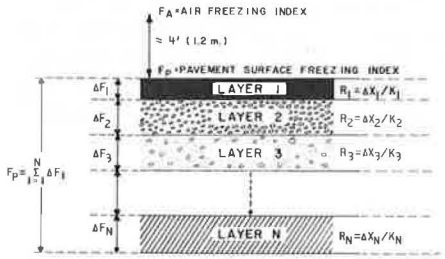

Figure 10. Soil parameters versus moisture content.

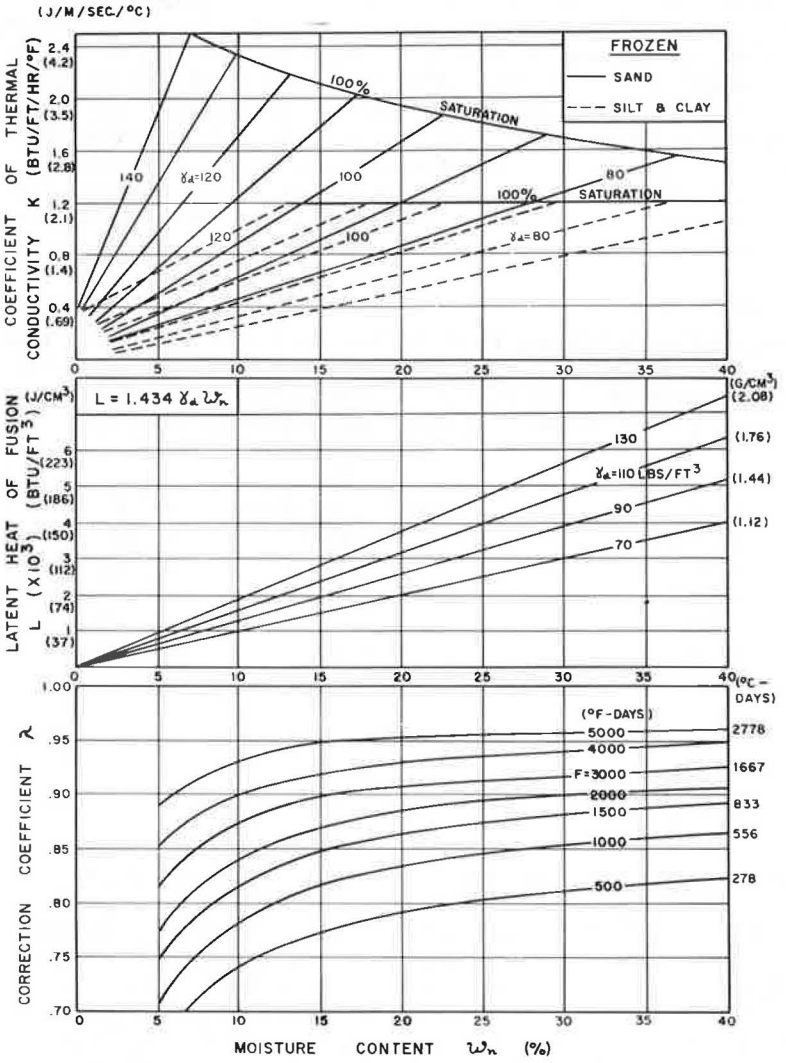

Berggren equation require the use of the pavement surface freezing index whereas the site data available usually consist of freezing indices computed with air temperatures measured 4 ft (1.2 m) above ground surface. Since average pavement surface temperatures are higher than their corresponding air temperatures, it follows that the freezing index of the pavement surface is lower than the air freezing index. As an engineering approximation, the surface freezing index may be estimated by applying a percentage correction factor N to the air freezing index:

$$F \text{ (pavement surface)} = N \times F \text{ (air)}$$

Information concerning surface/air correction factors is quite limited. Sanger (7) reports a value of 0.9 for bare pavements in the northern United States. Carlson (9), based on studies at Fairbanks, Alaska, reports values of 0.77 for portland cement concrete surfaces and 0.72 for asphaltic concrete surfaces.

Surface/air correction factors resulting from the Ministry of Transport's frost depth measurements are shown in Figure 11. The correction factors for each site were calculated by first computing the surface freezing index required to give the measured depth of frost penetration and then dividing this surface freezing index by the recorded air freezing index. For both asphalt and portland cement concrete surfaces, the freezing index surface/air correction factors determined show a tendency to decrease with decreasing site freezing index. Again, due to the black surface of asphalt pavements, the correction is greater for asphalt-surfaced pavements than for portland cement concrete pavements. The correction factor to use for a particular site may be estimated from the curves of Figure 11.

Accuracy of Computed Penetrations

In performing the frost depth calculations, layer thickness and moisture content data were available from bore holes drilled during installation of the frost depth indicators. Soil densities were not known in most cases and had to be estimated. Typical values of densities and thermal characteristics adopted for the calculations were as follows:

Layer	Density, lb/ft^3 (g/cm^3)	W_n, Percent	K, Btu/ft/hour/deg F (J/m/s/deg C)	L, Btu/ft^3 (J/cm^3)
Asphalt	150 (2.40)	1	0.83 (1.4)	Fig. 10
PC	150 (2.40)	1	0.54 (0.93)	Fig. 10
Base courses	140 (2.24)	Measured	Fig. 10	Fig. 10
Sand subgrades	110 (1.76)	Measured	Fig. 10	Fig. 10
Silt + clay subgrades	90 (1.44)	Measured	Fig. 10	Fig. 10

Maximum frost depths calculated were compared with measured values and the standard error of the computed values was of the order of 7 in. (18 cm) for asphalt surfaces and 6 in. (15 cm) for portland cement concrete surfaces. The error would likely have been less if actual soil densities had been available and used in the calculations.

Because the effect of variable soil properties is included, estimates of frost penetration in pavements are more accurate when based on the modified Berggren equation rather than on Figures 3 and 4. The empirical relationships of Figures 3 and 4 are useful, however, because only a knowledge of site air freezing index is required and these indices can usually be estimated for most sites from readily available freezing index contour maps. Subgrade soil conditions, and hence the depth of frost penetration, will vary throughout any stretch of pavement. In addition, the depth of frost penetration at any given location will vary from year to year, depending on the freezing tem-

Figure 11. Freezing index surface/air correction factor.

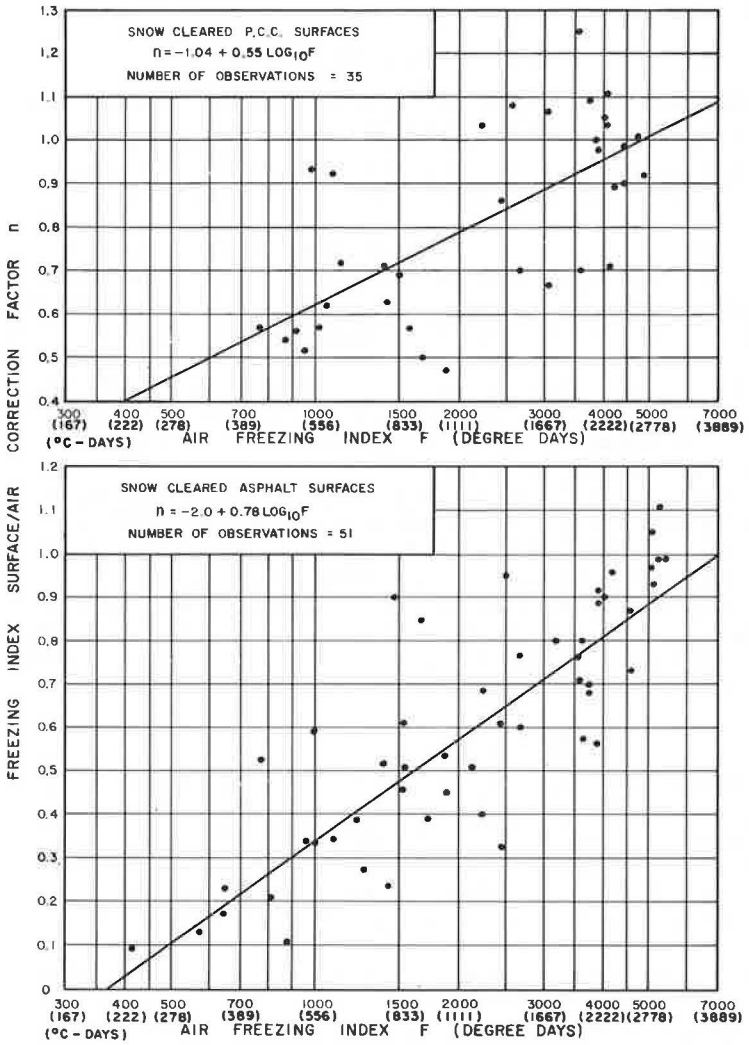

peratures experienced. Because of these variations, the accuracy of estimates obtained from Figures 3 and 4 is often sufficient.

SUMMARY AND CONCLUSIONS

The following conclusions were derived from the frost and thaw measurement program undertaken at Canadian airports from 1964 to 1971:

1. The Gandahl frost depth indicator is a simple, inexpensive device that enables comprehensive surveys to be undertaken in recording the depth of frost and thaw penetrations.
2. With a knowledge of site freezing index only, the maximum frost penetration in snow-cleared pavements can be estimated from the relationships established with a standard error in the order of 12 to 16 in. (30 to 41 cm). Estimates with a standard error of less than 6 in. (15 cm) can be calculated if the necessary soils information is available.
3. The depth of frost penetration in undisturbed snow-covered areas is quite variable due to variations in the depth of snow cover, snow density, and the time of season it is in place. An upper limit, representing the maximum penetration that can be expected, may be estimated from the site freezing index alone.
4. Because of limited data, only a general indication is presently available on the maximum depth of thaw to be expected in gravel-surfaced pavements established on permafrost. However, a limit has been established for the maximum depth of thaw that might be expected in undisturbed permafrost areas with organic cover.
5. The freezing index surface/air correction factor, which must be employed in frost penetration calculations, depends on the site air freezing index. The correction factor decreases with decreasing site air freezing index, and the correction is greater for asphalt-surfaced pavements than for concrete-surfaced pavements.

REFERENCES

1. Gandahl, R. Determination of the Ground Frost Line by Means of a Simple Type of Frost Depth Indicator. Statens Vaginstitut, Stockholm, Rept. 30A, 1963.
2. Berggren, W. P. Prediction of Temperature Distribution in Frozen Soils. Trans., American Geophysical Union, Pt. 3, 1943.
3. Aldrich, H. P., and Paynter, H. M. First Interim Report—Analytical Studies of Freezing and Thawing of Soils. New England Division, Arctic Construction and Frost Effects Laboratory, Boston, 1953.
4. Jumikis, A. R. The Frost Penetration Problem in Highways Engineering. Rutgers Univ. Press, New Brunswick, N. J., 1955.
5. Aldrich, H. P. Frost Penetration Below Highway and Airfield Pavements. HRB Bull. 135, 1956, pp. 124-149.
6. Calculation Method for the Determination of Depths of Freeze and Thaw in Soils. U.S. Corps of Engineers, Engineering Manual, Pt. 15, Chpt. 6, Oct. 1954.
7. Sanger, F. J. Degree-Days and Head Conduction in Soils. Proc., Permafrost International Conf., Purdue Univ., 1963.
8. Kersten, M. S. Thermal Properties of Soils. HRB Special Rept. 2, 1952, pp. 161-166.
9. Carlson, H. Calculation of Depth of Thaw in Frozen Ground. HRB Special Rept. 2, 1952, pp. 192-223.

ADFREEZING OF SANDS TO CONCRETE

J. T. Laba, Department of Civil Engineering,
University of Windsor, Windsor, Ontario, Canada

This paper presents experimental results obtained when the magnitude of the adfreezing force between frozen sands and concrete was investigated under laboratory conditions. Factors influencing the magnitude of the adfreezing force, called frost-grip, are introduced and discussed. Three different sands were used to provide more information relating to the influence of the sand's physical properties—i.e., particle shape, size, and gradation—on the magnitude of frost-grip. A simplified general equation to predict the values of the adfreezing force valid for all three sands is introduced as a function of five parameters.

•IN AREAS subject to temperatures below freezing, "frost-grip" between frozen soil and the material with which it comes in contact is a common occurrence. Researchers studying this phenomenon of frost-grip or adfreezing of soil to foundation units were mainly concerned with its contribution to the possible damage done to structures due to frost heaving (1, 2, 3). Their attention therefore was limited to frost-susceptible soils only. As a consequence, the effect that a frozen soil layer, even when non-frost-susceptible, can have on the stability of retaining walls, foundations, or any other structure was generally overlooked.

To avoid frost heave, non-frost-susceptible granular soils are used by many engineers as a select material in areas subject to frost action. Sandy soil when moist will adhere to concrete surfaces upon freezing. Consequently, this bonding force, referred to as frost-grip, will resist independent vertical movement of the unheated part of any structure or of the frozen soil layer. The frozen sand layer thus bonded to the structure could retard settlement of the unheated part of the structure during the winter months or, in the case of retaining walls, could provide a resisting force that must be overcome before failure of the wall could occur. In the latter case, frost-grip force could counteract the additional overturning force, i.e., the lateral thrust developed in a sand-ice layer due to temperature change that was discussed previously by the author (4, 5). For such cases, the knowledge of the magnitude of the frost-grip (even if obtained under laboratory conditions) and the parameters on which it may depend is of considerable importance and therefore was the main purpose of this investigation.

It was suspected that the magnitude of frost-grip that could be developed by frozen granular soils would be mainly the function of the following parameters: ice content, porosity, temperature, and particle shape, size, and gradation. Experiments were carried out to obtain comparable values of the frost adhesive force between frozen sands and concrete surfaces for various combinations of these variables. Three different sands were used in the investigation to provide more information relating to the effect of particle size, shape, and gradation. To avoid the effect of time-dependent creep or relaxation on measured frost-grip, the rupture strength developed between soil and concrete was measured under rapid loading. It is beyond the scope of this paper to also include the long-term loading effect on the magnitude of the adfreezing force, and therefore the frost-grip discussed represents the instantaneous adhesive force measured under rapid loading.

Publication of this paper sponsored by Committee on Frost Action.

SOILS STUDIED

Three different types of sand were used in the experimental investigation. Sand No. 1 was a crushed uniform sand from Ottawa, Illinois (uniformity coefficient 1.5 and specific gravity 2.65). Sand No. 3 was a natural variety of well-graded sand from Paris, Ontario (uniformity coefficient 3.8). Sand No. 2 (uniformity coefficient 2.85) was obtained from sand No. 3 mainly by eliminating the soil grains larger than 3.3 mm and smaller than 0.104 mm. Specific gravity for both sands No. 2 and No. 3 was virtually the same, 2.67. The grain size distributions are shown in Figure 1.

EXPERIMENTAL TECHNIQUE AND PROCEDURE

The experimental technique for measuring the frost-grip between the sand-ice system and concrete was as follows: The known weight of dry sand and required amount of water were thoroughly mixed together to give the desired water content of 5, 10, or 15 percent. The prepared soil was then placed in the hollow core of a concrete mold, shown in Figure 2, and compacted in the majority of cases by a manually operated standard Proctor hammer. The concrete molds were moistened before the specimens were compacted into them. To obtain a porosity range as wide as possible, the compaction effort was varied from zero blows (the soil being pushed in by a trowel and gently pressed by a mallet) to 50 blows (each of 5 layers being struck 10 times by a standard Proctor hammer). Further decrease in porosity was achieved by subjecting some of the specimens to vibration; this procedure was chosen because it eliminated the possible crushing of the sand particles under an increased compaction effort. During compaction, representative soil samples were taken from each mold for the purpose of determining the water content.

It has been indicated by Tsytovich (6) that in granular soils unfrozen water content is negligible; therefore, the ice content in each frozen specimen was assumed to be equal to its water content measured before freezing took place. Degree of ice saturation, however, was based on 9 percent volume expansion of the pore water upon freezing.

When preparing specimens for a high degree of ice saturation, a layer of heavy waxed paper was glued to the bottom of each mold to prevent water loss from the sand samples. The temperature of each sample was measured by means of two copper-constantan thermocouples placed in the specimen at two different levels—1 in. (2.54 cm) below the top surface and 1 in. from the bottom—and connected to the potentiometer through a multipolar rotary switch.

The filled molds were placed in the freezing chamber along with steel punch-out plates, and after completion of the necessary wire connection to the temperature potentiometer the specimens were frozen to the required temperature.

While in the freezer only the top of each soil sample was exposed to the atmosphere; the sides of each concrete mold were insulated and the bottom rested on a $1\frac{3}{4}$-in. (4.5-cm) thick wooden board covered with a layer of heavy waxed paper. Under these conditions, the specimens were subjected to unidirectional freezing, since the wooden board acted as insulation. The bottom insulation of soil samples changes the freezing pattern from that existing in nature because it prevents the upward flow of heat and moisture toward the cold front. All sands investigated were subjected to the same freezing pattern, and therefore comparable sand-ice specimens were obtained. Furthermore, the "closed" system used permitted easy preparation of the samples with the desired ice content, one of the most important parameters influencing the magnitude of frost-grip.

Before each test, the frozen samples were left at a selected constant temperature for not less than 6 hours to ensure uniform temperature distribution throughout the frozen sand-ice specimens. After that, specimens were removed from the freezer and placed in the compression tester one at a time. They were loaded quickly to avoid excessive plastic flow; the selected constant rate of induced deformation was 0.05 in./minute (0.12 cm/minute). This rate of loading corresponds to ASTM test method D 1633-63, recommended for determining the compressive strength of molded soil-cement cylinders. The ultimate force required to free the sand-ice core from the concrete mold was recorded; this, when divided by the surface contact area between specimen and concrete (measured at the time of failure), gave the frost-grip. It was observed that the decrease in height experienced by the sand-ice specimen during testing rarely exceeded 0.1 in. (0.25 cm).

Figure 1. Grain size distribution.

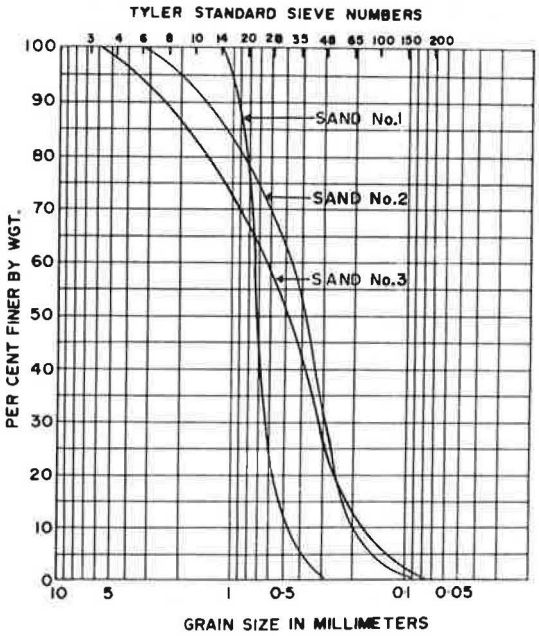

Figure 2. Dimension of molds and schematic testing arrangement.

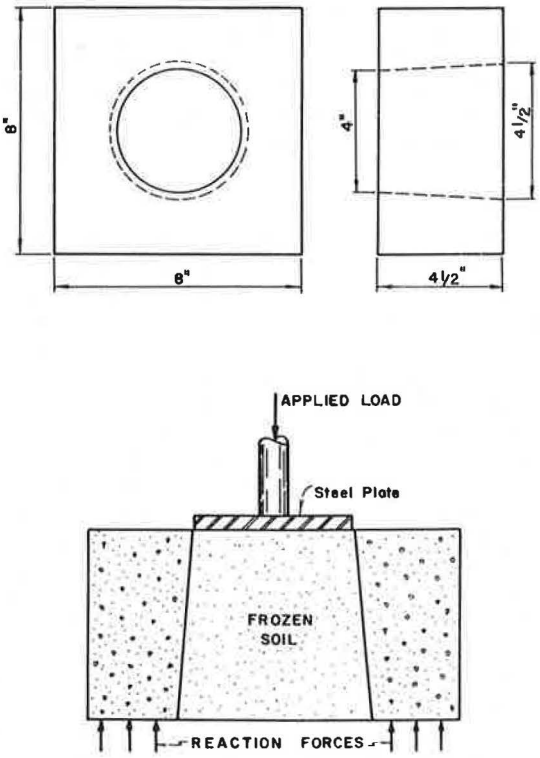

Figure 3. Frost-grip versus porosity for 5, 10, and 15 percent ice content: Sand No. 1, temperature 0 F.

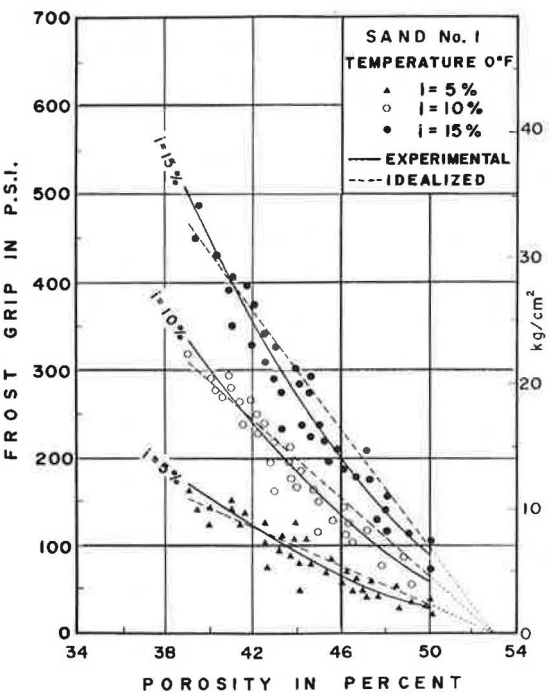

Figure 4. Frost-grip versus porosity for 5, 10, and 15 percent ice content: Sand No. 2, temperature 0 F.

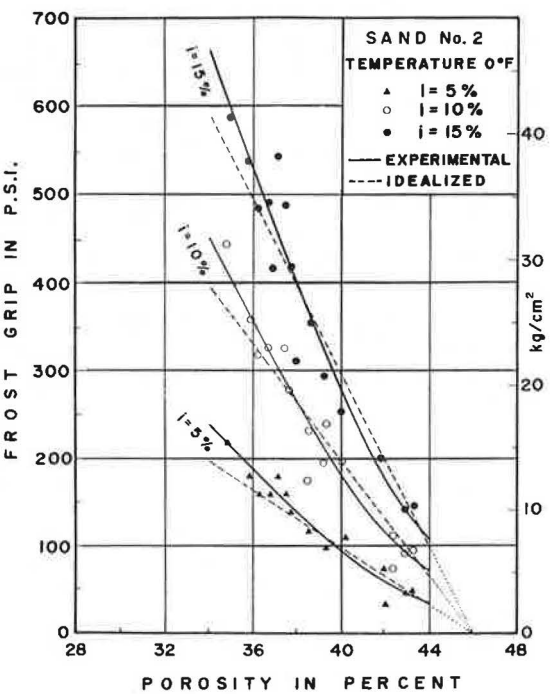

At this point it should be mentioned that the vertical deformation of 0.1 in. would reduce the effective frozen sand-concrete contact area by only 2 percent.

The molds were made of a rich concrete mix for increased strength and durability; the proportions were 1 part cement, 1 part sand, and 1 part $\frac{3}{8}$-in. (0.95-cm) crushed stone, with water added to give good workability. This mix provided a compressive strength of over 5,000 psi (34 500 kPa), using 3 in. × 6 in. (7.6 cm × 15 cm) test cylinders cured under water at room temperature for 28 days. No mold was used more than ten times, to preserve uniformity in the roughness of the concrete surface.

DISCUSSION OF RESULTS

Experimental results confirm that the parameters under investigation, namely, the sand porosity, n; ice content, i; temperature, T; and type of sand (defined by its origin; uniformity coefficient, U; and particle shape and size), have a significant effect on the magnitude of the adfreezing force, F. Graphs were plotted to obtain the relationship between these individual variables and frost-grip.

Figures 3 through 6 show the effect of porosity on the magnitude of frost-grip for three different constant values of ice content, i.e., 5, 10, and 15 percent. The type of sand used and the temperature of tested sand-ice specimens are indicated in each figure. All experimentally obtained curves show a rather rapid decrease in frost-grip stress with the increase in porosity. The rate of decrease in frost-grip is the largest at lower levels of the practical porosity range (where the curves are almost straight lines) and the smallest at the other end of the porosity range, where the highest values of obtained porosity are recorded. The nonlinearity shown by the F versus n curves can be attributed partly to the nonlinear change in degree of ice saturation resulting from changes in the sand's porosity under conditions of constant ice content.

Because the porosity in which all sands in nature are found is small, the F versus n curves can be reasonably approximated by straight lines converging at a point on the porosity axis, as shown by dotted lines in Figures 3 through 6. This idealization is done with the view to obtaining a simpler and more easily usable mathematical relationship between frost-grip and the related variables.

The convergence of the F versus n idealized lines at a point on the porosity axis suggests that every investigated type of sand has its own theoretical limiting value of porosity, above which no frost-grip will develop. On the other hand, the experimental curves, if extended to the level of intercept porosity, would indicate some small value of frost-grip. The error resulting from this difference is not important, because in all cases the intercept porosity was found to be outside the practically obtained porosity range.

Figures 3 through 6 also show that an increase in ice content results in a considerable increase in frost-grip for any constant porosity. It can be observed that frost adfreezing stress developed by a frozen sand is directly proportional to its ice content and therefore to its ice saturation. This manifests itself in the fact that at a given constant porosity the vertical distances between experimental curves representing 5, 10, and 15 percent ice content are practically equal.

Figure 7a shows a typical relationship between frost-grip and ice content obtained for three investigated sands all having the same porosity, n = 40 percent, and the same temperature, T = 0 F (-17.8 C). It should be noticed that crushed uniform Ottawa sand, referred to as sand No. 1, developed the largest frost-grip, followed by natural, medium-graded and well-graded sands No. 2 and No. 3 respectively. The combined effect of porosity and ice content on the magnitude of frost-grip obtained for sand No. 1 at the constant temperature of 0 F is shown in Figure 7b.

The three investigated sands, when compared at the same temperature, water content, and porosity, show a significant difference in the magnitude of the frost-grip developed. This leads to the conclusion that the frost-grip between frozen sand and concrete is influenced not only by the ice content (or degree of ice saturation) but also by the physical properties of the sand, i.e., the particle shape, size, and gradation.

When the concrete surface and frozen sand layer are forced to move vertically in respect to each other, it can be expected that not only shearing of the ice adhered to the concrete takes place but also some shear deformations in the sand's mineral skeleton. Therefore, it is not only the ice that comes in contact with the concrete surface that

Figure 5. Frost-grip versus porosity for 5, 10, and 15 percent ice content: Sand No. 3, temperature 0 F.

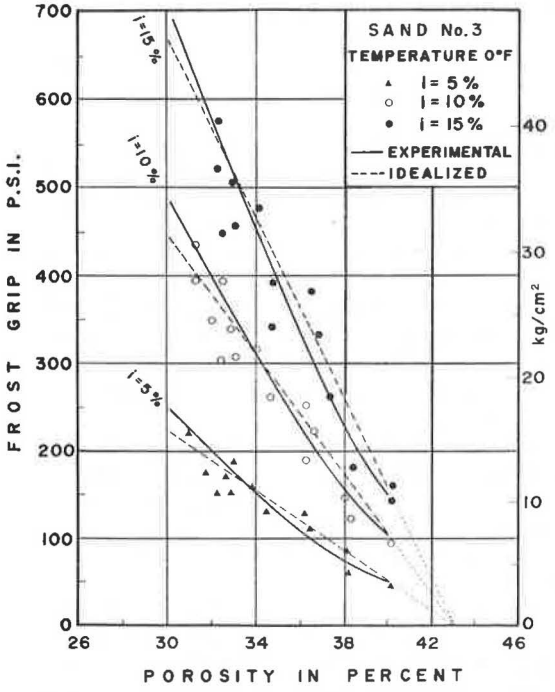

Figure 6. Frost-grip versus porosity for 5, 10, and 15 percent ice content: Sand No. 2, temperature 30 F.

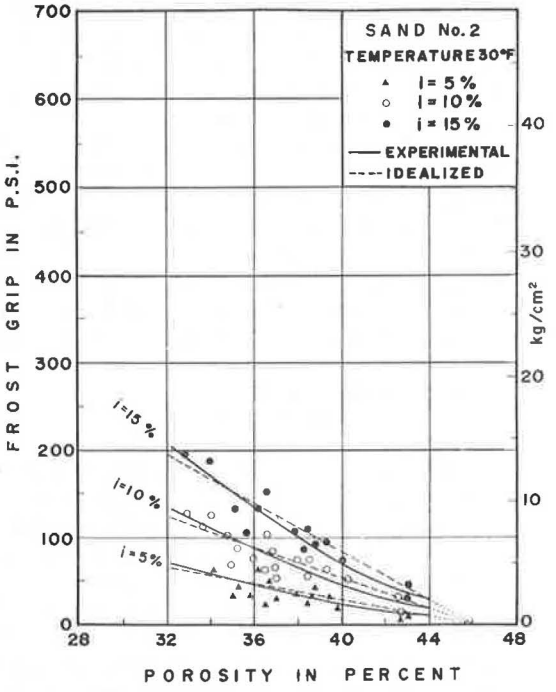

Figure 7. Frost-grip versus ice content: (a) Three investigated sands at porosity 40 percent and temperature 0 F; (b) Sand No. 1 at four different porosities and constant temperature 0 F.

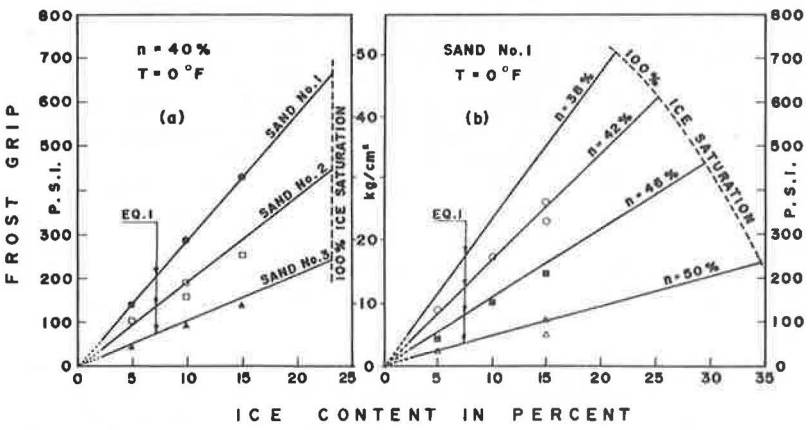

contributes to the frost-grip magnitude but also, to some extent, the ice that binds the sand particles together. Furthermore, in the specific case of sand No. 1, the large number of angular particles lodged in the concrete surface and forced to move while bound by ice contributed to the high results given by that sand. Visual inspection conducted after the testing of the specimens confirmed (especially in the case of sand No. 1) that some sand particles were forced to move or were broken off from the sand-ice surface during the testing.

In general, when comparing at the same porosity any three corresponding F versus n curves (the same temperature and ice content but different sand) shown in Figures 3 through 5, it can be observed that the sand's physical properties—dense packing, angular shape, and uniform particle size—contribute to the high values of frost-grip. On the other hand, loose packing, rounded shape, and nonuniform particle size have the opposite effect on the magnitude of frost-grip.

Figure 8 shows the effects of temperature on the frost adfreezing stress developed by the three investigated sands. The frost-grip increases with a decrease in temperature, the rate of increase being greatest close to the freezing point. The effect of temperature change on the magnitude of frost-grip is more pronounced in sands having a high ice content than in those having a low ice content.

Because the soil pore water increases its volume when converted to ice, it was considered desirable to study the effect that the rigid concrete molds may have on the magnitude of frost-grip, especially when investigating saturated or nearly saturated specimens. Therefore, in addition to the previously described solid samples obtained by packing moist sand into the hollow concrete mold, samples with a vertical hole in the middle and split concrete molds were introduced.

The samples with a hole were obtained by placing vertically in the middle of each mold a flexible rubber tube of 1.25 in. (3.175 mm) outside diameter pulled over an aluminum pipe. The area between the rubber tube and concrete mold was filled with moist sand, the sand was compacted, and the sample was placed in the freezer. Afterwards, the aluminum pipe was withdrawn, and the rubber tube left inside was packed loosely with insulating material. In the case of water-saturated or nearly saturated sands, this created favorable conditions for the possible outflow of excess pore water resulting from water expansion at freezing.

Split samples were obtained by cutting concrete molds in half vertically and placing them individually into a heavy steel frame. An impervious membrane was attached to the bottom and sides of each concrete mold to keep the water inside the sand samples. Two horizontal bolts passing through one side of the steel frame were designed to keep two halves of the mold tightly pressed together during the compaction of the specimen. The bolt pressure on the mold was released in the freezer after freezing of the specimen took place. Later, during testing, the bolts were used to support the concrete mold to prevent free lateral expansion during extraction of the sand-ice core.

The results obtained are shown in Figure 9, which indicates that, as long as the volume of ice formed is equal to or less than the volume of voids in the sand, there is no significant difference between frost-grip values obtained when using solid samples, samples with a vertical hole, or samples tested in a split mold. Therefore, it can be concluded that the rigidity of concrete molds did not influence the magnitude of frost-grip by any significant amount.

FROST-GRIP EQUATIONS

Referring to the idealized F versus n straight dotted lines shown in Figures 3 through 6, the magnitude of frost-grip can be expressed by the general equation

$$F = m (N - n) \tag{1}$$

where

F = frost-grip, in psi;
m = slope of the idealized F versus n line representing constant water content, in psi/percent;

Figure 8. Frost-grip versus temperature for three sands having ice content of 5, 10, and 15 percent.

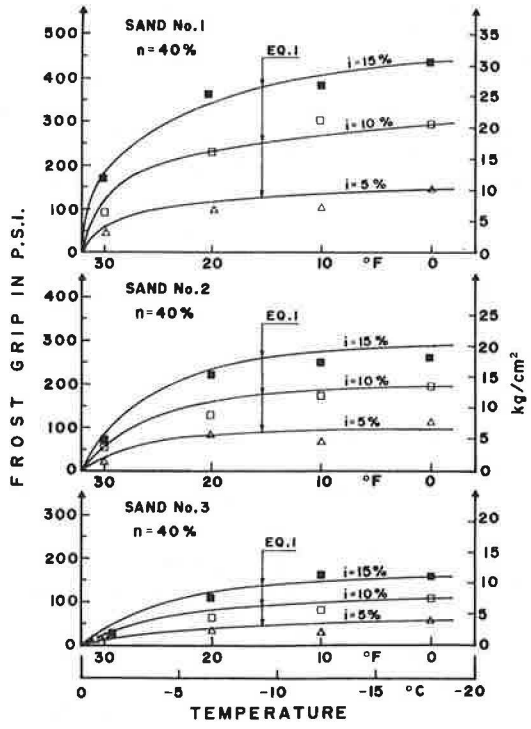

Figure 9. Frost-grip versus water content: Comparison of results using varied techniques.

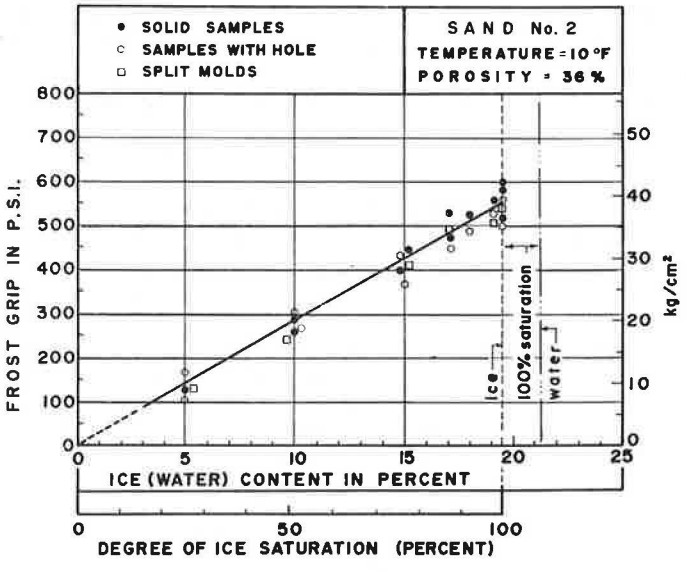

n = porosity, in percent; and
N = the intercept on the porosity axis at F = 0, referred to as "terminal porosity", in percent.

Based on experimental results, the values of slope m and terminal porosity N can be expressed in the form of the following empirical equations, derived by searching systematically for unknown functions by means of an electronic computer:

$$m = A\, i\, (32 - T)^{0.25} \tag{2}$$

valid for T < 27 F (-2.8 C), and

$$N = (1.0414 - 0.0053 \log_{10} U)^{100} \tag{3}$$

where

A = adfreezing factor, in psi/percent^2;
i = ice content, in percent;
U = uniformity coefficient of sand; and
T = temperature, in deg F.

Values of A and U can be found experimentally for any particular sand. The values of A and U obtained for three investigated sands are as follows:

Sand	Type	A	U
Sand No. 1	Crushed, uniform	0.95	1.5
Sand No. 2	Natural, medium-graded	1.40	2.85
Sand No. 3	Natural, well-graded	1.45	3.8

However, at temperatures near the freezing point, the adfreezing factor A was found to be somewhat lower in value and constant for all three sands. The value of A for temperatures between 27 F and 32 F (-2.8 C and 0 C) was found to be 0.79; hence the values of m in this temperature range can be expressed by

$$m = 0.79\, i\, (32 - T)^{0.25} \tag{4}$$

In the sands investigated, the relationship between ice content i (or water content w) and degree of ice saturation S_i can be expressed as

$$i = w = 0.917\, S_i\, n/G\, (100 - n) \tag{5}$$

where G = specific gravity of sand and n = porosity, in percent.

Thus, when the values of the adfreezing factor and uniformity coefficient are known for a given sand, then for any particular case of porosity, ice content, and temperature, the frost adfreezing stress can be calculated from the equations introduced. All idealized F versus n dotted lines representing various ice contents shown in Figures 3 to 6, and also the curves shown in Figures 7a, 7b, and 8, were obtained by using Eq. 1.

CONCLUSIONS

The ice content of a sand is one of the major factors influencing resultant frost-grip that can be exerted by that sand. The relationship is linear: For an ice content of zero percent there is no frost-grip and for an ice content greater than zero, the attendant frost-grip is directly proportional to the ice content.

The temperature of the sand-ice system has a significant influence on the magnitude of frost adfreezing. The frost-grip increases with a decrease in temperature, the rate of increase being the largest just below the freezing point. A change in temperature will produce larger changes in the frost-grip magnitude in sands having a high ice content (or degree of ice saturation) than in those having a low ice content.

Particle shape, size, and gradation also exert influence on the frost-grip. An angular particle will give higher results than a rounded particle. Under conditions of equal porosity, ice content, and temperature, uniform sand will develop higher frost-grip than well-graded sand.

ACKNOWLEDGMENT

This work was supported financially by the National Research Council of Canada.

REFERENCES

1. Saltykov, N. I. Calculating Frost Heaving Forces on Foundations. Izvestiia Akademii Nauk SSSR, Otdelenie Tekhnickeskikh Nauk, No. 6, Translation 46 (Peel, Jaroslov J., translator), SIPRE Bibliography Proj., Library of Congress, 1944, pp. 305-412.
2. Trow, W. A. Frost Action on Small Footings. HRB Bull. 100, 1955, pp. 22-35.
3. Penner, E., and Gold, L. W. Transfer of Heaving Forces by Adfreezing to Columns and Foundation Walls in Frost-Susceptible Soils. Canadian Geotechnical Jour., Vol. 8, No. 4, 1971, pp. 514-526.
4. Laba, J. T. Lateral Thrust in Frozen Granular Soils Caused by Temperature Change. Highway Research Record 304, 1970, pp. 27-37.
5. Laba, J. T., and Aziz, K. A. Pressure-Time Relationship in Laterally Stressed Frozen Granular Soils. Highway Research Record 393, 1972, pp. 79-87.
6. Tsytovich, N. A. Bases and Foundations on Frozen Soil. HRB Spec. Rept. 58, 1960, 93 pp.

MOISTURE VARIATION IN HIGHWAY SUBGRADES AND THE ASSOCIATED CHANGE IN SURFACE DEFLECTIONS

Gaylord Cumberledge, Gary L. Hoffman, Amar C. Bhajandas, and Ronald J. Cominsky,
Bureau of Materials, Testing, and Research,
Pennsylvania Department of Transportation

The objectives of this research are to determine the influence of subgrade moisture conditions on surface deflections and to develop a means of predicting relative changes in surface deflections from variations in pertinent pavement system properties. Five field test sites were established and pertinent data were collected for 3 years. A multilinear regression analysis technique was used to determine the relationship between the dependent variable (percent changes in surface deflection) and selected independent variables. Surface deflections are significantly influenced by changes in pavement surface temperature and subgrade moisture. A predicting equation for relative changes in surface deflections from pertinent pavement system properties is developed.

•THE seasonal change in moisture content of subgrade soils with its resultant effects on structural pavement performance is an area of interest to many highway engineers. It is well documented in the literature that the shearing strength of a subgrade soil can be greatly reduced by the influx of moisture during spring thaw or long periods of heavy rainfall (1, 2, 3, 4). This reduction in strength is generally attributed to an increase in moisture content of the subgrade soil resulting in high excess pore pressures between the soil particles and sometimes an associated decrease in soil density. Consequently, the bearing capacity of the subgrade will also be reduced significantly, and extensive deflection of the pavement may result (4, 5, 6, 7).

It is generally accepted that, in fine-grained soils, the shearing strength and bearing capacity of a subgrade reach their lowest value at the beginning of the thawing period in the spring when the excess pore pressures reach a maximum (4, 7, 8, 9). During this time frost boils, pumping, and pavement breakup may occur under a moving load (9). The excess pore pressures will gradually decrease with time, and consequently the subgrade will gradually gain in strength (4). An equation has been developed for the purpose of predicting seasonal changes in pavement surface deflections.

PROCEDURE OF THE INVESTIGATION

Field Sites and Data Collection

For this study, field test sites were selected throughout Pennsylvania. Five of the sites were flexible and three were rigid. Pits 3 ft (0.91 m) wide by 4 ft (1.21 m) long by 5 ft (1.52 m) deep were opened in the center of one of the travel lanes for the purpose of installing thermocouples and moisture cells. Moisture contents, densities, liquid limits, plastic limits, and gradations of all pavement materials were determined by the appropriate ASTM or AASHO standard test. In addition, the thicknesses of the pavement layers were measured.

Type T thermocouples (copper-constantan) from Omega Engineering, Inc., with an error tolerance of ±0.75 F (0.41 C) were employed in this study to monitor temperature fluctuations. Continuous readout was supplied by Esterline Angus Corporation Model

Publication of this paper sponsored by Committee on Environmental Factors Except Frost.

E1124E Multipoint Recorders, which cycle every 15-20 minutes, depending on the number of thermocouples in the pavement profile. The surface thermocouple was placed 0.25 in. (0.63 cm) from the surface of the wearing course to protect it from traffic damage. In addition, thermocouples were placed at the interface and midpoint of the surface, base, and subbase layers and every 6 in. (15.24 cm) into the subgrade to a depth of 5 ft (1.52 m).

The moisture-sensing devices consisted of Soiltest Model MC-310A fiberglass soil-moisture cells constructed of two Monel screen electrodes separated by and encased in a wrapping of fiberglass fabric. The units also contained thermistors, which were employed as a check against thermocouple readings, for monitoring temperature. A Soiltest Model MC-300A moisture meter was used to monitor the changes in electrical resistances with associated moisture changes. Calibration of the cells was done essentially by the method proposed by Turner and Jumikis (9). The cells were placed at the same elevations in the pavement profile as the thermocouples, except none were placed in the pavement surfaces.

Deflections were taken on the pavement surface using a Model RR-400 Road Rater manufactured by Foundation Mechanics, Inc. Attached to the front end of a vehicle, the Road Rater consists of a steel mass, hydraulic vibrator, and deflection sensors. The 160-lb (72.6-kg) mass was oscillated at 25 Hz. Pavement displacement, measured by deflection sensors, is clearly displayed on instrumentation located inside the supporting vehicle, adjacent to the operator. The methods of calibration and data collection are explained in detail elsewhere (5).

Data collection at all of the sites consisted of obtaining the moisture and temperature readings in the pavement profile and the associated surface deflection readings at points (2,5), (2,7), and (4,6) as shown in Figure 1. In addition, the accumulated monthly precipitation data were acquired from adjacent Weather Bureau stations. These data, plus the engineering index properties and thicknesses of the pavement layers, were then used in the analysis of the changes in deflections with time at the experimental field sites.

Variables Considered in This Study

A number of authors (3, 6, 10, 11, 12) have recognized the following variables to be contributing factors in the percentage change in subgrade support during the spring-thaw period: moisture content, temperature, density, liquid limit, plastic limit, plasticity index, gradation of the subgrade soil, and thickness of pavement section.

The primary factors of interest in determining the percent change in surface deflection (which can be related to subgrade support), as shown in the literature (4), are the changes in moisture content (ΔMC) of the subgrade and the temperature ($\Delta \bar{T}$) of the pavement surface. As indicated in the literature (12), the thickness of the various pavement layers (D_p) determines the relative stiffness of the pavement acting as a whole. Logically, therefore, these terms must be included as independent terms in predicting changes in surface deflection. Moreover, the nature of the subgrade soils as reflected by their engineering index properties—particle size distribution, liquid limit (LL), plastic limit (PL), plasticity index (PI), and density (γd)—significantly influence the overall pavement deflection. Consequently, a statistical mathematical model for establishing the prediction of percent change in deflection must compensate for different soil types.

In this investigation all the previous parameters were studied. The percentage change in surface deflection is expressed as

$$\Delta\delta = \frac{\delta - \delta_{min}}{\delta_{min}} \times 100 \qquad (1)$$

where $\Delta\delta$ = percent change in deflection from the minimum deflection (δ_{min}) and the deflection (δ) at any date. Likewise,

$$\Delta MC = \frac{MC_{\delta} - MC_{\delta min}}{MC_{\delta min}} \qquad (2)$$

where ΔMC = percent change in moisture content from the moisture content that corresponds with the minimum deflection ($MC_{\delta_{min}}$) and the moisture content associated with the deflection at any date (MC_{δ}). The particle size distribution or gradation of the subgrade soil is represented by the percent passing the No. 4 and No. 200 sieves.

RESULTS AND ANALYSES

Subgrade Moisture

Figure 2 shows the average change in actual subgrade moisture content as indicated by moisture data from 8 different sites and for the years 1970 through 1973. In addition to the 5 flexible pavement sites used in the deflection analyses, 3 rigid pavement sites are also included to arrive at these subgrade moisture change curves. It is presumed that the type of pavement surface has no significant effect on subgrade moisture variation as long as an adequate seal exists against vertical moisture movement through the surface. The sand curve is comprised of data from the Lairdsville, Wellsboro, and Wilkes-Barre sites, which have an A-2-4 subgrade soil classification. Data from the Clarion, Lantz Corners, and Meadville sites, which have an A-4 subgrade soil classification, make up the silt curve. State College and Washington sites, which have an A-7 and A-6 subgrade soil respectively, provide data for the clay curve.

It can be readily seen that all three subgrade soil types experience the greatest increase in moisture content in March and April. The sand soils show the greatest increase in moisture (3 to 4 percent) as compared to increases of 2 to 3 percent for silt soils and only 1 percent for clay soils. As anticipated, the increased moisture content in the sands drops back to a base level at a faster rate than do the silts. All subgrade soil types perennially reach a base level or minimum moisture content by September and October. The subgrade moisture variation, which occurs throughout the entire instrumented depth of 5 ft (1.52 m), can be associated with lateral movement from the shoulders, fluctuation in the water table and capillary zone, and, to a somewhat lesser degree, infiltration through surface cracks.

Influence of Temperature on Pavement Deflections

Among the variables that affect the deflection of a pavement is the temperature of its surface course. This variable could be included in the multiple linear regression program; however, it can be isolated from the other variables principally for two reasons:

1. A related study (5) by the authors has already established the relationship between the temperature of a pavement's surface course and its surface deflection; and
2. A better insight into the influence of all other variables can be attained.

To eliminate the influence of temperature on surface deflections, all readings must be corrected to some standard value. In this study a base temperature of 60 F (15.56 C) is used. Hence, the actual surface deflection values shown in the third column of Table 1 are corrected to values based on pavement surface temperature of 60 F using the appropriate temperature adjustment factor from Figure 3. This linear equation is developed by regression analysis of data recorded at two sites with similar subgrade soil during a period when the moisture remained unchanged.

Seasonal Relationship of Deflection, Moisture, and Precipitation

The effect of subgrade moisture variation on the change in corrected surface deflection is shown in Figures 4 through 8. A definite relationship between moisture and deflection is apparent. A corresponding increase in surface deflection generally occurs with an increase in subgrade moisture, except during winter months when deflections are constant because of the frozen conditions of both the pavement and the subgrade.

A comparison of monthly precipitation with moisture variation indicates erratic peaks and no definite increases in moisture due to periods of heavy rainfall. In some instances, however, points of maximum subgrade moisture are preceded by a few months by periods of high precipitation. It is also noted that after October the subgrade moisture content tends to increase each month during the winter up to a maximum in March or April. This trend was also found by Yao and Broms (4).

Figure 1. Plan view of test site.

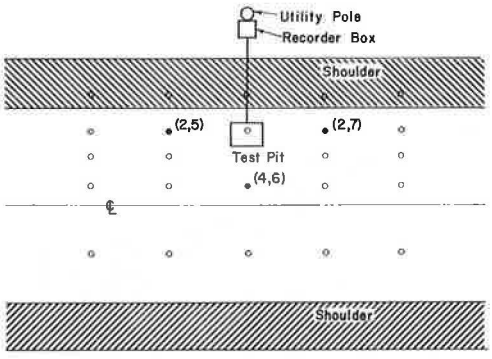

Figure 2. Seasonal change in subgrade moisture content.

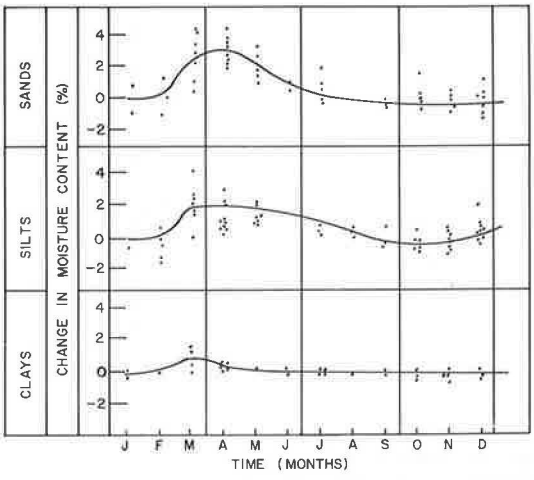

Table 1. Actual and corrected surface deflection data.

Site	Month-Year	Actual Deflection[a] (mils)	Pavement Temperature[b] (deg F)	Temperature Correction Factor[c] (60 F base)	Temperature-Corrected Deflection (mils)
Lairdsville	April-72	0.50	55	1.0365	0.52
	May-72	0.47	89	0.7747	0.36
	July-72	0.45	85	0.8055	0.36
	Sept.-72	0.46	91	0.7593	0.35
	March-73	0.49	51	1.0673	0.52
	April-73	0.47	64	0.9672	0.46
	May-73	0.47	85	0.8055	0.38
	July-73	0.46	86	0.7978	0.36
	August-73	0.45	110	0.6130	0.27
	Sept.-73	0.36	93	0.7439	0.26
Meadville	April-72	1.34	79	0.8517	1.13
	May-72	1.08	95	0.7285	0.78
	July-72	0.87	96	0.7208	0.62
	Sept.-72	0.85	79	0.8517	0.72
	March-73	0.97	46	1.1058	1.07
	April-73	1.05	83	0.8209	0.85
	May-73	1.01	69	0.9287	0.63
	July-73	0.94	100	0.6900	0.64
	August-73	0.98	82	0.8286	0.80
	Sept.-73	0.83	80	0.8440	0.70
State College	April-72	1.17	64	0.9672	1.12
	May-72	0.76	73	0.8979	0.68
	July-72	0.94	95	0.7285	0.68
	March-73	0.75	56	1.0288	0.77
	April-73	0.75	73	0.8579	0.67
	May-73	0.72	84	0.8132	0.58
	July-73	0.72	79	0.8517	0.60
	August-73	0.76	88	0.7824	0.59
	Sept.-73	0.81	74	0.8902	0.71
Washington	April-72	1.34	86	0.7978	1.06
	May-72	0.84	98	0.7054	0.59
	July-72	0.80	95	0.7285	0.58
	Sept.-72	0.80	94	0.7362	0.58
	March-73	0.90	60	0.9980	0.90
	April-73	0.86	71	0.9133	0.70
	May-73	0.84	64	0.9672	0.77
	July-73	0.83	91	0.7593	0.62
	August-73	0.71	82	0.8286	0.58
	Sept.-73	0.61	76	0.8748	0.53
Wilkes-Barre	April-72	0.95	49	1.0827	1.03
	May-72	0.63	83	0.8209	0.51
	July-72	0.58	83	0.8209	0.47
	Sept.-72	0.67	95	0.7285	0.48
	March-73	0.75	57	1.0211	0.77
	April-73	0.84	54	1.0442	0.87
	May-73	1.02	81	0.8363	0.85
	July-73	0.85	89	0.7747	0.65
	August-73	0.83	110	0.6130	0.50
	Sept.-73	0.73	90	0.7670	0.55

[a]Average of points (2,5), (2,7), and (4,6), which are nearest instrument pit in site grid system.
[b]Average of thermocouples inserted in surface course.
[c]See Figure 3.

Figure 3. Deflection adjustment factor for temperature.

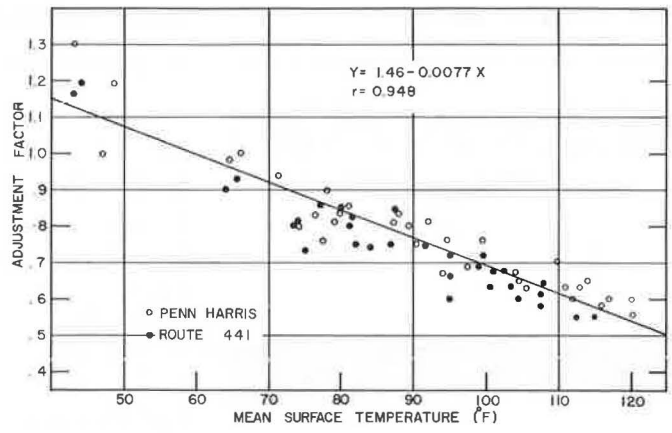

Figure 4. Seasonal relationship of precipitation, subgrade moisture, and corrected surface deflection for Lantz Corners.

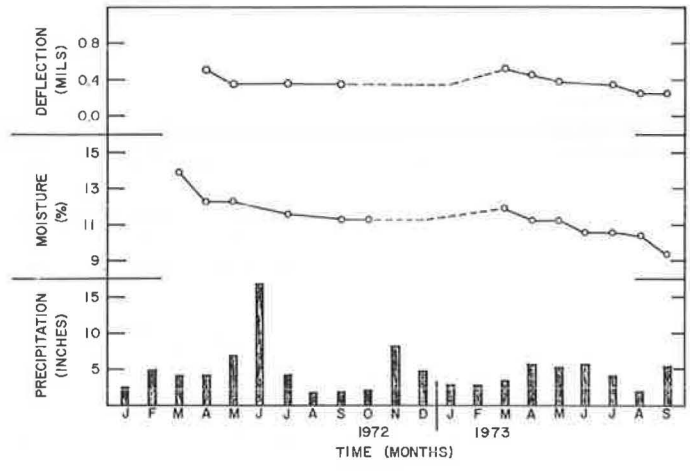

Figure 5. Seasonal relationship of precipitation, subgrade moisture, and corrected surface deflection for Meadville.

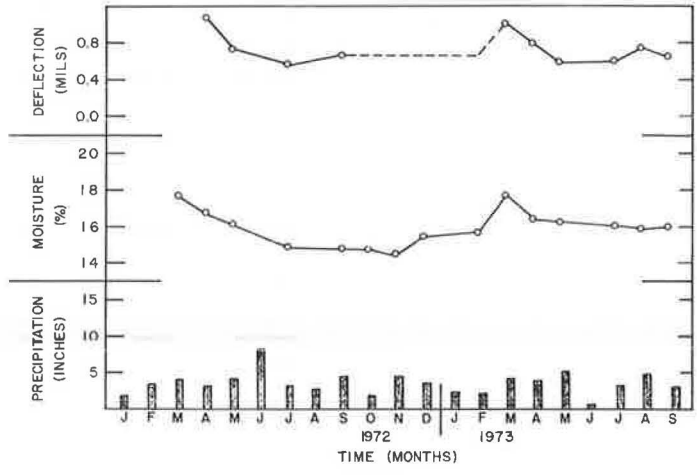

Figure 6. Seasonal relationship of precipitation, subgrade moisture, and corrected surface deflection for State College.

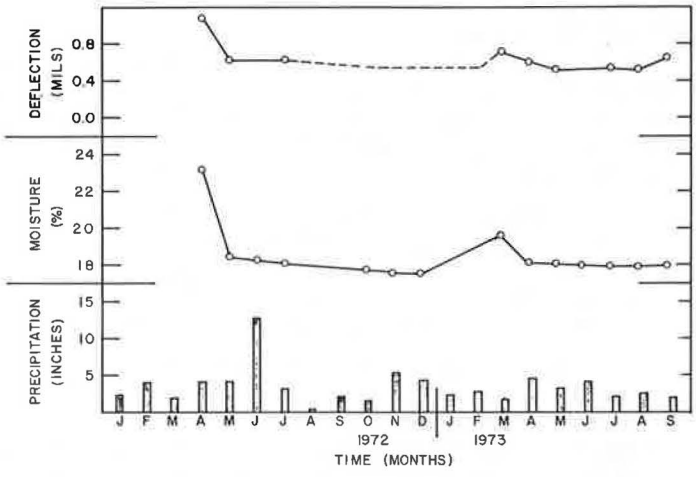

Figure 7. Seasonal relationship of precipitation, subgrade moisture, and corrected surface deflection for Washington.

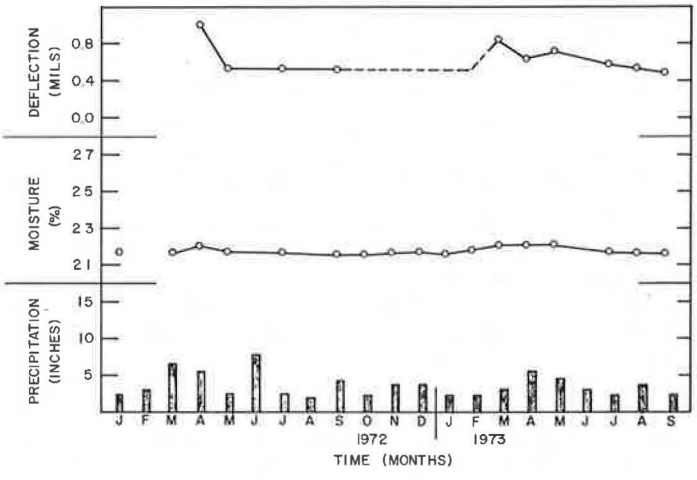

Figure 8. Seasonal relationship of precipitation, subgrade moisture, and corrected surface deflection for Wilkes-Barre.

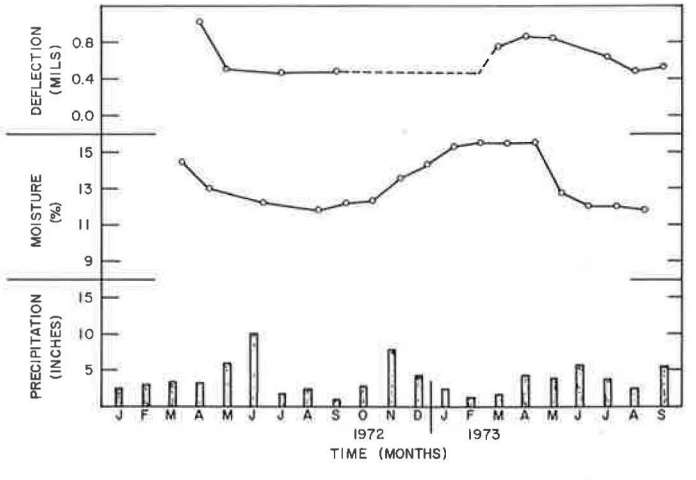

Statistical Analysis

A stepwise multilinear regression analysis was employed to establish the degree of relationship between the dependent variable (percent change in deflection) and the independent variables—the percent change in moisture content (ΔMC), thickness of entire pavement system (D_p), density (γ_d), liquid limit (LL), and percent by weight passing the No. 200 sieve (%200). The following statistical parameters were evaluated:

1. Coefficient of multiple correlation (R);
2. Coefficient of determination (R^2);
3. Analysis of variance ratio (F-ratio);
4. Standard error of the estimate (S_y); and
5. Regression coefficients for the associated variables.

Tables 2 and 3 show the field data that were analyzed in the development of the regression equation.

Multiple linearity was assumed to exist between the percent change in deflection and the associated variables. A high R-value would substantiate this assumption whereas a low R-value would negate linearity, indicating that possibly a polynomial relationship exists or that no relationship exists at all.

Initially, the percent passing the No. 4 sieve (%4), the plastic limit (PL), and the plasticity index (PI) of the subgrade soils were also included as independent variables. However, the correlation matrix for investigating correlation between two or more independent variables indicated the following variables were intercorrelated:

1. Liquid limit (LL) and plastic limit (PL);
2. Liquid limit (LL) and plasticity index (PI); and
3. Percent material passing No. 4 and No. 200 sieves.

If these independent variables are intercorrelated, then one of the variables may be removed without affecting the functional relationship. In selecting the independent parameters, the one contributing most significantly to the coefficient of determination value (R^2) must be considered. The logic for this is dictated by the fact that the R^2-value is defined as the ratio of the explained variation of the regression analysis to the total variation, which in turn indicates the percentage of the total variation that is attributable to the independent variables. With this point in mind, the percent passing the No. 4 sieve, the plastic limit, and the plasticity index were eliminated from the final relationship with no significant reduction in the R^2-value.

The multilinear regression analysis performed with field data from the 5 bituminous pavements produces the following equation for predicting percent changes in surface deflections:

$$\Delta\delta_{60F} = 2.8496\ (\Delta MC) + 0.7000\ (\%200) + 2.4484\ (D_p) - 0.8342\ (LL) - 0.3979\ (\gamma_d) \quad (3)$$

This equation gives computed values that produce relatively high multiple R- and R^2-values and reasonably low standard errors of estimate when compared with the actual values.

The "F" to remove, listed along with other pertinent statistical data in Table 4, is an indicator of the importance of the corresponding independent variable in predicting deflection changes. A higher F-value indicates a more significant variable. Therefore, the change in subgrade moisture content is certainly the most significant of the five variables, and the percent passing the No. 200 sieve is the second most significant variable. The remaining three variables are considerably less significant, and their introduction into the equation produces relatively small increases in the multiple R-value.

The multilinear regression analysis forces a linear equation that produces the best fit using combinations of all variables. As a result, a regression coefficient of any corresponding independent variable reflects not only the variation that is directly due to that independent variable but also the variation that is due to the other independent variables correlated with it (13). Therefore, it is not possible to relate any one independent variable to the dependent variable.

Table 2. Change in corrected surface deflection with associated change in subgrade moisture.

Site	Month-Year	Corrected Deflection (mils)	Moisture Content (percent)	Percent Change in Surface Deflection[a]	Percent Change in Moisture Content[b]
Lairdsville	April-72	0.52	12.3	100	30.9
	May-72	0.36	12.3	38	30.9
	July-72	0.36	11.6	38	23.4
	Sept.-72	0.35	11.3	35	20.2
	March-73	0.52	11.9	100	26.6
	April-73	0.46	11.3	77	20.2
	May-73	0.38	11.3	46	20.2
	July-73	0.36	10.6	38	12.8
	August-73	0.27	10.4	4	10.6
	Sept.-73	0.26[c]	9.4	—	—
Meadville	April-72	1.13	16.9	82	12.7
	May-72	0.78	16.3	26	8.7
	July-72	0.62[c]	15.0	—	—
	Sept.-72	0.72	14.9	16	-0.7
	March-73	1.07	17.8	73	18.7
	April-73	0.85	16.1	37	7.3
	May-73	0.63	16.4	2	9.3
	July-73	0.64	16.2	3	8.0
	August-73	0.80	16.0	29	6.7
	Sept.-73	0.70	16.1	13	7.3
State College	April-72	1.12	23.3	90	28.7
	May-72	0.68	18.5	15	2.2
	July-72	0.68	18.2	15	0.6
	Sept.-72	—	—	—	—
	March-73	0.77	19.8	31	9.4
	April-73	0.67	18.3	14	1.1
	May-73	0.59	18.2	-2	0.6
	July-73	0.60	18.1	2	0.0
	August-73	0.59[c]	18.1	—	—
	Sept.-73	0.71	18.1	20	0.0
Washington	April-72	1.06	22.2	100	2.3
	May-72	0.59	21.9	11	0.9
	July-72	0.58	21.8	9	0.5
	Sept.-72	0.58	21.7	9	0.0
	March-73	0.90	22.2	70	2.3
	April-73	0.70	22.2	32	2.3
	May-73	0.77	22.2	45	2.3
	July-73	0.62	21.8	17	0.5
	August-73	0.58	21.7	9	0.0
	Sept.-73	0.53[c]	21.7	—	—
Wilkes-Barre	April-72	1.03	14.5	119	18.9
	May-72	0.51	13.0	9	6.6
	July-72	0.47[c]	12.2	—	—
	Sept.-72	0.48	11.8	2	-3.3
	March-73	0.77	15.5	64	27.0
	April-73	0.87	15.5	85	27.0
	May-73	0.85	15.5	81	27.0
	July-73	0.65	12.7	38	4.1
	August-73	0.50	12.0	6	-1.6
	Sept.-73	0.55	11.8	17	-3.3

[a]Computed as $(\delta - \delta_{min})/\delta_{min}$.
[b]Computed as $(MC - MC @ \delta_{min})/(MC @ \delta_{min})$.
[c]Corrected minimum surface deflection (δ_{min}).

Table 3. Pertinent engineering characteristics of field test sites.

Site	Corrected Minimum Deflection (mils)	Moisture Content at Minimum Deflection (percent)	Depth of Pavement Section (in.)	Engineering Properties of Subgrade Soils				
				Density (pcf)	Liquid Limit	Plasticity Index	Percent Passing No. 200 Sieve	Subgrade Classification
Clarion[a]	—	—	24.5	117	31	8	61.5	A-4(3)
Lairdsville	0.26	9.4	16.0	124	24	3	26.0	A-2-4(0)
Lantz Corners[a]	—	—	17.0	112	25	2	65.1	A-4(0)
Meadville	0.62	15.0	12.0	110	24	3	66.2	A-4(0)
State College	0.59	18.1	18.0	100	55	20	74.9	A-7-5(17)
Washington	0.53	21.7	15.0	105	37	11	85.9	A-6(10)
Wellsboro[a]	—	—	19.0	116	21	1	29.4	A-2-4(0)
Wilkes-Barre	0.47	12.2	24.0	127	16	NP	29.2	A-2-4(0)

[a]Concrete pavement.

Table 4. Multilinear regression analysis data.

Independent Variable[a]	Coefficient	"F" to Remove	Multiple R	Increase R
ΔMC	2.8496	40.79[b]	0.8423	0.8423
#200	0.7000	7.29[c]	0.8824	0.0692
D_p	2.4484	4.13	0.8859	0.0035
LL	-0.8342	3.98	0.8898	0.0039
γ_d	-0.3979	2.96	0.8980	0.0082

$\Delta\delta_{60\,F} = 2.8496\ (\Delta MC) + 0.7000\ (\#200) + 2.4484\ (D_p) - 0.8342\ (LL) - 0.3979\ (\gamma_d)$

[a]Dependent variable is percent change in surface deflection ($\Delta\delta$) corrected to 60 F temperature base.
[b]Significant at 1 percent level.
[c]Significant at 5 percent level.

Figure 9. Actual versus computed percent change in deflections (adjusted to 60 F temperature base).

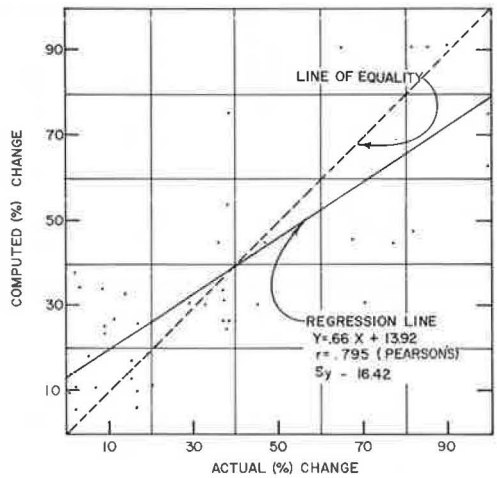

Figure 9 shows a scatter diagram and the associated statistical parameters of the percent change in deflection computed with the multilinear regression equation versus the actual percent change measured in the field. When the regression line coincides with the line of equality, perfect correlation is established. The moderately high r-value and low standard error of estimate indicate a good correlation between predicted and actual change in deflection values. Thus, the prediction of the change in deflection appears to be suited for bituminous pavements placed on plastic subgrade soils. Furthermore, the validity of the equation predicting deflection change, Eq. 3, is established for the five investigated sites.

SUMMARY

1. Surface deflections of flexible pavement systems are significantly affected by temperature variation in the surface and moisture variation in the subgrade.
2. Seasonal variations in subgrade moisture occur as anticipated.
3. Percent change in surface deflection of flexible pavements can be predicted with reasonable confidence by the following equation:

$$\Delta\delta_{60\,F} = 2.8496\ (\Delta MC) + 0.7000\ (\#200) + 2.4484\ (D_p) - 0.8342\ (LL) - 0.3979\ (\gamma_d)$$

RECOMMENDATIONS FOR APPLICATION

1. Along with field testing, spring load restrictions can be established.
2. Maximum and minimum surface deflection values can be predicted from field conditions.
3. Fatigue life of flexible pavement surfaces can be predicted from change in surface deflection.

ACKNOWLEDGMENTS

The authors wish to express their appreciation to the Bureau of Materials, Testing, and Research of the Pennsylvania Department of Transportation for the sponsorship and financial assistance that made this research possible; to L. D. Sandvig, Director, and W. C. Koehler, Engineer of Tests, for allotting the time and personnel for conducting this study; H. F. Lahr, Jr., and T. E. Keiter for drafting the illustrations in the text; and Mrs. N. J. Myers for her skill and patience in the typing of the manuscript.

REFERENCES

1. Broms, B. B. Effect of Degree of Saturation on Bearing Capacity of Flexible Pavements. Highway Research Record 71, 1965, pp. 1-14.
2. Cominsky, R. J., Cumberledge, G., and Bhajandas, A. C. Frost Action Phenomena in Soils and Pavements. PennDOT Bureau of Materials, Testing, and Research, Research Project 68-30, July 1972.
3. Cumberledge, G. A Study of Factors Influencing the Reduction of Highway Subgrade Support During the Spring Thaw Period. MSCE thesis, West Virginia Univ., 1967.
4. Yao, L. Y. C., and Broms, B. B. Excess Pore Pressures Which Develop During Thawing of Frozen Fine-Grained Subgrade Soils. Highway Research Record 101, 1965, pp. 39-57.
5. Bhajandas, A. C., Cumberledge, G., and Cominsky, R. J. Flexible Pavement Evaluation and Overlay Design Through Deflection Measurements With the Dynaflect. PennDOT Bureau of Materials, Testing, and Research, Research Project, July 1971.
6. A Guide to the Structural Design of Flexible and Rigid Pavement in Canada. Canadian Good Roads Association, Sept. 1965.
7. Williams, A. A. B. The Deformation of Roads Resulting From Moisture Changes in Expansive Soils in South Africa. In Moisture Equilibria and Moisture Changes in Soils—A Symposium in Print, (Aitchison, C. D., ed.), Butterworths, 1965.
8. Russam, K. The Prediction of Subgrade Moisture Conditions for Design Purposes. In Moisture Equilibria and Moisture Changes in Soils—A Symposium in Print, (Aitchison, C. D., ed.), Butterworths, 1965.
9. Turner, K. A., Jr., and Jumikis, A. R. Subsurface Temperatures and Moisture Contents in Six New Jersey Soils, 1954-1955. HRB Bull. 135, 1956, pp. 77-108.
10. Bleck, A. T. Pavements and Influences Affecting or Determining Their Performance. HRB Bull. 20, 1949, pp. 21-170.
11. Helmer, R. A. Results of Oklahoma Flexible Paving Research Project. Highway Research Record 71, 1965, pp. 39-68.
12. Sowers, G. F. Georgia Satellite Flexible Pavement Evaluation and Its Application to Design. Highway Research Record 71, 1965, pp. 151-171.
13. Ezekiel, M., and Fox, K. A. Methods of Correlation and Regression Analyses. John Wiley, New York, 1967.

EFFECTS ON HIGHWAY SUBDRAINAGE OF GRADATION AND DIRECTION OF FLOW WITHIN A DENSELY GRADED BASE COURSE MATERIAL

Thomas J. Moynahan, Jr., and Yaron M. Sternberg,
Department of Civil Engineering, University of Maryland

Because of the relatively high content of fine-grained particles, densely graded base course aggregates will not readily drain once saturated with water. An investigation of permeability and its effect on drainage of densely graded base course material specified by the Maryland State Highway Administration was conducted using a prototype permeameter. The experimental permeameter provided values of permeability of a compacted sample both in the vertical and horizontal direction without removing or disturbing the compacted specimen. The horizontal permeability was found to be only slightly greater than the vertical permeability. Experimental permeability data were applied to an example of lateral drainage from the midpoint of a roadway to a shoulder drain under conditions proposed by the Army Corps of Engineers for base course drainage. The direction of flow in the base course material was found to have little effect on the drainage characteristics; fines content is the more significant factor in determining the rate of highway subdrainage.

•ADEQUATE drainage of base course materials has long been considered essential for maintaining the integrity and service life of highway wearing surfaces. Surface water that infiltrates through minor cracks and other openings in the pavement may become trapped between the slab and an impermeable base. Pumping may result when vehicles passing over concrete slabs force water and suspended fines upward through expansion joints and cracks, leaving voids in the base course. The resultant nonuniform slab support may lead to major cracking and failure of pavement sections. In addition, water trapped between a wearing surface and base may contribute to pavement failure by creating a potential for deleterious frost action. Recent studies and examples of highway failure due to excessive quantities of water within the structural section are reported by Cedergren, Arman, and O'Brien (1).

The Army Corps of Engineers (2) has proposed a base course drainage criteria for airfields by which adequate drainage is said to be achieved if a 50 percent reduction in water drainable by gravity from an initial saturated condition occurs within a 10-day period. Barber (3) and Strohm, Nettles, and Calhoun (4) have stated that this criterion as applied to highway base courses may not be met if the gradation of the base contains fine material in excess of 5 percent passing the No. 200 sieve. Excessive fines tend to lower the hydraulic conductivity or permeability and provide poor drainage by sealing the water-transmitting void network within the base course aggregates.

When a highway pavement is constructed over an impervious subgrade soil that is prone to pumping, such as silt and clay, water beneath the pavement cannot percolate vertically into the subgrade. The primary lines of seepage are restricted to a horizontal direction through the base and into the shoulder area, where a lateral drain pipe

Publication of this paper sponsored by Committee on Subsurface Drainage.

system is sometimes provided. Horizontal permeability values would therefore appear to be more applicable than the traditional vertical values in determining the rate of water movement through the base course to the intercepting laterals.

According to Reeve (5), horizontal permeability of homogeneous gravel beds may be considerably greater than its vertical permeability. This condition may be greatly amplified in a nonhomogeneous material. Thin interstratified layers of fine material may occur during the construction of a highway base course when compaction is performed in layers and fines accumulate between the compacted layers. It is suspected that the interstratified layers of fines decrease the vertical permeability of the total section while not appreciably changing its average horizontal permeability.

This layering phenomenon may similarly occur when permeability test samples are compacted in layers within a cylindrical mold in the laboratory. Because only vertical permeability values are reported from such tests, these values may be overly conservative when applied to horizontal drainage situations. The dual purposes of this study, therefore, are to develop an apparatus that can determine and compare horizontal and vertical permeabilities of stratified granular base course samples and to investigate the effects of fines content in general on both vertical and horizontal permeabilities. Previously, a permeameter similar to the prototype apparatus described in the following was developed by Post and Jouanna (6) to measure only the horizontal permeability of a nonstratified granular earth dam fill material.

DEVELOPMENT OF A HORIZONTAL PERMEAMETER

The basis for the prototype apparatus was a standard vertical permeameter consisting of a 6-in. inside diameter compaction mold conforming to ASTM D-1883-67, a mounting plate, a collar, and a top plate. The assembled permeameter was made watertight by the installation of neoprene ring gaskets at each joint of the individual components. The vertical permeameter is shown in Figure 1.

Several modifications to the standard assembly were necessary before horizontal flow could be induced and the horizontal hydraulic conductivity thus evaluated. An inflow pipe, perforated along its length, was installed at the center of the permeameter mold and drain holes were drilled into the body of the mold on the same horizontal planes as the perforations in the inflow pipe. The detailed modifications to the standard permeameter are shown in Figure 2. A complete description of the prototype permeameter was given by Moynahan (7).

Water introduced under pressure into the center pipe flowed horizontally through a compacted soil sample and emerged from the drain holes in the body of the mold. The seepage lines resembled a radial-horizontal flow pattern analogous to the flow net of a recharge well in a confined aquifer. The confining layer within the modified apparatus was a 6-in. diameter copper bearing plate that pressed against the top of the sample and restricted the flow to the radial-horizontal direction.

The ability to evaluate vertical coefficients of permeability was retained in the prototype horizontal apparatus by providing a seal for the inflow pipe and plugs for the drain holes in the body of the mold. The installation of the watertight seals and plugs restricted the flow to a vertical direction and did not appreciably disturb a sample that had previously been tested for horizontal values. The modified apparatus prepared for vertical testing is shown in Figure 3.

EQUATIONS OF FLOW

The equations governing the flow for both the vertical and horizontal directions are derived from Darcy's Law:

$$Q = KiA \tag{1}$$

where Q = flow rate, K = hydraulic conductivity, i = hydraulic gradient, and A = sectional area through which the flow passes. The equations derived to evaluate the vertical hydraulic conductivity for both the constant and variable head flow conditions of this study are

Figure 1. The standard permeameter.

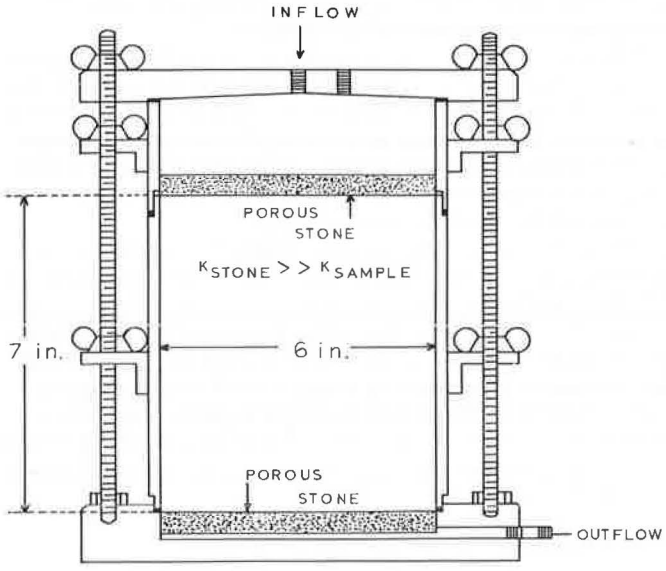

Figure 2. The modified permeameter in the horizontal test configuration.

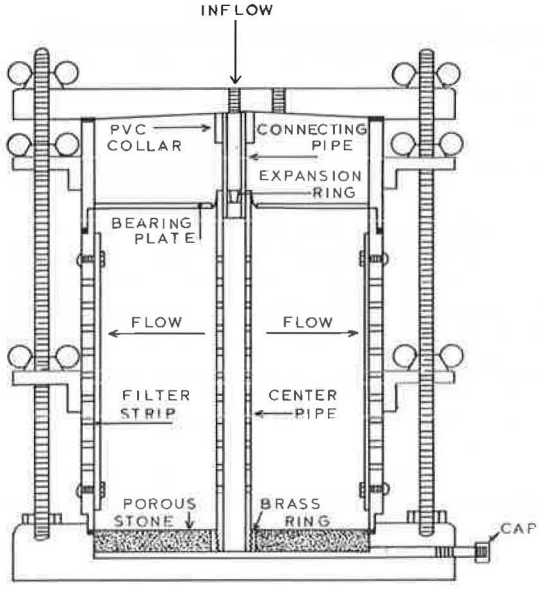

Figure 3. The modified permeameter in the vertical test configuration.

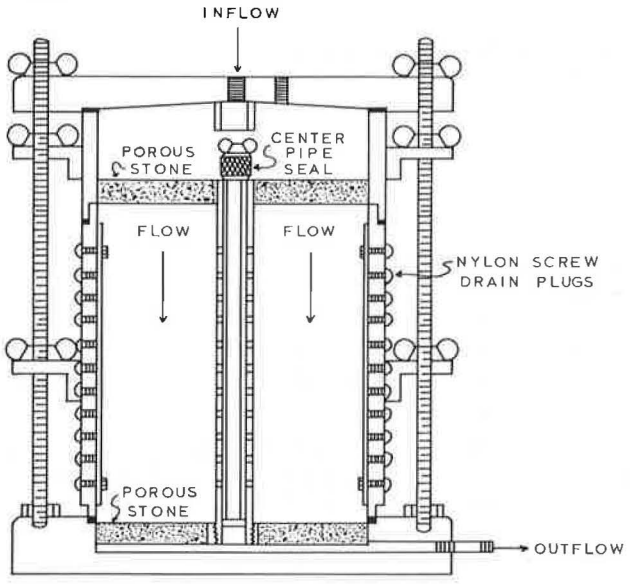

Figure 4. Experimental gradation curves.

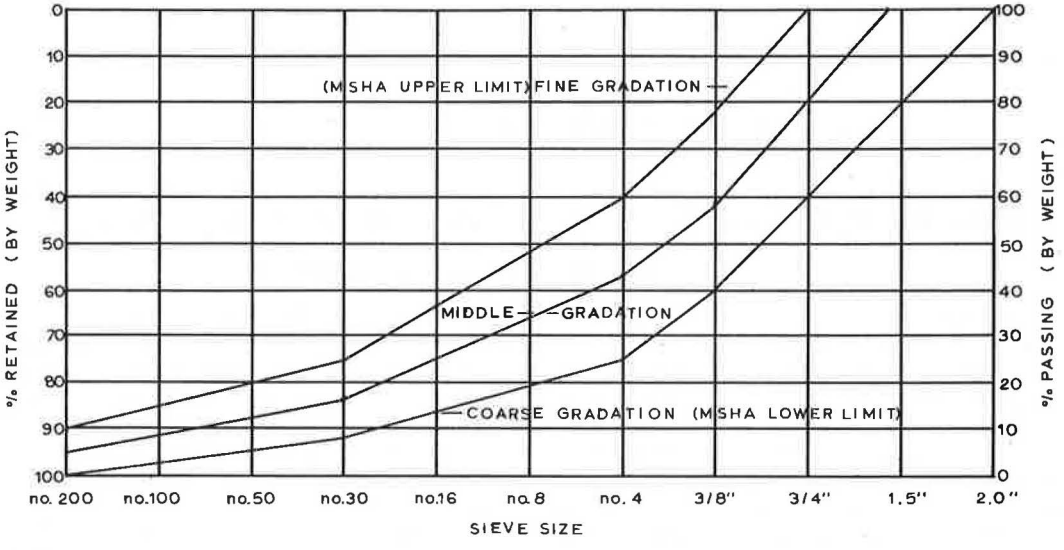

$$K_v = \frac{q \cdot L}{\Delta t \cdot A \cdot (h_1 - h_2)} \quad \text{(constant head)} \tag{2a}$$

$$K_v = \frac{\pi \cdot r_s^2 \cdot L}{\Delta t \cdot A} \ln\left(\frac{h_i - h_2}{h_f - h_2}\right) \quad \text{(variable head)} \tag{2b}$$

where

K_v = vertical hydraulic conductivity,
q = volume of discharged water,
L = height (length) of sample,
Δt = duration of flow,
A = sectional area of sample through which flow passes,
h_1 = height of water in standpipe during steady flow,
h_2 = height of water in the permeameter holding basin,
h_i = initial height of water in the standpipe during non-steady flow,
h_f = final height of water in standpipe during non-steady flow, and
r_s = inside radius of the standpipe.

The following equations relate the horizontal hydraulic conductivity to the constant and variable head flow conditions respectively for the horizontal test configuration; these equations were derived from Darcy's Law by methods employed in well flow analysis:

$$K_h = \frac{q}{2 \cdot \pi \cdot \Delta t \cdot L\,(h_1 - h_2)} \cdot \ln\left(\frac{r_m}{r_o}\right) \quad \text{(constant head)} \tag{3a}$$

$$K_h = \frac{\ln\left(\frac{h_i - h_2}{h_f - h_2}\right) \cdot r_s^2 \cdot \ln\left(\frac{r_m}{r_o}\right)}{2 \cdot L \cdot \Delta t} \quad \text{(variable head)} \tag{3b}$$

where q, L, Δt, h_1, h_2, h_i, h_f, and r_s are as defined earlier and

K_h = horizontal hydraulic conductivity,
r_m = inside radius of the permeameter, and
r_o = outside radius of the center flow pipe.

The physical parameters on the right side of Eqs. 2 and 3 are determined experimentally in the laboratory, and hydraulic conductivities are calculated from the ensuing data.

SAMPLE DESCRIPTION AND PREPARATION

The base course material tested in this study was crushed limestone with a gradation within the allowable range for densely graded aggregates as specified by the Maryland State Highway Administration (MSHA). Densely graded aggregate was chosen for testing because it provided a wide range of fines content relative to other base course aggregates specified by state agencies. The range of fines, from 0 to 10 percent by weight, was necessary for the investigation of the proposed effect on directional permeability by fines accumulation in layers during compaction and the effect of fines content in general on both vertical and horizontal permeability.

The MSHA allowable range for gradation of densely graded aggregates is shown in Figure 4. The fine gradation of this study corresponded to the upper limit of the MSHA range and contained 10 percent fine material by weight passing the No. 200 sieve. The coarse gradation was identical to the lower limit of the MSHA band, with 0 percent fines passing the No. 200 sieve, and the middle gradation was the median of the upper and lower limits, with 5 percent fines passing the No. 200 sieve.

The original quantity of base course aggregates received from the producer was sieved into its constituent sizes and remixed according to the three experimental curves described. In accordance with AASHO T-180, Method "D", aggregates retained on the 2-in. sieve were discarded. The aggregates passing the 2-in. sieve and retained on the $\frac{3}{4}$-in. sieve were removed and replaced by an equal weight of material smaller than $\frac{3}{4}$ in. and larger than No. 4.

Base course samples were compacted in the prototype horizontal permeameter mold at optimum moisture content to a dry density at least 96 percent of maximum dry density. The compaction technique employed a 10-lb hammer with an 18-in. drop falling alternately on 5 equal layers 86 times each. The total compacted height of the sample was 7 in. After compaction, the samples were immersed in water and allowed to reach saturation before permeability testing commenced. Vertical permeability tests were also conducted with a standard permeameter as a control for both the density and the vertical coefficients of permeability obtained with the modified permeameter.

EXPERIMENTAL RESULTS

Experimental values of permeability are shown in Figure 5. These values have been corrected for temperature variations within the permeating water by the following equation:

$$K_{20} = \frac{\mu_t}{\mu_{20}} \cdot K_t \qquad (4)$$

in which

K_{20} = standardized coefficient of permeability at 20 C,
K_t = coefficient of permeability determined at test temperature t,
μ_t = viscosity of water at temperature t, and
μ_{20} = viscosity of water at 20 C.

The experimental permeability values obtained from the standard permeameter and from the vertical test of the prototype permeameter are shown in Figure 6. An analysis of variance revealed that the mean of the prototype vertical permeability values is significantly larger than the mean of the standard values at the 0.05 level of significance in all the gradations tested. The difference, which was unexpected, was initially attributed to possible variation in dry densities whereby the dry densities of the modified method were less than those of the standard permeameter. However, an analysis of variance for the dry density data suggested that there was no difference between the mean of the prototype dry densities and the mean of the standard dry densities at a level of significance of 0.05.

Another explanation for the greater values of vertical permeability in the prototype apparatus was that the addition of the center pipe increased the net outflow from the permeameter during the vertical test. Possible sources of extraneous flow were seepage through the center pipe caused by a leaky center pipe seal and seepage between the granular sample and the outside surface of the center pipe. Either occurrence would result in greater flows and larger permeability values when using the prototype vertical permeameter.

In order to account for the effects of the center pipe, correction factors were determined. The ratios of the standard to the modified vertical coefficients of permeability were calculated for samples of similar dry densities within each gradation. The average of the ratios was used to adjust the modified permeability values as shown in the following equation:

$$K_{vadj} = \frac{\sum_{i=1}^{n} \frac{K_{vstd}}{K_v}}{n} \cdot K_v$$

where

K_{vadj} = vertical permeability coefficient of the modified permeameter adjusted for center pipe effects,
K_{vstd} = vertical coefficient of permeability from the standard permeameter,

Figure 5. Experimental data.

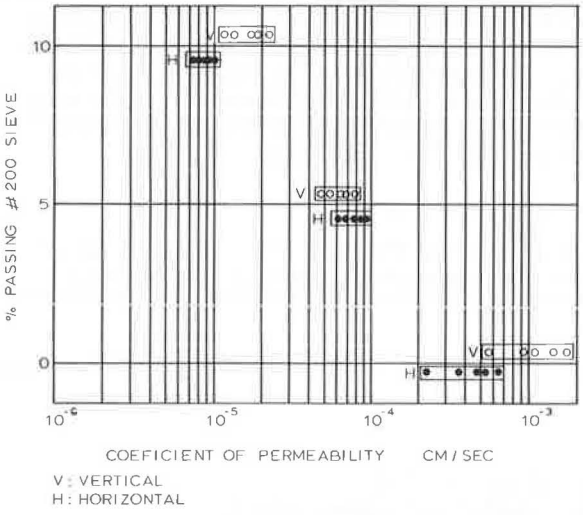

Figure 6. Vertical permeability values.

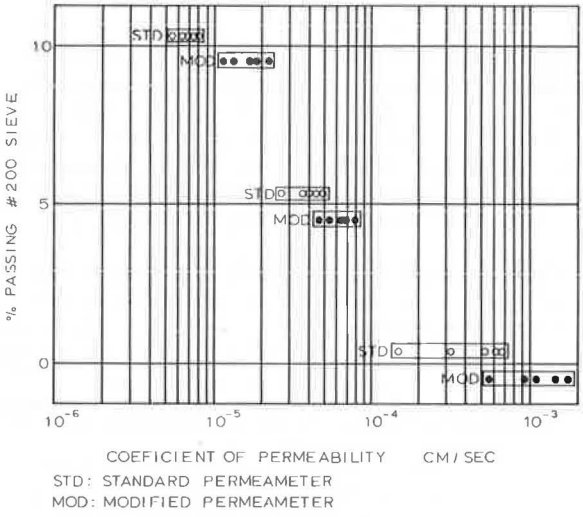

K_v = vertical coefficient of permeability from the modified permeameter, and
n = number of tests for each gradation.

The correction factors were found to be 0.35 for the coarse gradation, 0.70 for the middle gradation, and 0.41 for the fine gradation. The adjusted vertical coefficients of permeability are shown in Figure 7.

A comparison of the results by gradation in Figure 7 indicates that the samples containing fines of 10 percent passing the No. 200 sieve have the lowest coefficients of permeability, followed by the progressively higher values for each reduction in fines content. The average experimental coefficients of permeability for each gradation are given in Table 1. In general the values for hydraulic conductivity differ by an order of magnitude, with the coarse gradation having values on the order of 10^{-4} cm/sec (approximately 1.0 ft/day), the middle gradation having values of 10^{-5} cm/sec (0.1 ft/day), and the fine gradation having values of 10^{-6} cm/sec (0.01 ft/day).

The average horizontal coefficients of permeability were found by an analysis of variance to be statistically greater than the vertical values for both the middle and fine gradations. No difference could be detected between the means of the horizontal permeability values and the adjusted vertical coefficients of the coarse gradation. These findings would appear to be the result of fine material accumulating between the compacted layers within the samples. Since the coarse gradation contained no fine material, the layering effect could not theoretically occur. Consequently, no detectable difference was found between vertical and horizontal permeability of this gradation.

APPLICATION OF RESULTS TO CORPS OF ENGINEERS DRAINAGE CRITERIA

Relating the experimental permeability results to the Corps of Engineers airfield base course drainage criteria as applied to highways by Strohm et al. included the following equation for predicting the time t_{50} required for 50 percent drainage to occur from a saturated state:

$$t_{50} = \frac{n_e \cdot D^2}{a \cdot K \cdot H_o}$$

where

t_{50} = time in days required for 50 percent drainage to occur from a saturated state,
n_e = effective porosity or specific yield,
D = horizontal drainage distance in feet,
K = permeability of the base course in feet/day, and
H_o = hydrostatic head in feet.

Figure 8 shows the relative positions and dimensions of a highway pavement, base course, and underdrain system. The parameters determined for the experimental densely graded base course are given in Table 2, with the corresponding times for 50 percent drainage in the last column. The times for both the horizontal and vertical hydraulic conductivities are listed for comparison.

The times required for 50 percent drainage given in Table 2 indicate that the experimental data do not agree with Barber's statement (1) that only base course aggregates containing fines less than 5 percent passing the No. 200 sieve will meet the Corps of Engineers drainage criteria. The coarse gradation of this study with no fine material would have been expected to drain within the 10-day limit; however, the data in Table 2 indicate that the Corps drainage criteria will be satisfied only after a lapse of approximately 30 days from initial saturation. The direction of flow does not appreciably affect the times required to meet the Corps criteria.

CONCLUSIONS

It is believed that the following conclusions are warranted based on the data obtained in this study:

Figure 7. Adjusted vertical permeability values.

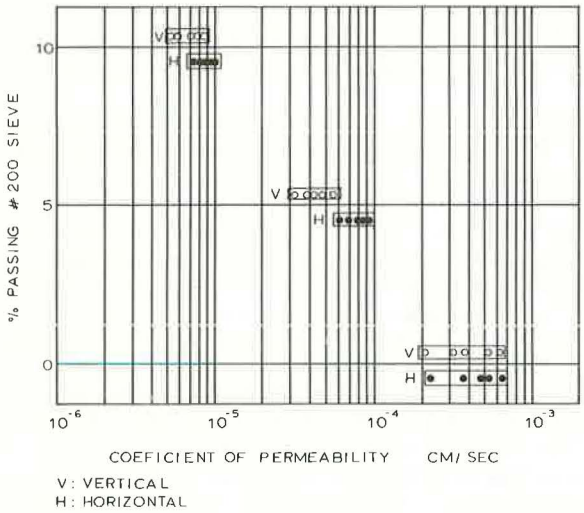

Table 1. Average experimental coefficients of permeability.

Gradation	Percent Passing No. 200 Sieve	Coefficient of Permeability (cm/s)	
		Vertical	Horizontal
Coarse	0	4.06×10^{-4}	4.53×10^{-4}
Middle	5	4.27×10^{-5}	7.60×10^{-5}
Fine	10	6.80×10^{-6}	8.48×10^{-6}

Figure 8. Corps of Engineers drainage diagram.

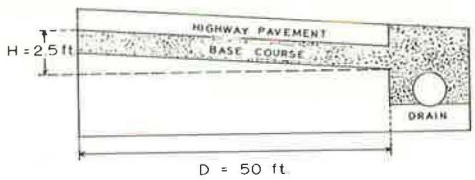

Table 2. Data for Corps of Engineers drainage criteria.

Gradation	γ_{dry}	Percent Passing No. 200 Sieve	S_y, n_e	Coefficient of Permeability (ft/day)		Time t_{50} (days)	
				Vertical	Horizontal	Vertical	Horizontal
Coarse	143.06	0	0.071	1.15	1.28	31	28
Middle	149.95	5	0.057	1.21×10^{-1}	2.15×10^{-1}	236	133
Fine	149.18	10	0.043	1.92×10^{-2}	2.40×10^{-2}	1,120	896

1. The horizontal permeability of a densely graded base course sample is only slightly greater than its vertical permeability.
2. The greater horizontal permeability values are attributed to the effect of interstratified fine material that accumulates between compacted layers.
3. Both the vertical and horizontal permeabilities of densely graded base course mixes were found to be inversely related to fines content.
4. Even the most permeable samples of a densely graded base do not provide acceptable drainage under the Corps of Engineers drainage criteria as adapted to highway base courses by Strohm, Nettles, and Calhoun (4).

As Cedergren et al. point out (1), base course materials with permeabilities as low as those found in this study should be restricted from highway subdrainage systems if competent drainage of the structural section is to be accomplished. The possibility that horizontal flow within a densely graded base course may be sufficiently large to exhibit acceptable subdrainage characteristics was not substantiated by the findings of this study. These conclusions are valid only for densely graded base course samples, and further research should be conducted on base or filter material where horizontal flow predominates.

ACKNOWLEDGMENTS

The authors are grateful for the support provided by the Maryland Department of Transportation, State Highway Administration. This paper is a portion of the research work on surface and subsurface drainage of highways carried out at the Department of Civil Engineering of the University of Maryland.

REFERENCES

1. Cedergren, H. R., Arman, J. A., and O'Brien, K. H. Development of Guidelines for the Design of Subsurface Drainage Systems for Highway Pavement Structural Sections. Office of Research, Federal Highway Administration, Final rept., 1973.
2. Drainage and Erosion Control, Subsurface Drainage Facilities for Airfields. U.S. Army Corps of Engineers, Part 13, Ch. 2, 1955.
3. Barber, E. S. Subsurface Drainage of Highways and Airports. HRB Bull. 209, 1958, 21 pp.
4. Strohm, W. E., Nettles, E. H., and Calhoun, C. C. Study of Drainage Characteristics of Base Course Materials. Highway Research Record 203, 1967, pp. 8-28.
5. Reeve, R. C. Drainage Investigation Methods in Drainage of Agricultural Lands. American Society of Agronomy, 1957.
6. Post, G., and Jouanna, P. Horizontal Permeability of Compacted Gravelly Material. Proc., International Conf. on Soil Mechanics, Vol. 3, 1969.
7. Moynahan, T. J., Jr. Investigation of the Vertical and Horizontal Hydraulic Conductivity of Dense Graded Base Course Aggregate. Department of Civil Engineering, Univ. of Maryland, MS thesis, 1973.

HYDRAULIC EROSION OF COHESIVE SOILS

Arumumgam Kandiah and Kandiah Arulanandan,
Department of Civil Engineering, University of California, Davis

The mechanism of erosion of saturated and unsaturated soils was studied by examining the effect of initial water content on the critical shear stress required to initiate erosion. Erosion tests on saturated and unsaturated soils were carried out in a rotating cylinder and a flume apparatus respectively. To provide a valid comparison of the critical shear stresses obtained on two different measuring devices, identical saturated samples were tested in both to show that the critical shear stress is independent of the testing apparatus. Critical shear stresses obtained as a function of water content on saturated and compacted samples were compared. The mechanism causing erosion in both cases has been shown to be due to swelling. The mechanism causing swelling in the saturated samples is shown to be due to differences in concentration gradient. Test results are also presented to show the influence of structure and water content on the slaking of soils.

IN recent years increasing emphasis has been placed on the study of erosion characteristics of soils. Knowledge of the factors influencing erosion is especially useful in the design of road cuts, drainage ditches, embankments, and other surfaces from which vegetation has been removed.

A significant body of information on the causes and mechanisms of cohesive soil erosion has been assembled (1) and presented at the Highway Research Board Soil Erosion Symposium held in 1973. One of the contributions made at the symposium was the successful adaptation of the modified rotating cylinder test apparatus of Masch, Espey, and Moore (2) for erosion measurement of saturated soils (3). At the panel discussion no general agreement was reached as to the validity of the critical shear stresses obtained by using the rotating cylinder apparatus. It may be argued that tests conducted in open flumes may give different critical shear stresses. The first objective of this paper, therefore, is to compare the results of critical shear stresses obtained on saturated samples of Yolo loam by using a flume and the rotating cylinder apparatus.

Numerous studies on the erosion of compacted clays have been carried out by various researchers (4, 5, 6). Evidence presented in previous studies has dealt mainly with erosion rates, and the testing conditions are not reported in sufficient detail in all cases to reach any definite conclusions. The erodibility index, which depends on the physicochemical and compositional properties of soils, is defined as the shear stress required for zero erosion rate, also called the critical shear stress τ_0. The influence of clay mineral type and pore and eroding fluid composition on the erodibility index τ_0 for saturated soils has been demonstrated earlier (3), but the influence of water content of saturated and unsaturated soils on the erodibility index of soils has not been reported. The second objective of the paper, therefore, is to examine the effect of water content on the erodibility index of soils in order to provide more insight into the mechanism of erosion of saturated and unsaturated soils. The third objective of the paper is to present some results to show the influence of structure and water content on the slaking of cohesive soil systems.

Publication of this paper sponsored by Committee on Physicochemical Phenomena in Soils.

SAMPLES FOR TESTING

Results reported in this study were obtained on a local natural soil called Yolo loam. Its composition is 40 percent sand, 49 percent silt, and 11 percent clay. X-ray analysis from the same soil group showed that montmorillonite, kaolinite, mica, and vermiculite were the clay minerals present.

Sample Preparation

For shear stress comparison, saturated soil samples were prepared by consolidating samples of Yolo loam from a slurry. Soil samples weighing 1.5 kg were mixed in 20-litre bottles containing 10 litres of solutions of various SAR and salt concentrations. Samples were agitated from time to time to obtain equilibrium between soil and solution. Samples were filtered and consolidated for 2 weeks with increasing loads up to a pressure of about 100 kPa. The effluent was used to determine the chemical composition of the pore fluid.

Compacted samples were prepared by mixing thoroughly a known weight of the soil with a given amount of water to obtain the desired molding water content. The sample was then allowed to equilibrate overnight in plastic bags placed in a humidity room. All samples were compacted according to the modified AASHO standard.

Measurement of Shear Stress

Lane (7) in his investigation on the design of stable channels used the following equation for determining the fluid-induced shear stress:

$$T_o = \gamma D S$$

where

T_o = critical shear stress,
γ = unit weight,
D = depth of flow, and
S = slope of the water surface.

For a two-dimensional flume or in the case of a very wide channel this equation is quite correct. However, for small, narrow flumes as used in this study the equation may give erroneous results because of varied nonuniform flow and turbulence.

Two kinds of instruments are currently available for the measurement of shear stress; one is the shear meter or shear balance and the other is the Preston tube.

The Preston tube consists of a circular tube with an outside diameter d_p resting on the surface and reading the total pressure P_t. Preston (8) showed that the total pressure p_t measured relative to the static pressure p_s depends on the independent variables ρ, v, T_o, and d_p. The equation developed by Preston takes the form

$$\log \frac{T_o d_p^2}{4\rho v^2} = -2.604 + \frac{7}{8} \log \frac{(p_t - p_s)}{4\rho v^2} d_p^2$$

where

ρ = mass density of fluid in slugs/ft^3;
v = kinematic viscosity of fluid in ft^2/second;
T_o = boundary shear stress in lb/ft^2; and
d_p = diameter of Pitot tube in feet.

If the left side becomes smaller than 4.5, then Preston's equation renders incorrect results; if larger than 6.5, no experimental data are available. Preston points out that for the equation to hold true the Pitot tube must lie in the laminal sublayer, which is expected to be about one-tenth of the boundary layer thickness.

The Preston tube has been successfully used to measure shear stress by several workers, including Ippen and Drinker (9); Gosh and Roy (10); and Hwang and Laursen

(11). Ippen and Drinker used the Preston tube to measure the shear stress distribution around bends in open channels. It was found that the shear stress distribution over the entire sample was reasonably uniform and that the Preston tube was a simple and accurate enough device to measure shear stress for erosion studies.

TESTING EQUIPMENT AND PROCEDURE

Erosion tests were performed in the rotating cylinder and a small flume. The rotating cylinder apparatus and testing procedure were described earlier by Arulanandan et al. (3).

The Flume

A small circulating flume, 8 ft (2.5 m) long, 6 in. (0.15 m) wide, and 12 in. (0.3 m) deep was modified to test the erosion of molded soil samples. The flume has three controls for varying the velocity of fluid flow: one discharge control valve with a pressure gauge and two controls for varying the slope of the flume. Figures 1 and 2 show the essential features of the flume. The soil samples were introduced from the bottom of the flume at a distance of 5 ft (1.5 m) from the tailgate. The sample was confined inside an aluminum ring and fitted to the bottom of the flume. A threaded screw was used to keep the surface of the sample flush with the bottom of the flume at any time during the erosion test.

Shear Stress Measurement

Shear stress is measured using a Preston tube (8) designed to suit the required condition of flume. Pressure differences are measured using two open inclined manometers. The flume was precalibrated by obtaining pressure differences for 0, 1, 2, and 3 percent slopes and two settings of headgate position, and the discharge control valve was operated to give the desired shear stress. After 1 minute of erosion, the sample was removed and weighed. The surface was trimmed and the sample was again soaked in water for 5 minutes before the next erosion test; 5 minutes of soaking was considered adequate for the surface to absorb sufficient water to produce maximum swell.

RESULTS OF EROSION MEASUREMENTS

Comparison of Erosion Rate Versus Shear Stress Measurements

The critical shear stresses obtained using the rotating cylinder and the flume are shown in Figure 3. Data shown indicate that the same critical shear stresses are obtained at different sodium absorption ratios (SAR) by the two methods. The results also show that τ_o, the critical shear stress, decreases with an increase in SAR. This result is expected because the degree of flocculation decreases with an increase in SAR at a given salt concentration (3, 12, 13).

The rates of erosion obtained by the two methods are different, however. Further study is necessary to provide a reasonable explanation for this behavior.

Effect of Water Content

The effects of varying the water content of a saturated sample of a silty clay containing 20 percent kaolinite (Hydrite R) and prepared at low SAR are shown in Figure 4. It may be observed that the water content has hardly any effect on the critical shear stress, even though it does affect the erosion rate, once the critical shear stress is exceeded. It is known, however, that samples at high SAR are less flocculated and hence would undergo particle orientation during consolidation. The critical shear stresses may thus be a function of water content. Conclusive results are not yet available to confirm this.

The relationships of erosion rate versus shear stress obtained on compacted samples of Yolo loam (see Fig. 5 for compaction curve) prepared at low SAR are shown in Figure 6. The samples were compacted in cylindrical molds and tested in the flume. The results show that the critical shear stress increases with increasing water content.

Figure 1. Schematic diagram of the flume.

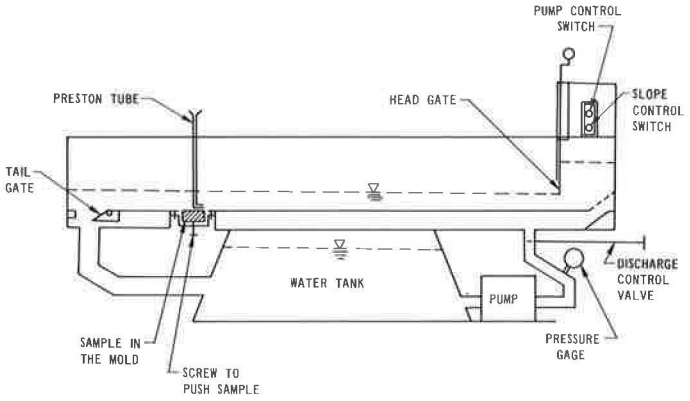

Figure 2. Photograph of the flume.

Figure 3. Plot of erosion rate versus shear stress for Yolo loam obtained from rotating cylinder apparatus and the flume.

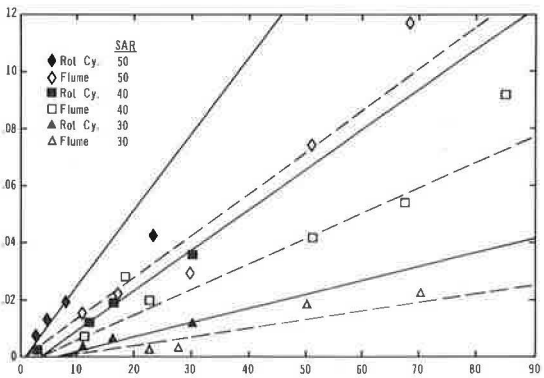

Figure 4. Effect of water content on critical shear stress and erosion rate in a kaolinitic soil at very low SAR (15).

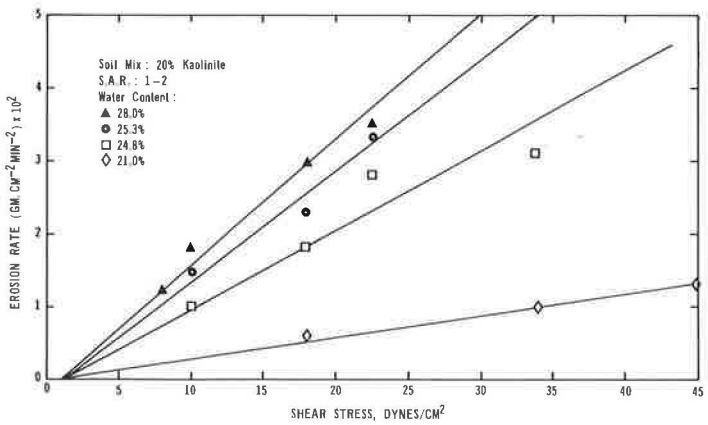

Figure 5. Compaction curve for Yolo loam.

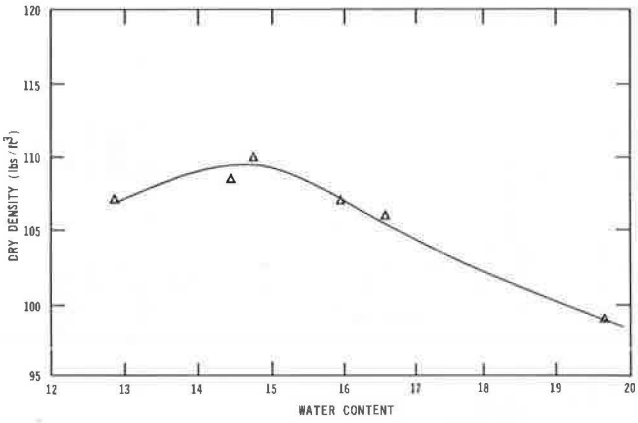

Figure 6. Shear stress versus loss in weight for compacted Yolo loam at various molding water contents.

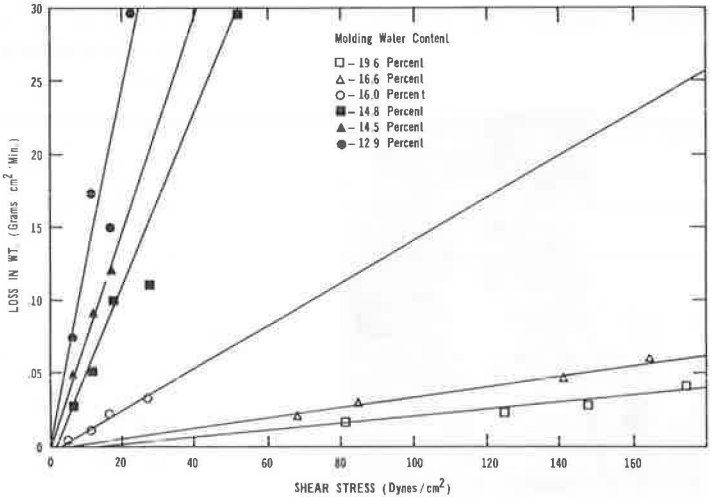

Figure 7. Influence of water content on the critical shear stress of compacted Yolo loam.

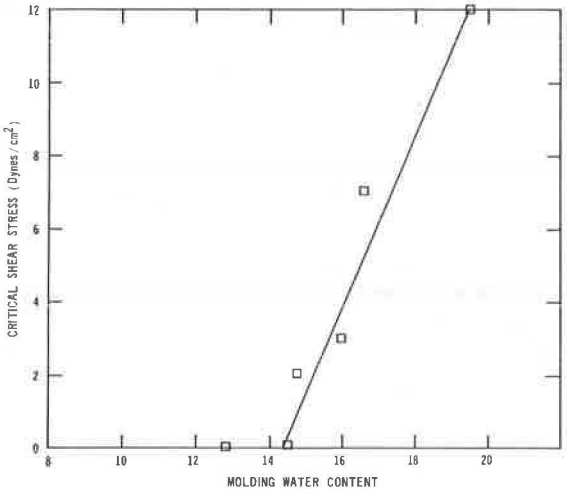

The amount of swelling is known to decrease with increase in water content. These results suggest that for a given soil the critical shear stress would increase with a decrease in the swelling of the soil and that for compacted soils the critical shear stress is a strong function of water content and density. A relationship between molding water content and critical shear stress is shown in Figure 7. At a water content of about 15 percent, which for this compaction curve is the optimum water content, the critical shear stress required to initiate erosion is zero. This result indicates that a different process of particle detachment is involved on the dry side of the line of optimum. This process is generally described as flaking.

Effect of Water Content and Structure on Flaking

Although the actual mechanism of flaking is complicated and not well understood, it is generally accepted that the flaking of dry cohesive soil when in contact with water is due to air pressure in the capillaries (17, 18). When a lump of dry soil is soaked in water, the dipolar water molecules are attracted by the clay particles and thus the water moves into the pores. The rate of water entry depends on the magnitude of the driving forces, which are a function of the matrix potential and osmotic potential. In the pore the water forms menisci, which react against the air in the pores of the dry soil. The entrapped air in the extremely small pores exerts enormous pressure and this breaks loose small bits of soil on the surface. This weakens the resisting forces of the dry soil system and suddenly the pressure in the soil is released and the expanding air throws the soil from the surface with explosive force.

Winterkorn (19) reported that the rate of slaking depends on the relative magnitudes of the driving and the resisting forces. Among the resisting factors are the resistance to water permeation, resistance of internal soil surface to wetting, electrochemical bonds, and cementing agents such as organic matter and other glutinous material. If the rate of water penetration exceeds that of the bond destruction, then the system fails slowly after a prolonged period. On the other hand, if the rate of bond destruction equals or exceeds the water penetration, the breakdown process is very orderly and sometimes instantaneous.

Flaking rate studies on compacted samples of Yolo loam indicate that flaking is instantaneous when samples are compacted on the dry side of the line of optimum. The flaking rates decreased with increased water content, and the flaking was practically negligible at 19.3 percent water content, as shown in Figure 8.

The influence of pore fluid composition on the structure of soils has been well documented (3, 12, 13). The higher the SAR and lower the concentration, the higher is the dispersion of clays, or at a given concentration an increase in SAR produces an increase in deflocculation. The influence of structure on erodibility of saturated soils has also been well demonstrated (3). The effect of structure on the flaking of soils was reported earlier (14, 15) and the results are discussed later. Samples of silty clay containing 20 percent kaolinite (Hydrite R), illite, or montmorillonite were prepared at low and high SAR at a concentration of 0.01 N. The samples were consolidated from a slurry under 100 kPa, allowed to air-dry, weighed, and then suspended in a beaker of distilled water. The flaking rates for the three different clays are shown in Figure 9.

The flaking times are shown to be greater for soils with more dispersed structure. A soil with a higher SAR in the saturated state develops a less flocculated structure than one with a low SAR. The air-dried soils appear to maintain the same structure. A more dispersed soil also has a low permeability and hence would require a longer time for the flow of water into the pores of the soil to produce the flaking observed.

The results also show the influence of minerology on the time of flaking. Montmorillonite with a lower permeability would take a longer time to flake than kaolinite, as shown by the results in Figure 9.

CONCLUSIONS

1. A comparison of the results of critical shear stresses obtained on saturated samples of Yolo loam using a flume and the rotating cylinder apparatus show that the critical shear stress is independent of the testing device. Compacted samples cannot,

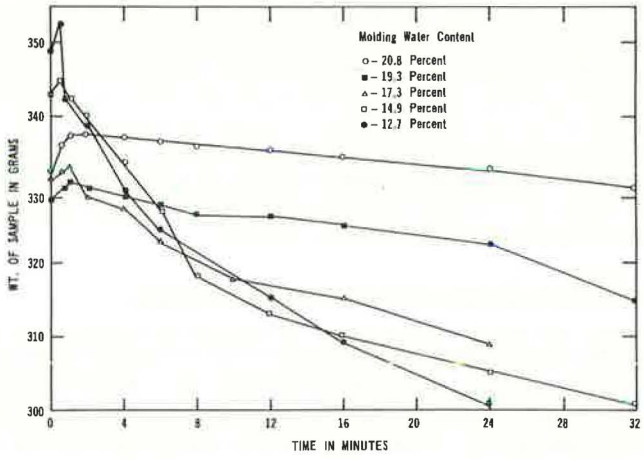

Figure 8. Effect of water content on the flaking of compacted Yolo loam.

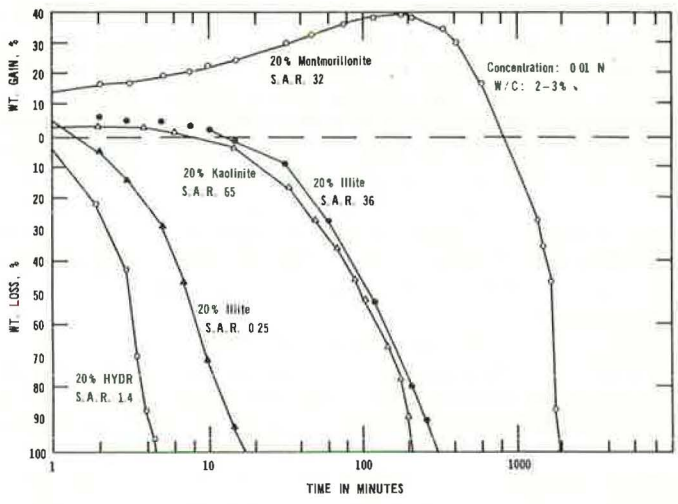

Figure 9. Effect of soil type and pore fluid composition on the slaking of dry soil samples.

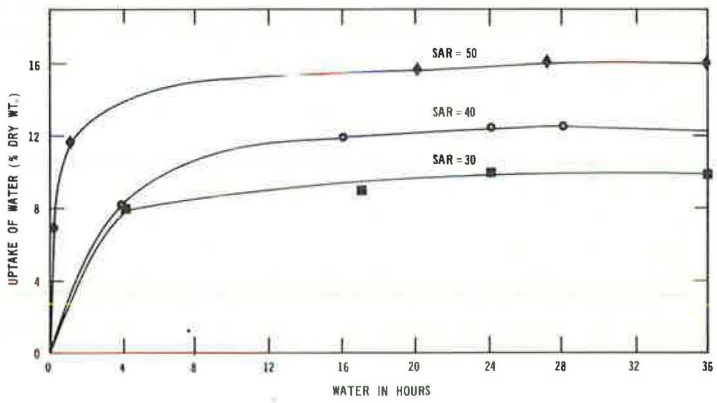

Figure 10. Water uptake of saturated Yolo loam at three different SAR and at a salt concentration of 0.05 N.

however, be tested in the rotating cylinder, whereas both saturated and compacted samples can be tested in the flume. The different testing methods appear to give different erosion rates under the same shear stress. Further studies are necessary to explain this behavior.

2. Samples of saturated soils prepared at low SAR exhibit critical shear stresses that are independent of water content, whereas in compacted soils the critical shear stress is highly dependent on the water content. The higher the water content, the lower the swell is and hence the higher the shear stresses required to initiate erosion. The mechanism of initiation of erosion in saturated soils is controlled both by structure and the osmotic pressure gradient developed due to the difference in concentration of the pore and eroding fluids (3). Structure and osmotic pressure gradient control the swelling of clays. The larger the swelling, the lower is the critical shear stress. For the samples of saturated clays prepared at low SAR, the osmotic pressure gradient and particle orientation are not significantly changed during consolidation, and hence the swelling is not significantly affected. Thus the critical shear stress is seen to be independent of water content for the low SAR samples. Increasing the SAR of a soil at a given concentration does change the osmotic swell behavior (Fig. 10), and hence the critical shear stresses (Fig. 3). The critical shear stress in both compacted and saturated soil is controlled by the swell behavior of the soil. In compacted soils the osmotic pressure concept can satisfactorily explain a good portion of the swelling (19) Structure also affects the swelling of compacted clays (16). In saturated soil the swelling behavior is dictated by the structure and osmotic pressure gradient created by the differences in concentrations of the pore and eroding fluids. It is to be noted that different methods of compaction will induce different structures and hence different amounts of swell (16), and thus should produce different critical shear stresses.

3. Flaking is instantaneous for samples compacted on the dry side of the line of optimum, and thus the shear stress required to initiate erosion is zero. The flaking rate is slower for a dispersed soil than a flocculated one. Slaking rate is shown to be controlled by the permeability of the system, because a montmorillonitic clay with a lower permeability exhibits a larger flaking time than a kaolinite clay with a larger permeability.

ACKNOWLEDGMENTS

Support for this research project by the Davis Faculty Research Grant and the National Science Foundation is gratefully acknowledged. Special thanks are due to Ranjan Ariathurai for assistance in the development of the flume apparatus and the interest taken in this study. Part of the flume tests were carried out by Kiruppa Ariathurai, to whom the authors are grateful.

REFERENCES

1. Paaswell, R. E. Causes and Mechanisms of Cohesive Soil Erosion: The State of the Art. HRB Special Rept. 135, 1973, pp. 52-74.
2. Masch, F. D., Jr., Espey, W. H., Jr., and Moore, W. L. Measurements of the Shear Resistance of Cohesive Sediments. Agr. Res. Service, Pub. 970, 1965.
3. Arulanandan, K., Sargunam, A., Loganathan, P., and Krone, R. B. Application of Chemical and Electrical Parameters to Prediction of Erodibility. HRB Special Rept. 135, 1973, pp. 42-51.
4. Abdel-Rahman, N. N. The Effect of Flowing Water on Cohesive Beds. Laboratory for Hydraulic Research and Soil Mechanics, Swiss Federal Institute of Technology, Zurich, thesis, 1962.
5. Grissinger, E. H. Remarks at HRB Workshop on Soil Erosion, Jan. 26, 1973.
6. Christensen, R., and Das, B. Hydraulic Erosion of Remolded Cohesive Soils. HRB Special Rept. 135, 1973, pp. 8-19.
7. Lane, E. W. Design of Stable Channels. Trans., ASCE, Vol. 120, 1955.
8. Preston, J. H. Determination of Turbulent Skin Friction by Means of Pitot Tubes. Jour. Royal Aeronautical Society, Vol. 8, 1954.

9. Ippen, A. T., and Drinker, P. A. Boundary Shear Stress in Curved Trapezoidal Channels. Jour. Hydraulics Div., Proc. ASCE, No. HY5, 1962.
10. Gosh, S. N., and Roy, N. Boundary Shear Stress Distribution in Open Channel Flow. Jour. Hydraulics Div., Proc. ASCE, Vol. 96, No. HY2, 1970.
11. Hwang, L., and Laursen, E. M. Shear Measurement Technique for Rough Surfaces. Jour. Hydraulics Div., Proc. ASCE, Vol. 89, No. HY2, 1963.
12. Aitchison, G. D., and Wood, C. C. Some Interactions of Compaction, Permeability and Post Construction Deflocculation Affecting the Probability of Piping Failure in Small Earth Dams. Proc. 6th International Conference on Soil Mechanics and Foundation Engineering, Montreal, Vol. 2, 1965.
13. Quirk, J. P., and Schofield, R. K. The Effect of Electrolyte Concentration on Soil Permeability. Jour. Soil Science, Vol. 6, 1955.
14. Arulanandan, K. Discussion of "Experimental Study of the Attack of Water on Dry Cohesive Soil Systems," by Winterkorn, H. F. HRB Workshop on Soil Erosion, Jan. 26, 1973.
15. Sargunam, A. Influence of Minerology, Pore Fluid Composition and Structure on the Erosion of Cohesive Soils. Univ. of California, Davis, PhD thesis, 1973.
16. Seed, H. B., and Chan, C. R. Structure and Strength of Compacted Clays. Jour. Soil Mechanics and Foundations Div., ASCE, Vol. 85, 1959.
17. Winterkorn, H. F. Mechanism of Water Attack on Dry Cohesive Soil Systems. Soil Science, Vol. 54, No. 4, Oct. 1942, pp. 259-273.
18. Means, R. E., and Parcher, J. V. Physical Properties of Soils. Charles E. Merrill Books, Columbus, Ohio, 1963.
19. Winterkorn, H. F. Experimental Study of the Attack of Water on Dry Cohesive Soil Systems. HRB Special Rept. 135, 1973, pp. 1-7.
20. Ladd, C. C. Mechanisms of Swelling by Compacted Clay. HRB Bull. 245, 1960, pp. 10-26.

DETERMINATION OF ATTERBERG LIMITS USING MOISTURE TENSION METHODS

Ahmed Atef Gadallah, Eugene R. Russell, and Eldon J. Yoder,
School of Civil Engineering, Purdue University

This paper presents the results of a laboratory investigation of the relationship between the Atterberg limits and the moisture content as obtained by the moisture tension method. The study was conducted in two basic parts. First, a series of tests was made on 38 soils for the purpose of establishing mathematical models for predicting liquid and plastic limits. The results of these tests showed very good correlation between the standard test results and the moisture tension test results. The soils used had liquid limit values <50 percent and plasticity index <21 percent. Second, the mathematical models were verified by using a total of 144 samples having a wide range of plasticity values. The results showed good correlation for the liquid limit and fair correlation for the plastic limit. The results of the investigation indicate that a linear relationship exists between the consistency limits and the moisture content obtained at various pressure intensities. The results also strongly suggest that the moisture tension test can be used on a routine basis for determining the consistency limits of soils.

•THE Atterberg limits have been extensively used for identifying engineering properties of soils and specifying quality of base courses. Almost all specifications for base course materials set some limits on these constants. To get consistent test results for the liquid and plastic limits and to minimize the time required for such tests, attempts have been made either to modify the standard method for determination of these limits or to correlate the limits obtained by the standard method with those obtained from a completely different method.

The moisture tension method (10, 14, 15, 16, 18) has been studied as an alternate procedure for estimating the liquid and plastic limit. The results obtained by this method show a higher degree of reproducibility (10, 15, 16) than the ASTM standard method. The method also permits testing a large number of soil samples simultaneously.

However, there are some limitations relative to the use of the moisture tension method for determining the consistency limits. Previous studies have utilized textural classification of soils as a basis for determining the relationship between moisture tension and liquid limit. Generally, a specific pressure intensity has been recommended for a given soil textural group (14, 15, 16, 18). The use of this technique for the plastic limit determination and for the identification of nonplastic soils has not been fully explored.

The primary purpose of this study was to investigate the possibility of using a unique pressure intensity in the moisture tension test for establishing the moisture tension-consistency limits relationship for various soil types, regardless of their textural classification, and thus specifying a limit on the moisture content values, as obtained from the moisture tension method utilizing a unique pressure intensity, below which a soil could be classified as nonplastic.

Publication of this paper sponsored by Committee on Exploration and Classification of Earth Materials.

MATERIALS

This investigation was conducted using 38 soils obtained from the Indiana State Highway Commission. The liquid limit values of these soils ranged from 18 to 50 percent and the plasticity index values were less than 21 percent. Four basic soil types were tested:

1. Inorganic clays of low to medium plasticity, silty clays, lean clays.
2. Inorganic silts and silt clays.
3. Inorganic clays and silts of low plasticity.
4. Nonplastic materials, mostly silty sands.

MOISTURE TENSION METHOD EQUIPMENT

The apparatus used in this investigation essentially consisted of a commercially available ceramic plate extractor capable of holding three ceramic plates. The ceramic plates used were approximately 10¼ in. (26 cm) in diameter and of a design permitting the tests to be run in the 0 to 1 bar (0 to 100 kPa) pressure range. They are commonly designated as "1 bar ceramic plates" (Fig. 1).

Soil samples are placed in rubber rings 2 in. (5.08 cm) in inner diameter and ½ in. (1.27 cm) high on the ceramic plates, which are mounted in the extractor. A maximum of 12 soil samples of this size can be placed on each plate. When the pressure is applied in the extractor, a pressure difference is maintained across each porous plate, the bottoms of which are at atmospheric pressure. Water from the soil is forced out of the extractor through the ceramic plate cells and the outflow tubes until an equilibrium moisture state is reached, and flow then ceases.

TEST PROCEDURES

The liquid and plastic limits were determined in accordance with ASTM D 423-61T and D 424-59 respectively. Four replicated tests were performed by one trained operator on each soil used in this study.

The general procedure for the moisture tension test is as follows. Each soil sample of 50 grams weight (consisting of the fraction passing the No. 40 sieve) was put into a glass jar. A sufficient amount of distilled water was added and carefully mixed with a spatula until the soil mass could be slowly poured out of the jar. Care was taken that the soil was not so wet as to have free water on the surface when standing. The samples were allowed to stand in the capped jars for 2 hours before placing them on the plates.

The ceramic plates were placed in the extractor and saturated with distilled water prior to placing the soil samples on the plate. Twelve rubber rings of 2 in. (5.08 cm) inside diameter and ½ in. (1.27 cm) height were placed on the plate. Each soil sample was placed in the rubber rings on the plate using a spoon. Care was taken to ensure that the mixing and preparation process was consistent to minimize the effects of pore sizes and state of packing on the test results. Although these two factors cannot be precisely controlled by the techniques used in this study, previous studies have shown that good results can be obtained as long as consistency in the method of preparation was maintained (15, 16).

The tubes were next connected and the lid of the extractor was closed and tightened with bolts. The ends of the outflow tubes were kept constantly under approximately 1 in. (2.5 cm) of water in a beaker to ensure outflow into a constant environment as far as humidity was concerned and to check against air leaks (15). Pressure was then applied and adjusted to the required value. The pressure was maintained for 24 hours to ensure reaching an equilibrium state. At the close of a run the outflow tube was pinched to prevent possible backflow of water when the pressure in the extractor was released. The pressure was released and the lid of the extractor was opened. The soil samples were transferred to containers, and the moisture content of these samples was determined in accordance with ASTM D 2216-63T.

This method of preparation was selected and used in this research after a preliminary study was conducted to evaluate the effect of method of preparation of soil samples

on the moisture tension test results (6). Six soils were prepared using five different methods of preparation, three of which had been utilized and tested in previous research (10, 14, 15). A statistical analysis of the results indicated that the method of preparation of the soil samples had no significant effect on the moisture tension test results (at $\alpha = 0.05$). This conclusion, however, should be viewed with some caution because the test results apply only to the relatively limited inference space consituted by the soil test samples and methods of preparation that were used. Also, the statistical analysis indicated significant interaction between the method of preparation and soil type. This suggests that for some soil types the method of preparation may have an effect on the test results and further indicates that a standardized method of preparation of soil samples is important.

The authors believe that consistency in the method of mixing and preparing the soil samples is of essential value in minimizing changes in the pore sizes and packing state of the soil samples that would affect the moisture tension test results, at least to the extent that such changes do not affect its reproducibility.

RESULTS

Prediction of Liquid and Plastic Limits of Soils

Previous studies (15, 16) suggested that the region between the upper and lower flex points in the moisture tension curves could represent the plasticity index of the soil and that this hypothesis is consistent with the mechanism of plasticity as set forth by Grim (7). Furthermore, the interpretation of two pressure intensities, 3 psi (20.7 kPa) and 20 psi (137.9 kPa), relative to the moisture tension curves obtained in a study by Nishio (10) approximately corresponds to the two flexes.

To determine the Atterberg limits-moisture tension relationships, four pressure intensities, 6, 10, 12, and 18 psi (41.4, 68.9, 82.7, and 124.1 kPa), were used. These pressure intensities lie in the range of 3-20 psi (20.7-137.9 kPa) in which the soil samples exhibit plastic behavior, as suggested in previous studies (10, 15, 16).

For each pressure intensity and using the previously described moisture tension test procedure, the moisture content of each soil was determined. For each of the pressure intensities, four replications were made.

Linear regression models were hypothesized to study the relationships between the measured variables (liquid limit and plastic limit) and the independent variable, WC_i (the symbol WC_i will be used to represent the moisture content obtained under "i" psi pressure intensity). A separate model was evaluated for each of four pressure intensities. Nonplastic soils were excluded from this part of the study.

The data for the regression analysis were handled by two different statistical procedures. The first is commonly referred to as "random combination" and the other as "average values".

In the "random combination" scheme, liquid limit values from the four replications on each soil by the standard method were randomly combined with the four moisture content values obtained at a corresponding pressure intensity to form a set of four readings. The data obtained for the 28 soil samples were tested for homogeneity of variance. The assumption of homogeneity of variance for both LL and PL test data was accepted and there was no need of transforming the dependent variables.

In the "average values" scheme, the mean value of the four replicates of the standard liquid and plastic limit tests for each soil was used as the dependent variable. Similarly, the mean WC_i value for each soil was used as the independent variable. Using these average values in the regression analysis eliminates a part of the variation among the replicate measurements, which may make the coefficient of determination R^2 misleadingly high. However, this study indicated that there is very little difference in R^2 due to the use of the two schemes (random combination versus average values). The use of the prediction models obtained by utilizing the random combination scheme could better represent the inference space for this study.

Interpretation of Regression Analysis Results

The models obtained from the regression analysis of the test data were examined

and those providing the best fit of the data were selected. The criterion used to evaluate the best regression equation was the coefficient of determination, R^2, the ratio of the variation explained by the regression equation to the total variation of the data about the mean. Also, the significance of the regression was tested by an F-test at an α level of 0.05. The residuals obtained from the regression analysis were examined to determine if they were correlated. It was observed that the residuals did not show any predominant trend.

The results of the regression analysis using the random combination scheme are summarized in Table 1. An examination of these results indicates that these linear first-order regression models are appropriate for representing the relationship between consistency limits (LL and PL) and the moisture content WC_1. The data show that

1. The prediction models obtained for both the liquid and plastic limits show a high coefficient of determination, R^2. Also, a linear relationship exists between the liquid or plastic limit and the equilibrium moisture content for each of the pressure intensities utilized in this investigation, namely, 6, 10, 12, and 18 psi (41.4, 68.9, 82.7, and 124.1 kPa).
2. The regression models obtained for the prediction of the liquid limit show a higher R^2 value than that obtained for the prediction of the plastic limit values.
3. For the liquid limit prediction models, the R^2 values remain almost the same (0.92-0.95) with changes in the pressure intensity. Conversely, for the plastic limit prediction models, the R^2 values decrease directly with the increase in pressure intensity utilized [the prediction model obtained at 6 psi (41.4 kPa) has an R^2 value of about 0.94, and that at 18 psi (124.1 kPa) has an $R^2 = 0.78$].
4. The deviations of the predicted LL and PL values from the observed values are within the range of those obtained in replicated standard LL and PL test results (6, 9, 10, 15). To make the prediction models less cumbersome and easier to handle, it was decided to simplify the regression coefficients. Because the liquid and plastic limit values are generally determined to the nearest whole percent moisture content, rounding off the regression coefficients in the prediction equations will not affect the results appreciably.

Detection of Nonplastic and Low-Plasticity Soils

Another aspect of the study was concerned with the identification of nonplastic soils by the moisture tension method. [Nonplastic soils are defined as those sandy or noncohesive soils for which it is difficult or impossible to determine the plastic limit.] The moisture contents (WC_1) of the nonplastic soils were obtained by using four different pressure intensities. Study of the moisture content values indicated that WC_1 values of the nonplastic soils had an approximate upper-bound limit depending on the pressure intensity used. Similarly, for the soils exhibiting a plasticity index (PI) less than 3 percent as well as those with PIs between 3 and 6 percent, the moisture content (WC_1) values were within specific ranges. Therefore, it appears that nonplastic and low-plasticity soils can be identified by their limiting WC_1 values. These limiting values for various pressure intensities are given in Table 2.

Figure 2 shows the relationship of the liquid and plastic limits to the moisture content values WC_1 at various pressure intensities (using the simplified regression coefficients). These relationships can be divided into several distinct segments. The lowest segment A indicates the nonplastic region, the region B signifies the range from nonplastic to a PI < 3 percent, and region C approximates the WC_1 values for soils exhibiting PI values between 3 and 6 percent. The region beyond C is for soils exhibiting a PI greater than 6 percent.

Verification of the Proposed Mathematical Models

To verify the proposed relationships, additional soil samples with previously determined consistency limits were obtained from a laboratory outside Indiana. A total of 144 samples representing a large range in soil texture were tested. The liquid limits of these samples ranged between 15 and 80 percent; the highest plasticity index was 60

Figure 1. Setup of equipment showing two extractors.

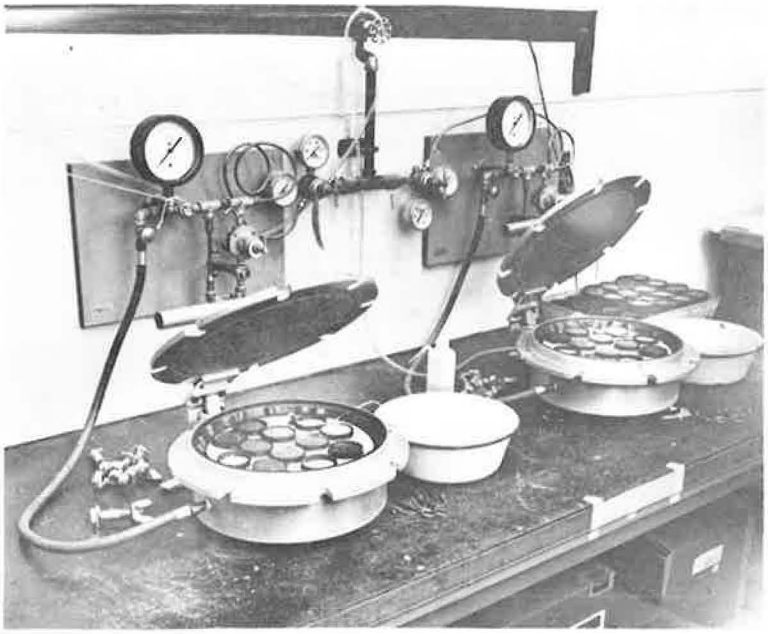

Table 1. Prediction equations for the liquid and plastic limits.

Pressure	Model	R^2	Standard Error	No. of Samples
6 psi (41.4 kPa)	LL = -3.5863 + 1.3201 WC_6	0.93	2.58	112
	PL = 1.4094 + 0.7097 WC_6	0.94	1.22	112
10 psi (68.9 kPa)	LL = -3.5437 + 1.4867 WC_{10}	0.95	2.18	112
	PL = 1.9906 + 0.7737 WC_{10}	0.90	1.59	112
12 psi (82.7 kPa)	LL = -2.7809 + 1.4892 WC_{12}	0.95	2.09	112
	PL = 2.7699 + 0.7570 WC_{12}	0.87	1.85	112
18 psi (124.1 kPa)	LL = -1.9158 + 1.5029 WC_{18}	0.92	2.68	108
	PL = 3.9766 + 0.7299 WC_{18}	0.78	2.41	108

Table 2. WC_i ranges for nonplastic and low-plasticity soils.

Pressure	WC_i Range for Nonplastic Soils[a]	WC_i Range for Soils With PI <3 Percent[a]	WC_i Range for Soils With PI Between 3 and 6 Percent[a]
6 psi (41.4 kPa)	<10	10-15	15-20
10 psi (68.9 kPa)	<9	9-14	14-19
12 psi (82.7 kPa)	<8	8-13	13-18
18 psi (124.1 kPa)	<7	7-12	12-17

[a]Values are in percent moisture content.

Figure 2. Relationship of liquid and plastic limits to moisture content at various pressure intensities.

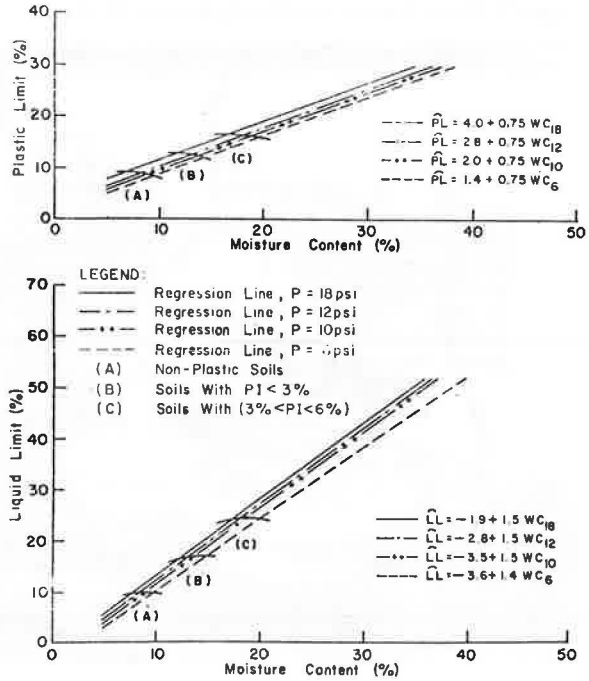

Figure 3. Relationship between liquid limit and moisture content at 10 psi (68.9 kPa) for the check samples (144 data points).

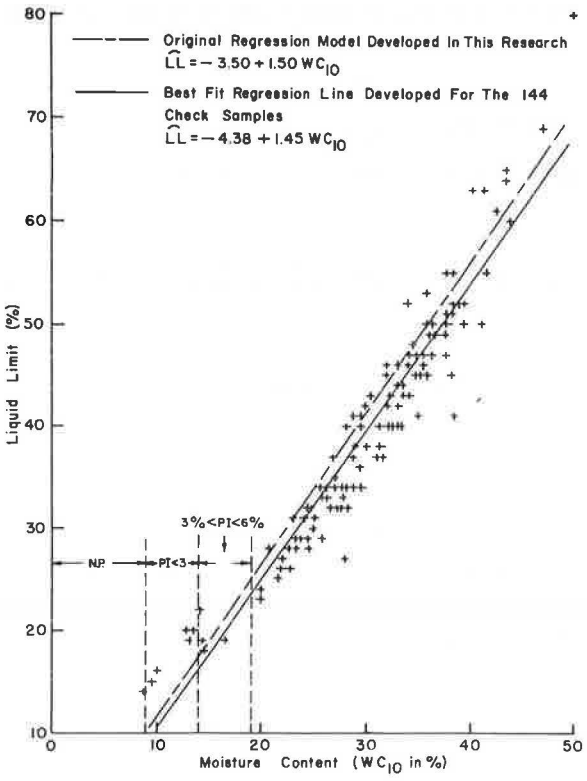

percent. The moisture tension method test was run on these samples at a pressure intensity of 10 psi (68.9 kPa) because a high R^2 value was obtained for both the liquid and plastic limit prediction models for this pressure. Although the models indicate that utilizing a pressure intensity of 6 psi (41.4 kPa) would result in an even higher coefficient of determination R^2, using such a relatively low pressure intensity requires more experimental control and more careful adjustments of the pressure regulators than the higher pressures. The equilibrium moisture content is a function of the pressure intensity applied, i.e., for low pressure, WC_t is higher than that obtained under high pressures. Also, it was observed that transferring the soil samples from the ceramic plates to the containers after releasing the pressure was easier at 10 psi (68.9 kPa) pressure intensity.

Liquid Limit Relationships

The liquid limit prediction model,

$$LL = -3.50 + 1.50\ WC_{10} \quad (1)$$

was applied to the check sample data. The coefficient of determination, R^2, resulting from applying model 1 to the check sample data was 0.89.

To investigate the possibility of a better fitting model for the check samples, a regression analysis of the check sample data was made. The analysis resulted in the following linear model with a coefficient of determination, $R^2 = 0.92$:

$$LL = -4.38 + 1.45\ WC_{10} \quad (2)$$

A plot of standard LL values versus WC_{10} for the check samples together with models 1 and 2 is shown in Figure 3. The deviations of the predicted values from the standard values using both models 1 and 2 are summarized in Table 3.

The next step in this analysis was to compare statistically the original and check sample models. Both models have a general form of the type

$$LL = b_0 + b_1\ WC_{10} \quad (3)$$

It was found that the slope b_1 and the intercept b_0 of the Purdue sample model lie within the 95 percent confidence limits for the regression coefficients β_1 and β_0 respectively of the check sample model. The shift in intercept values could be attributed primarily to operator variability.

These models suggest that a linear model may be the best fit to define the LL versus WC_{10} relationship for any soil. However, for good correlation one might have to adjust the parameters b_0 and b_1 for soils from different geographic areas.

Plastic Limit Relations

A correlation analysis of PL and WC_{10} for the 144 check samples resulted in a simple correlation coefficient, $r = 0.63$. Because of the apparent low correlation when the results of all 144 samples were used, it was decided to restrict the verification of the PL relationship to just those soils having a PI < 21 percent and an LL < 50 percent. This constitutes the inference space of the model developed earlier (Purdue data) and it also covers the majority of soils that an agency would test under normal circumstances.

The data lying inside the prescribed range were included for the analysis (91 data points). The plastic limit prediction model (Purdue data),

$$PL = 2.0 + 0.75\ WC_{10} \quad (4)$$

the best fitting linear regression model (from check samples),

$$PL = 4.77 + 0.54\ WC_{10} \quad (5)$$

Table 3. Summary of deviation of predicted LL values from the standard values.

Deviation[a]	Purdue Sample Model[b]		Check Sample Model[c]	
	No. of Observations	Percent of Observations	No. of Observations	Percent of Observations
1-2	65	45.2	87	60.5
3-4	42	29.2	36	25.0
>4	37	25.6	21	14.5

[a]Standard LL minus predicted LL in percent.
[b]Using the model LL = -3.50 + 1.50 WC_{10}.
[c]Using the model LL = -4.38 + 1.45 WC_{10}.

Figure 4. Relationship between plastic limit and moisture content at 10 psi (68.9 kPa) for the check samples (91 data points).

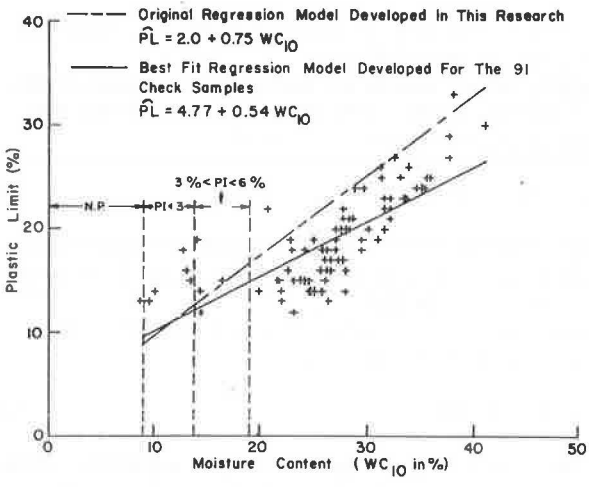

Table 4. Summary of deviation of predicted PL values from the standard values.

Deviation[a]	Purdue Sample Model[b]		Check Sample Model[c]	
	No. of Observations	Percent of Observations	No. of Observations	Percent of Observations
1-2	19	21.0	57	62.5
3-4	27	29.5	29	32.0
>4	45	49.5	5	5.5

[a]Standard PL minus predicted PL in percent.
[b]Using the model PL = 2.0 + 0.75 WC_{10}.
[c]Using the model PL = 4.77 + 0.54 WC_{10}.

and the reduced data (91 data points) are shown in Figure 4. Model 5 resulted in a coefficient of determination $R^2 = 0.60$. The simple correlation coefficient, r, between PL and WC_{10} for the reduced data increased to 0.78.

The deviations of predicted values, using both models 4 and 5, from the standard plastic limits are summarized in Table 4.

Nonplastic and Low-Plasticity Soils

It was observed that the ranges of WC_{10} values postulated for nonplastic and low-plasticity soils are valid for the check sample data. These ranges are indicated in Figures 3 and 4.

CONCLUSIONS

The objective of this study was to investigate the feasibility of using the moisture tension method to determine Atterberg limits. The conclusions are as follows:

1. Linear relationships were developed between the consistency limits (LL and PL) and the moisture content, WC_1, obtained at 6, 10, 12, and 18 psi (41.4, 68.9, 82.7, and 124.1 kPa) pressure intensity. These relationships offer the possibility of using linear models, correlating the consistency limits with the moisture content for predicting liquid and plastic limits.
2. The nonplastic and low-plasticity soils can be identified by their WC_1 values as obtained by the moisture tension method.
3. The results of the verification of the consistency limits-WC_{10} relationships indicated that the liquid limit prediction model showed good agreement with the best-fitting linear regression model for the check sample data. A linear relationship for these parameters explains 92 percent of the variation in the data. The plastic limit model resulted in a relatively poor prediction of the plastic limit values of the check samples. The analysis to determine the best-fitting linear model for the check sample data resulted in an R^2 value of 0.60. This low value can possibly be explained by the fact that forces other than capillarity affect the moisture tension test results, especially in the case of clays. Baver (1) suggested that the water-holding capacity of soils is a function of the clay content, the type of clay minerals, amount of organic matter, and porosity. It is possible that different mineralogical characteristics and origin of the check soils may have caused the differences observed during the verification of these models. Further, some of the difference can be attributed to the variability between different operators. The range of WC_{10} values suggested previously for nonplastic soils as well as those with low plasticity (based on original data) was verified by the check sample data.

ACKNOWLEDGMENTS

This research was sponsored by the Indiana State Highway Commission.

REFERENCES

1. Baver, L. D. Soil Physics, 3rd Ed. John Wiley, New York, 1956.
2. Casagrande, A. Research on the Atterberg Limits of Soils. Public Roads, Oct. 1932, pp. 121-130.
3. Casagrande, A. Classification and Identification of Soils. Trans. ASCE, Vol. 113, 1948, pp. 901-991.
4. Dawson, R. F. Investigations of the Liquid Limit Test on Soils. Symposium on Atterberg Limits, ASTM Special Tech. Publ. 254, 1959, pp. 190-195.
5. Draper, N. R., and Smith, H. Applied Regression Analysis. John Wiley, New York, 1966.
6. Gadallah, A. A. Determination of Consistency Limits of Soils by Moisture Tension Method. Joint Highway Research Project, Purdue Univ., Research Rept. 4, Feb. 1973.
7. Grim, R. E. Applied Clay Mineralogy. McGraw-Hill, New York, 1962.
8. Livneh, M., Kinsky, J., and Zaslavsky, D. Correlation of Suction Curves With the

Plasticity Index of Soils. Jour. of Materials, JMLSA, Vol. 5, No. 1, March 1970, pp. 209-220.
9. Morris, M. D., Ulp, R. B., and Spinna, R. J. Recommendations for Changes in the Liquid Limit Test. Symposium on Atterberg Limits, ASTM Special Tech. Publ. 254, 1959, pp. 203-211.
10. Nishio, T. K. An Investigation of the Use of the Moisture Tension Method for Determination of Liquid and Plastic Limit Values of Soil. Joint Highway Research Project, Purdue Univ., Research Rept. 15, July 1972.
11. Ostle, B. Statistics in Research. Iowa State Univ. Press, Ames, 1963.
12. Richards, L. A. Methods of Measuring Soil Moisture Tension. Soil Science, No. 68, 1949, pp. 95-112.
13. Richards, L. A. Porous Plate Apparatus for Measuring Moisture Retention and Transmission by Soil. Soil Science, No. 66, 1948, pp. 105-110.
14. Rollins, R. L., and Davidson, D. T. The Relation Between Soil Moisture Tension and Consistency Limits of Soils: Methods for Testing Engineering Soils. Iowa Engineering Experiment Station, Bull. 192, 1960, pp. 210-220.
15. Russell, E. R., and Mickle, J. L. A Study to Correlate Soil Consistency Limits With Soil Moisture Tensions. Engineering Research Institute, Iowa State Univ., Final Rept., Project 490-S, 1965.
16. Russell, E. R., and Mickle, J. L. Liquid Limit Values by Soil Moisture Tension. Jour. Soil Mechanics and Foundations Div., ASCE, Vol. 96, No. SM3, May 1970, pp. 967-989.
17. Seed, B. H., Woodward, R. J., and Lundgren, R. Fundamental Aspects of Atterberg Limits. Jour. Soil Mechanics and Foundations Div., ASCE, Vol. 90, No. SM6, Nov. 1964, pp. 75-109.
18. Sultan, H. A. Relation Between Soil Moisture Tension and the Consistency Limits for Utah Soils. Univ. of Utah, unpublished MS thesis, 1961.
19. Terzaghi, K., and Peck, R. B. Soil Mechanics in Engineering Practice. John Wiley, New York, 1967.
20. Uppal, H. L. A Scientific Explanation of the Plastic Limit of Soils. Jour. of Materials, Vol. 1, No. 1, March 1966, pp. 164-179.

DISCUSSION

J. Neil Kay, School of Civil and Environmental Engineering, Cornell University

A definite need exists to find alternative methods for determination of Atterberg limits. As the authors have indicated, the conventional methods are time-consuming and, in addition, subject to considerable human error. In any attempt to develop alternative methods, however, the full significance of the results of these tests must be kept in mind. The standard tests appear crude and unscientific to those who are unfamiliar with soil classification, but this is far from the truth. In fact, as far as engineering purposes are concerned no facet of soil classification comes closer to gaining universal acceptance than application of Atterberg limit tests. This is no coincidence. Judicious consideration of both the liquid and plastic limits sometimes in conjunction with other index properties has proved over the years to be a remarkable indicator of soil performance for engineering applications.

In their paper the authors suggest that both the liquid limit and the plastic limit may be obtained from a single test result. This is entirely contrary to the basic meaning and significance of the Atterberg limit tests. The implication for such a proposal is that the liquid limit and plastic limit (and consequently the liquid limit and plasticity index) are uniquely related. This is seen by combining the authors' respective prediction models:

$$LL = -3.50 + 1.50\ WC_{10} \quad (1)$$

$$PL = 2.0 + 0.75\ WC_{10} \quad (4)$$

Combining (1) and (4) leads to

$$LL = 2.0\ PL - 7.50 \quad (6)$$

and introducing the plasticity index gives

$$PI = 0.5\ LL - 3.75 \quad (7)$$

A further implication of Eq. 7 is that the liquid limit may replace plasticity index as a predictor of soil performance.

Equation 7 may be plotted on the standard plasticity chart. This has been done in Figure 5 together with some typical soils as described by Terzaghi and Peck (19). It becomes obvious from this diagram that the very basis for distinction between soil types is lost in the method proposed by the authors. It is absolutely essential that determination of liquid and plastic limits be made from independent tests. A calibration of the method would be possible within a given soil type, but then one might as well measure liquid limit alone. At any rate, the most frequent use of the Atterberg limits is to define the soil type in the first place.

The moisture tension method appears to be valid as a reliable predictor of liquid limit. However, even for a large number of samples there is some question of feasibility from a time and cost standpoint. This writer is of the opinion that the liquid limit may be most cheaply and reliably predicted for a wide range of fine-grained soils by use of the Swedish fall-cone as discussed by Sherwood and Riley (21).

REFERENCE

21. Sherwood, P. T., and Riley, M. D. An Investigation of a Cone Penetrometer Method for the Determination of the Liquid Limit. Geotechnique, Vol. 20, No. 2, June 1970, pp. 203-208.

AUTHORS' CLOSURE

The authors wish to thank Professor Kay for his review and discussion of our paper. We would like to point out that his discussion is based on extrapolation of our data and prediction models, which would not be appropriate when using a statistical analysis approach.

During the first phase of the study, the liquid and plastic limit prediction models 1 and 4 respectively were developed using soils with a PI < 21 percent and an LL < 50 percent. This constitutes the inference space of the prediction models. In the second phase, which dealt with verifying these prediction models, the liquid limit prediction models gave a good result when used for the check samples, which represent a large range of normal soil texture. At the same time, because of the low correlation between the PL and WC_{10} for the check samples, the verification of the PL relationship using the check samples was restricted to just those soils having a PI < 21 percent and LL < 50 percent, which in turn constitutes the inference space of the models developed using Purdue data.

In other words, the liquid limit prediction models are valid for a wide range of normal soil texture, while the plastic limit prediction models presented were found to be valid only within the range of soils used in the study. It must be kept clearly in mind that the method is primarily recommended for agencies that run hundreds of these tests on soils within the ranges normally encountered, i.e., the ranges that constitute the inference space of the models. The method is not recommended in areas where there are troublesome soils such as clays of very high plasticity. Nor is the method, without a great deal of additional study, applicable to soils that plot far from

Figure 5. Plasticity chart showing implications of proposed method.

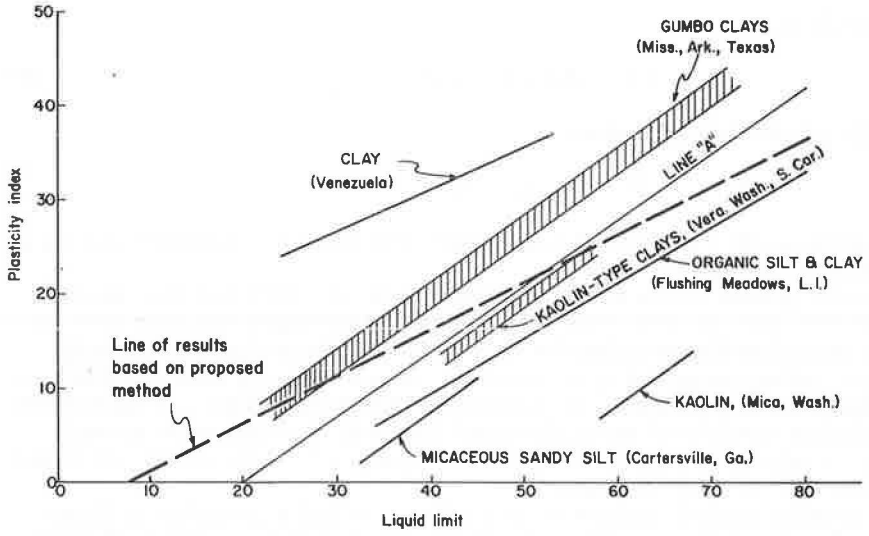

Figure 6. Plasticity chart.

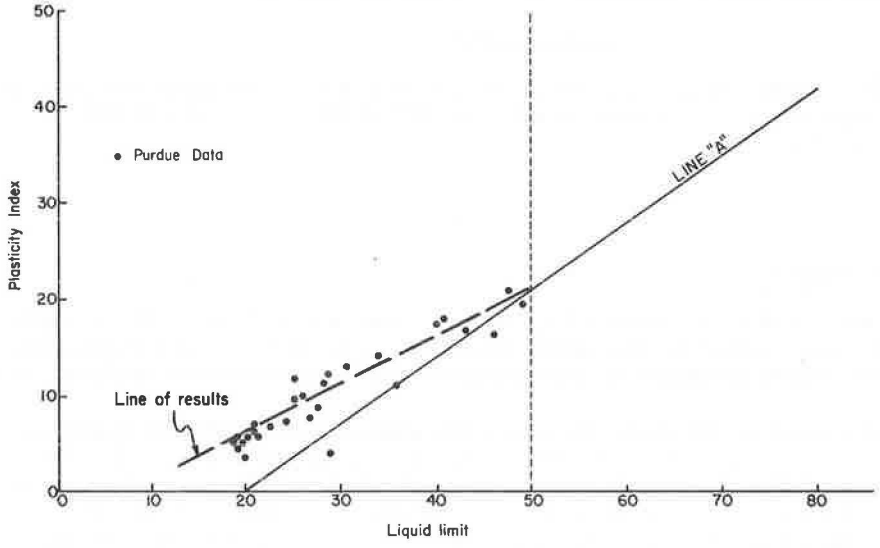

the A line (micaceous soils, highly organic soils, etc.). The authors intend that the method be an engineering tool, which must be used with sound engineering judgment or common sense. Furthermore, the line of results of our study, which is shown in Figures 5 and 6, does not provide a conflict with the basis for distinction between soil types within the inference space of the study. Although we do not place great importance on it, we are pleased that the line of results based on our method is as close to the A line as the figure shows. We feel this is another "proof" of its validity.

THE INFLUENCE OF CUP FRICTION AND GRADING ON THE LIQUID LIMITS OF SOME GHANAIAN SOILS

N. K. Kumapley and K. E. Inkabi, Department of Civil Engineering,
University of Science and Technology, Kumasi, Ghana

ABRIDGMENT

•THE history of the development of soil consistency limit tests from the pioneering work of the Swedish soil scientist, Atterberg, in 1911 to the present stage has been well documented (1, 15). Starting in the late 1920s, extensive research in America on the consistency limits (4, 5, 7) culminated in the standardization of the method of determining the liquid limit and the evolution of soil identification and classification systems based on these limits and particle size distribution of the soil.

The basic condition for the validity of these classification systems is that both the particle size distribution test and the Atterberg limit tests should yield reproducible results using standard testing procedures. Most temperate-zone soils and some laterites meet this condition and can therefore be reliably classified using existing standard procedures. These procedures, however, appear to break down when they are applied to the identification and classification of the so-called troublesome soils that do not yield reproducible results of particle size distribution and Atterberg limits. This group of soils includes micaceous soils (14, 23) and silty or sandy soils of low plasticity (24). The main difficulty with the Atterberg limit tests appears to be the tendency of these soils to either slip in the liquid limit cup or liquefy with shock during the test, thus giving inconsistent results. The difficulties experienced in attempting to classify these "troublesome" soils using standard testing procedures call for a reexamination of the validity of these standard testing procedures when applied to these soils.

ENGINEERING SIGNIFICANCE OF THE ATTERBERG LIMITS

Notwithstanding their essentially empirical and arbitrary origin, the Atterberg limits rapidly assumed increasing importance with the establishment of useful empirical and semi-empirical correlations between them and other more fundamental soil properties. Some of these correlations are between the Atterberg limits and such soil properties as the consolidation characteristics of remolded clays (20), percentage of clay content (17, 19), cone penetration resistance (24), soil moisture tension (16), California bearing ratio (2), swell potential of expansive soils (25), and shear strength.

The considerable research effort directed toward a study of the soil consistency limits has highlighted some serious shortcomings of the present method of determining the liquid limit and has led to attempts to replace the use of the Casagrande liquid limit device with more "reliable" techniques. Some of the methods proposed in the literature are the use of cone penetrometers (9, 24), laboratory vane tests (6), and the measurement of soil moisture tension (16). In spite of the fact that most of these methods have been claimed to be superior to the conventional Casagrande device, none, with perhaps the exception of the cone penetrometer test, has found universal acceptance to date. It is reasonable to suppose, therefore, that the conventional Casagrande device will continue to be used for a long time to come. This paper proposes a possible modification to the conventional device to overcome one of its main drawbacks, namely the inability of the present device to give reproducible results in micaceous and silty soils of low plasticity.

Publication of this paper sponsored by Committee on Soil and Rock Properties.

LIMITATIONS OF THE CONVENTIONAL LIQUID LIMIT TEST

Various investigators have discussed in detail the main limitations of the conventional liquid limit device in relation to the design of the apparatus and its accessories (5, 8, 13), operator errors (11, 18), and soil type, particularly the difficulty of obtaining reproducible results of the liquid limits of micaceous soils and silty and sandy soils of low plasticity (24). For example, Tubey and Bulman (23) reported that consistency limit tests on a sample of a Ghanaian micaceous soil yielded liquid limits ranging from 54 to 65 percent and plastic limits varying from 43 to 36 percent, resulting in a range of plasticity indices from 11 to 29 percent. Ruddock (14), who also experienced considerable difficulty in obtaining meaningful consistency limit values on similar soils, appeared to have reached the same conclusion as Tubey and Bulman (23) and Newill (12) that linear shrinkage probably provided a more reliable basis for the classification of these soils.

In order to obtain consistent liquid limit results on these "troublesome" soils it has been suggested that the roughness of the inside of the cup also be standardized (5, 22). However, as far as the authors are aware, no attempt has been made to evaluate the influence of the roughness of the inside of the cup on liquid limit values. The present study investigates this influence.

THE SHEAR STRENGTH OF A SOIL AT THE LIQUID LIMIT

Probably because of the realization that the mechanized liquid limit test is essentially a dynamic shear test (5) and because of the desire, therefore, to substitute more reliable shear tests for the determination of the liquid limit, the shear strength aspects of the Atterberg limits have received considerable attention from researchers (5, 6, 9, 13, 21, 24).

The value of the undrained shear strength of a soil at the liquid limit reported in the literature varies between 0.1 psi (0.68 kPa) and 0.52 psi (3.58 kPa). Various factors may account for this relatively wide range of variation in shear strength, but perhaps the main factor is the difficulty associated with the measurement of low values of shear strength. Most laboratories use the miniature laboratory vane apparatus for this purpose, but it has been established that the value of the undrained shear strength obtained is influenced by the size of sample and the size of vane (6), the accuracy with which the failure torque can be measured, and the assumptions made regarding the distribution of shear stresses across the ends of the vane.

It is therefore fair to conclude that, while the shear strength of a soil at the liquid limit may fall within a small but measurable range of values, such a range would have to be established for a given situation. The first part of this study therefore concerned the establishment of such a range of shear strength values for some typical plastic Ghanaian clays.

SOIL TYPES INVESTIGATED

Two groups of soils were tested. The first group was composed of plastic clays of sedimentary or residual origin. These soils do not slip in the liquid limit cup and therefore give fairly reproducible results. The second group of soils included the residual soils derived from the chemical decomposition of local rocks, particularly granites. Most of these residual soils, which are micaceous, sandy, or silty clays of low plasticity, occur extensively in Ghana. Typical particle size distribution curves for both groups of soils are shown in Figure 1.

LIQUIDITY INDEX-UNDRAINED SHEAR STRENGTH RELATIONSHIP FOR SOME GHANAIAN CLAYS

The soils selected for this study were plastic clays of the type that would not normally slip in the liquid limit cup. The investigation involved the measurement of the undrained shear strength of these soils over a wide range of consistencies, using a motorized laboratory vane apparatus with a $\frac{1}{2}$-in. diameter vane.

The Atterberg limits of these soils were also determined according to methods

stipulated in the relevant British Standards (3), thus enabling graphs of undrained shear strength to be plotted against liquidity index for these soils (Fig. 2). It can be seen from this figure that the undrained shear strengths corresponding to a liquidity index of unity (i.e., the liquid limit) ranged from 0.15 lb/in.^{2} to 0.25 lb/in.^{2} (1.03 to 1.72 kPa). This range of undrained shear strength values has therefore been accepted as defining the "true" liquid limit for local soils.

THE REPRODUCIBILITY OF THE ATTERBERG LIMITS

In a comparative study of this nature, likely to involve the performance of numerous Atterberg limit tests by various operators extending over a long period, it was considered essential that the inherent range of variability in the Atterberg limits be established for the set of operators used. Liquid and plastic limit determinations were made on two soil types by a set of fairly experienced operators. Based on a statistical analysis of the results using the method of variance, it was concluded that, while there were significant differences between operators even at the 5 percent level, for a given operator there were no significant differences between trials even at the 1 percent level. It was further concluded that for a confidence limit of 95 percent the set of operators used in this study could reproduce both the liquid and plastic limits to an accuracy of ±2 percent. Similar conclusions have been reached by other research workers on the basis of more detailed studies (11, 18). As a result of these findings, steps were taken to ensure that during the study the same operator performed all the tests on a particular sample and that the same liquid limit device was used in performing a set of tests.

INFLUENCE OF ROUGHNESS OF THE INSIDE OF THE CUP ON THE LIQUID LIMIT

In order to study the influence of the roughness of the inside of the cup on the liquid limits of soils, the insides of various liquid limit cups were roughened with portions of washed beach sand retained on B.S. sieve Nos. 14, 18, 36, 60, 100, 150, 200, and 240. The roughening was done by applying a thin film of araldite to the inside of the cup prior to sprinkling the sand lightly to cover the whole of the inside of the cup with the exception of the central part, which was kept clear to facilitate easier cutting of the groove. This was achieved by pasting a $\frac{1}{8}$-in. wide strip of paper along the center of the cup before sprinkling the sand. The cups were then cured in the oven for 24 hours at a temperature of 105 C. The roughening produced by this technique was effective enough to be used for a long time without the sand particles mixing with the soil being tested. It was only necessary to wash the inside of the cup under running water and mop it dry after each blow-count.

The liquid limits of six soils were determined using the eight roughened cups in addition to the standard smooth cup. The soils tested included three plastic clays and three micaceous soils. The liquid limit values were plotted against the nominal size of roughening taken as the aperture of the sieve on which the roughening sand was retained (Fig. 3). It may be seen from this figure that, while the liquid limits of the plastic clays appeared to be unaffected by the size of roughening, those of the micaceous soils generally increased with increasing size of roughening up to a nominal size of roughening of 0.015 in. (0.38 mm), after which they remained essentially constant.

It would appear, therefore, that the minimum size of roughening that would eliminate the tendency of these micaceous soils to slip in the liquid limit cup is of the order of 0.015 in. (0.38 mm), which is close to the aperture of the No. 36 B.S. sieve, 0.0166 in. (0.4216 mm). The cup roughened with sand retained on the No. 36 B.S. sieve was therefore adopted as the standard rough cup in the subsequent study.

THE "TRUE" LIQUID LIMIT OF A SILTY OR MICACEOUS SOIL

Liquid limits of selected plastic clays and silty and micaceous soils were determined using both the conventional liquid limit cup and the roughened cup. Plastic limits were also determined for these soils as well as their undrained shear strengths, which

Figure 1. Typical particle size distribution of (a) plastic clays and (b) micaceous and silty soils.

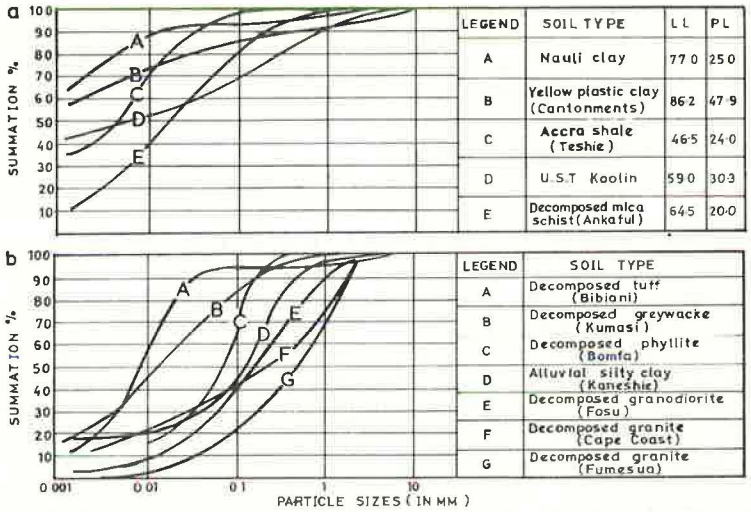

Figure 2. Liquidity in index-undrained shear strength relationship for some plastic Ghanaian clays.

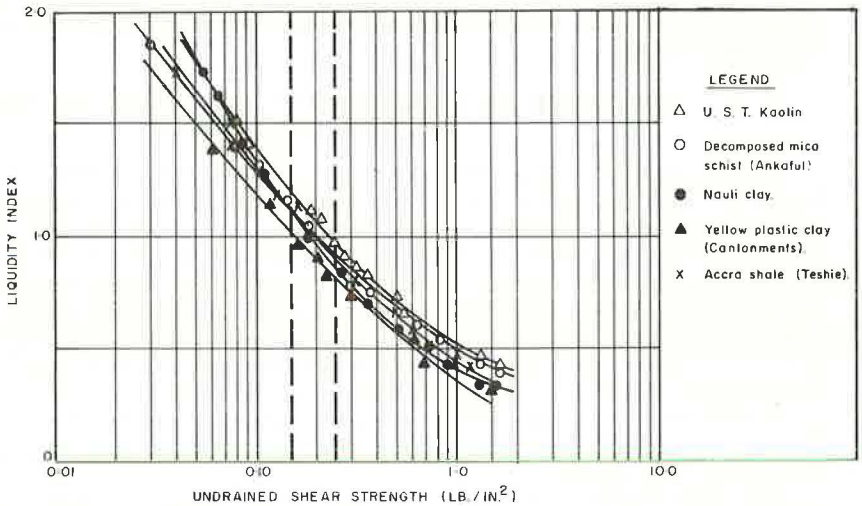

Figure 3. Effect of the nominal size of roughening of cup on the liquid limit.

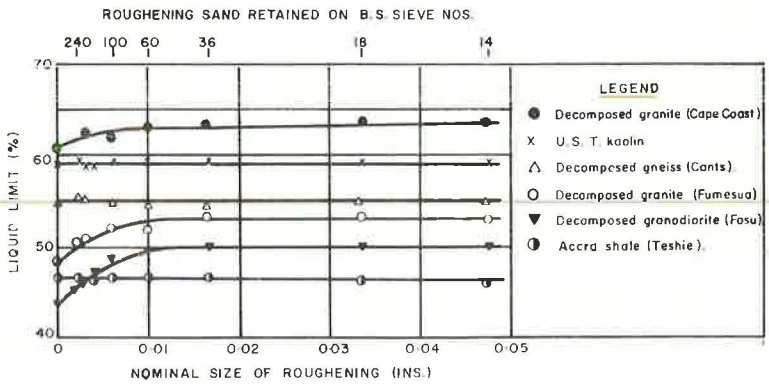

were measured at various consistencies. Typical curves of liquidity index versus undrained shear strength for six of the "troublesome" soils and two plastic clays are given in Figure 4. It is clear from Figures 4a to 4f that for the silty and micaceous soils the liquidity index-undrained shear strength relationships based on the roughened cup liquid limits gave values of undrained shear strength within the range 0.15 psi to 0.25 psi (1.03 to 1.72 kPa) at the liquid index of unity and that the curves based on standard cup liquid limits gave shear strength values outside this range.

For the plastic clays (Figs. 4g and 4h) both curves lie within the established range of shear strength at the liquidity index of unity. In general, the liquid limits obtained using the roughened cup were higher than those obtained from the conventional cup, the percentage increases in liquid limit varying between 3.7 and 80 percent for the 12 micaceous and silty clays tested.

This tends to indicate that the use of the roughened cup instead of the standard cup would only alter the liquid limits of soils that give "erroneous" results with the standard cup and would not substantially affect the liquid limits of soils that do not slip in the standard cup. Unpublished results of tests currently in progress show that, for the silty and micaceous soils, liquid limits determined using cone penetrometers also correlate fairly well with those determined using the roughened cup.

INFLUENCE OF MAXIMUM PARTICLE SIZE ON THE LIQUID AND PLASTIC LIMITS

Current standards stipulate that the Atterberg limits be determined on the portion of the soil finer than No. 40 sieve in American practice and No. 36 sieve in British practice. The reasoning behind the choice of these sieve sizes as the upper limit of particle sizes for the consistency limit tests is not clear. Lambe (10), for example, questioned the choice and suggested that it would appear more logical to run the Atterberg limit tests on portions of the soil finer than No. 140 or No. 200 U.S. standard sieves.

In order to investigate the possibility that the use of the portion of soil with a smaller maximum particle size may eliminate flaky mica particles and reduce the possibility of these micaceous soils slipping in the conventional cup, it was decided to study the influence of maximum particle size on the liquid and plastic limits of soils. The liquid and plastic limits of soils passing B.S. sieve numbers 14, 18, 25, 36, 60, 100, 150, and 200 were determined using the conventional liquid limit device. The soils investigated included both plastic clays and micaceous and silty soils.

It was found that there were only slight increases in the liquid and plastic limits of the portions of the soils passing B.S. sieve No. 14 and retained on B.S. sieve No. 60. The liquid and plastic limits of the portions finer than the No. 60 B.S. sieve, however, increased sharply with decreasing maximum particle size. Figure 5 shows that the relationship between the plasticity indices (PI) and the maximum particle size is of a similar form.

While it is recognized that the difference between the plasticity indices of the portions of soil passing the No. 36 and No. 60 B.S. sieves may be negligible, it is suggested that the No. 60 B.S. sieve, which appears to represent the maximum particle size beyond which there is a rapid increase in plasticity, be adopted as the lower limit of particle size for the determination of the liquid and plastic limits.

ACKNOWLEDGMENT

Some of the work reported in this paper was an extension of a project done under the supervision of the senior author by the junior author and A. S. Bawa in partial fulfillment of the requirements of the B.Sc. (Eng.) degree at the University of Science and Technology, Kumasi, Ghana.

REFERENCES

1. Bauer, E. F. History and Development of the Atterberg Limit Tests. Symposium on Atterberg Limits, ASTM Spec. Tech. Publ. 254, 1959.

Figure 4. Effect of roughening of cup on the liquidity index-undrained shear strength relationship.

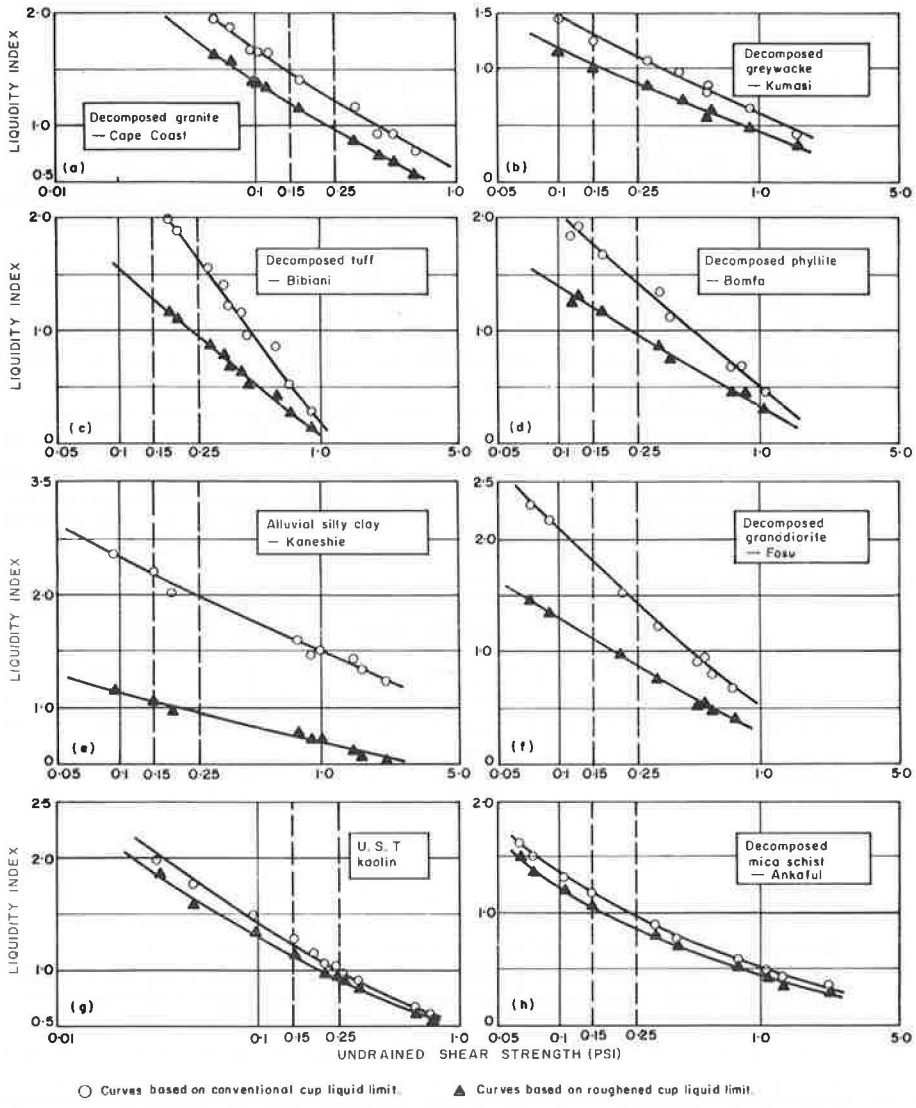

Figure 5. Influence of maximum particle size on the plasticity index.

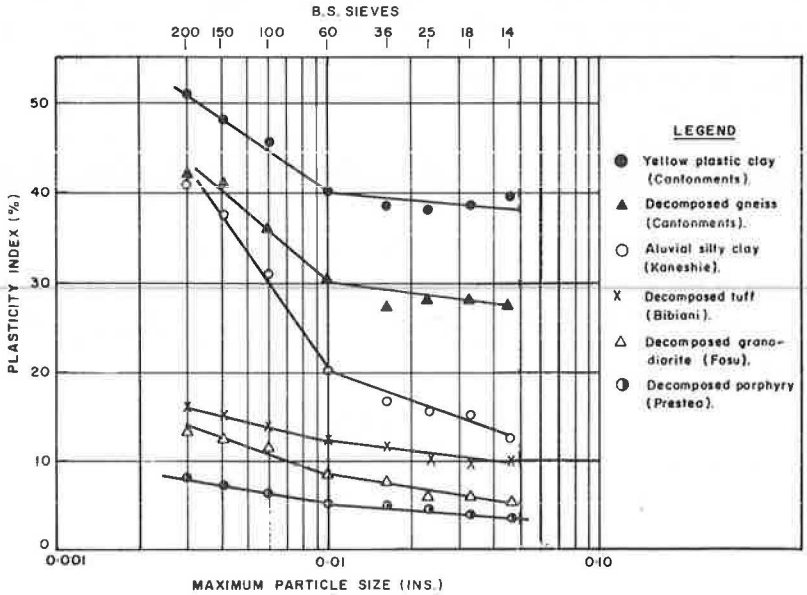

2. Black, W. P. M. A Method of Estimating the California Bearing Ratio of Cohesive Soils From Plasticity Data. Geotechnique, Vol. 12, 1962, pp. 271-282.
3. Methods of Testing Soils for Civil Engineering Purposes. British Standards Institution, B. S. 1377, 1961.
4. Casagrande, A. Research on the Atterberg Limits of Soils. Public Roads, Vol. 13, 13, No. 8, pp. 121-130, 1932.
5. Casagrande, A. Notes on the Design of the Liquid Limit Device. Geotechnique, Vol. 8, No. 2, June 1958.
6. Darienzo, M., and Vey, E. Consistency Limits of Clay by the Vane Method. HRB Proc., Vol. 34, 1955, pp. 559-566.
7. Hogentogler, C. A., Wintermyer, A. M., and Willis, E. A. The Subgrade Soil Constants, Their Significance, and Their Application in Practice. Public Roads, Vol. 12, No. 5, 1931, pp. 117-144.
8. Hovanyi, P. A New Grooving Tool. Geotechnique, Vol. 8, No. 2, June 1958.
9. Karlsson, R. Suggested Improvements in the Liquid Limit Test, With Special Reference to Flow Properties of Remoulded Clays. Proc. 5th International Conf. on Soil Mechanics and Foundation Engineering, Paris, Vol. 1, 1961.
10. Lambe, T. W. Soil Testing for Engineers—6th Ed. John Wiley, New York, 1960, p. 24.
11. Liu, T. K., and Thornburn, T. M. Study of the Reproducibility of Atterberg Limits. Highway Research Record 63, 1964, pp. 22-31.
12. Newill, D. An Investigation of the Linear Shrinkage Test Applied to Tropical Soils. British Road Research Laboratory, Road Research Note RN/4106/DN, unpublished, 1961.
13. Norman, L. F. J. A Comparison of Values of Liquid Limit Determined With Apparatus Having Bases of Different Hardness. Geotechnique, Vol. 8, No. 2, June 1958.
14. Ruddock, E. C. Residual Soils of Kumasi District in Ghana. Geotechnique, Vol. 18, No. 4, December 1967.
15. Russell, E. R., and Mickle, J. L. A Study to Correlate Soil Consistency Limits With Soil Moisture Tensions. Engineering Research Institute, Iowa State Univ., final rept., Project 490-S, 1965.
16. Russell, E. R., and Mickle, J. L. Liquid Limit Values by Soil Moisture Tension. Jour. Soil Mechanics and Foundations Div., ASCE, No. SM 3, May 1970.
17. Seed H. B., Woodward, R. J., and Lundgren, R. Clay Mineralogical Aspects of the Atterberg Limits. Jour. Soil Mechanics and Foundations Div., ASCE, Vol. 90, No. SM4 1964.
18. Shook, J. F., and Fang, H. Y. A Study of Operator Variability in the Determination of Liquid and Plastic Limits of Soil. Highway Research Abstracts, Vol. 31, No. 9, special paper, 1961, pp. 26-28.
19. Skempton, A. W. The Colloidal Activity of Clays. Proc., 3rd International Conf. on Soil Mechanics and Foundation Engineering, Zurich, Vol. 1, 1953.
20. Skempton, A. W. Notes on the Compressibility of Clays. Quarterly Journal of the Geological Society, Vol. 100, London, 1944.
21. Skempton, A. W., and Bishop, A. W. Soils. In Building Materials, Their Elasticity and Inelasticity (Reiner, M., ed.), North Holland Publishing, Amsterdam, 1954.
22. Sowers, G. F., Vesic, A., and Grandolfi, M. Penetration Tests for Liquid Limit. Symposium on Atterberg Limits, ASTM Spec. Tech. Publ. 254, 1959.
23. Tubey, L. W., and Bulman, J. N. Micaceous Soils—Methods of Determining Mica Content and the Use of Routine Tests in the Evaluation of Such Soils. Proc., 2nd Conf., Australian Road Research Board, Vol. 2, 1964.
24. Uppal, H. L., and Aggarwal, H. R. A New Method of Determining the Liquid Limit of Soils. Central Road Research Institute, New Delhi, Bull. 19, 1958.
25. Williams, A. A. B. Discussion of Jennings, J. E. B., and Knight, K. The Prediction of Total Heave From Double Oedometer Test. Symposium on Expansive Clays, South African Institution of Civil Engineering, 1957-58.

DILATANCY OF GRANULAR MEDIA IN TRIAXIAL SHEAR

K. P. George, Department of Civil Engineering, University of Mississippi; and
N. S. Shah, Sargent and Lundy, Chicago

ABRIDGMENT

•COHESIONLESS (granular) aggregates depend on the friction and the interlocking action between the individual particles for strength and stability. Crushed rock and natural river gravel, both widely used in flexible pavements, are examples of this type of material.

The fundamental assumptions of the strength theories ignore the fact that granular soil consists of individual grains rather than a homogeneous mass with certain mechanical properties. A particulate approach is emphasized in this study; that is, granular soils consist of randomly arranged, irregularly shaped, discrete particles that are free to displace relative to each other.

Idealizing the granular media to a continuum, the criterion of failure under the triaxial stress system, where the effective principal stresses are $\bar{\sigma}_1$ and $\bar{\sigma}_2 = \bar{\sigma}_3$, is given by

$$\bar{\sigma}_1 = \bar{\sigma}_3 \tan^2 \frac{\pi}{4} + \frac{\phi_d}{2} \quad (1)$$

in which $\bar{\sigma}_1$ and $\bar{\sigma}_3$ = maximum and minimum principal effective stresses respectively and ϕ_d = drained angle of friction. A straight slip line is predicted at failure that subtends an angle of $(\pi/4 + \phi_d/2)$ to the major principal plane. Equation 1 suggests that the assembly slides at failure with no volume change, just as in the case of two blocks of material in a simple friction test. Nevertheless, Osbourne Reynolds as early as 1885 reported that dense sands expand at failure, a condition which he named dilatancy. Several other researchers (4, 7, 8) investigated this problem and concluded that, in general, all specimens weak at yield (very loose) must be compacting and that all specimens strong at yield (dense) must be dilating.

In this study equations for volume change are derived in accordance with the particulate model advanced by Rowe (10). Using the stress-deformation results obtained from triaxial compression tests, the volumetric strain of two granular materials (a natural gravel and a crushed limestone) during triaxial loading are predicted and compared with the observed data. We also discuss how dilatancy/contraction is influenced by (a) surface texture of particles, (b) elastic properties of individual grains, (c) geometrical factors such as grain size and shape factors, and (d) packing of the mix.

ANALYSIS OF A SIMPLIFIED MODEL OF COHESIONLESS SOIL

The behavior of granular masses subject to external forces and displacement is governed by the individual forces and displacements occurring at each particle contact. Thurston and Deresiewicz (12) used a regular array of perfectly uniform spheres, in which each sphere was in contact with 12 others (face-centered cubic array), and discussed the conditions under which sliding of adjacent layers occurs. They derived a ratio of shearing to normal forces on the potentially sliding layer of spheres, given as

Publication of this paper sponsored by Committee on Soil and Rock Properties.

$$\frac{D \cos \beta}{2\sqrt{3}\, R^2 \sigma_3 + D \cos \gamma} = \frac{3 + 4\sqrt{2}\mu}{2(\sqrt{6} - \mu)} \tag{2}$$

in which D = the force tending to cause movement; R = radius of a single sphere; σ_3 = initial hydrostatic pressure to which the assembly is subjected; μ = coefficient of physical friction; and β and γ = respectively the angles made by D with the $\bar{y}$- and $\bar{z}$-axis. In the absence of friction, shearing force is required to do work in order to lift the sliding balls toward the crest against the hydrostatic stress, which can be obtained by setting $\mu = 0$ in Eq. 2. This latter component of shear strength is often designated as the dilatancy component.

PROPORTIONING THE MATERIALS

Two contrasting granular materials were selected for the laboratory testing: a natural gravel (specific gravity 2.82) and a crushed limestone (specific gravity 2.65). Each of these materials was separated into various fractions; for example, 25.4 mm to 19.0 mm, 19.0 mm to 12.7 mm, and so on. Various components stored separately were then combined to result in a graded material, as shown in Figure 1.

TRIAXIAL TEST DETAILS

The granular aggregates were tested in triaxial compression using samples measuring approximately 100 mm (4 in.) in diameter and 200 mm (8 in.) in height. Complete saturation was ensured before testing under a confining pressure of 100 kPa (15 psi). A constant rate of strain, 0.3 percent per minute, was maintained throughout the test.

The volume change of the sample was estimated by reasoning that in a fully saturated sample the volume of water expelled or drawn in is a direct measure of the volume change of the sample. As described by Bishop and Henkel (1), the volume of water expelled or drawn in is measured by a 100-ml burette.

The observed strength results were adjusted for membrane correction, as proposed by Henkel and Gilbert (3), and for the chamber piston friction by direct measurement. The nonuniformity in deformation resulting from possible end restraints was minimized by using lubricated end plates.

STRESS-DEFORMATION CHARACTERISTICS OF THE MATERIALS

Stress ratio and volumetric strain are plotted in Figure 2 as functions of axial strain for the two gravels compacted to respective maximum densities. During the initial stage the strains are small and nearly proportional to stress. Sliding between particles does not begin until the stress increment exceeds some critical stress ratio, approximately 3 and 4 for round gravel and limestone respectively. Due only to slippage, both materials exhibited nonlinear stress-strain relationships, the more so in the round gravel. In both gravels, as the shear motion continues, the degree of interlocking decreases, as evidenced by the decrease in shear resistance. Of the two mixes, round gravel experiences considerable shear motion accompanied by an increase in dilatancy (Fig. 2) to give rise to a somewhat sharp drop in shear strength beyond the peak.

As expected, these mixes decrease in volume under the initial increments of stress followed by an increase in volume with a net volume increase.

DILATANCY PREDICTION

Using a rigid plastic model, Yamaguchi (13) derived expressions for the Poisson's ratio and for unit expansion in the flow state during triaxial testing. The expression for unit expansion v is

$$v = \frac{\epsilon_1 \sin^2 \phi \left(\frac{\sigma_1}{\sigma_3} + 2\right)}{\frac{\sigma_1}{\sigma_1} - (1 + \sin \phi)^2} \tag{3}$$

in which ϕ = angle of shearing resistance and ϵ_1 and ϵ_3 = major and minor principal strains respectively. These results show that dilatancy increases with an increase in the angle of friction mobilized during loading.

Dilatancy of limestone is predicted in accordance with Eq. 3 and is plotted in Figure 3. The computed curve overpredicts the experimental volumetric strain shown by data points. The large difference can be attributed to, among other factors, the fact that in this analysis no allowances have been made for the elastic compression of the specimens.

To improve on the volumetric strain prediction, an alternate expression—in accordance with the stress-dilatancy theory—is derived here. According to this theory, soil particles in a dense mass move in such a way that a minimum of internal energy is absorbed. Rowe (11) computed an expression for the energy ratio (ratio of the instantaneous rate of work done on the sample by $\bar{\sigma}_1$ to that done by the sample against $\bar{\sigma}_3$) as

$$\dot{E} = \tfrac{1}{2}\left(\frac{\bar{\sigma}_1}{\bar{\sigma}_3}\right)\frac{d\epsilon_1}{d\epsilon_3} = \tan^2\left(\frac{\pi}{4} + \frac{\phi}{2}\right) \tag{4}$$

where ϕ_μ = angle of physical (solid) friction.

The stress-strain relation obtained from a drained triaxial test can be approximated by a series representation,

$$\epsilon_1 = A\left(\frac{\bar{\sigma}_1}{\bar{\sigma}_3}\right)^n \tag{5}$$

in which A and n are empirical constants determined by a least-squares curve-fitting procedure. The differential $d\epsilon$ from Eq. 5 is substituted in Eq. 4. The resulting expression is integrated to give ϵ_3, which when divided by ϵ_1 gives the Poisson's ratio of the aggregate, $\bar{\nu}$:

$$\bar{\nu} = \frac{n}{2(n+1)\tan^2\left(\frac{\pi}{4} + \frac{\phi}{2}\right)}\left(\frac{\bar{\sigma}_1}{\bar{\sigma}_3}\right) \tag{6}$$

Since the Poisson's ratio is known, the volumetric strain, v, is computed by

$$v = \epsilon_1(1 - 2\bar{\nu}) \tag{7}$$

Figure 3 shows a comparison of the experimental data points and the volumetric strain predicted by Eq. 7 for round gravel and limestone. For all six limestone mixes of various gradations, the predicted volumetric strain agrees with the experimental data. In round gravel, however, the volumetric strain values developed from theoretical calculation are significantly larger than observed in the laboratory test. In actual test, due to slippage, not all the grains will move in an expanding direction during shear; the measured behavior, therefore, is a result of the statistical averaging of the movements of many grains.

MATERIAL PROPERTIES RELATED TO DILATANCY

The various material characteristics that govern the strength and dilatancy of granular materials may be classified into two groups: intrinsic factors, such as surface texture, shape, size, and elastic properties of grains, and extrinsic factors, such as grading and porosity or packing of aggregations.

Dilatancy in Relation to Surface Texture

Surface texture is often expressed by the angle of surface friction, ϕ_μ. As in Eq. 1, the strength of a granular medium increases with increasing ϕ_μ, which in turn is a function of ϕ_μ. Morris (9), for example, has documented that an increase in texture alone would increase the strength by about 37 percent.

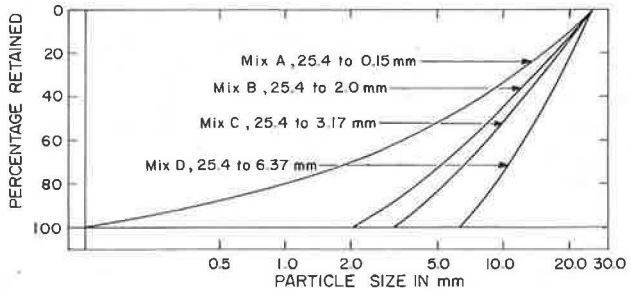

Figure 1. Particle size distribution curves for various mixes, material smaller than 25.4 mm.

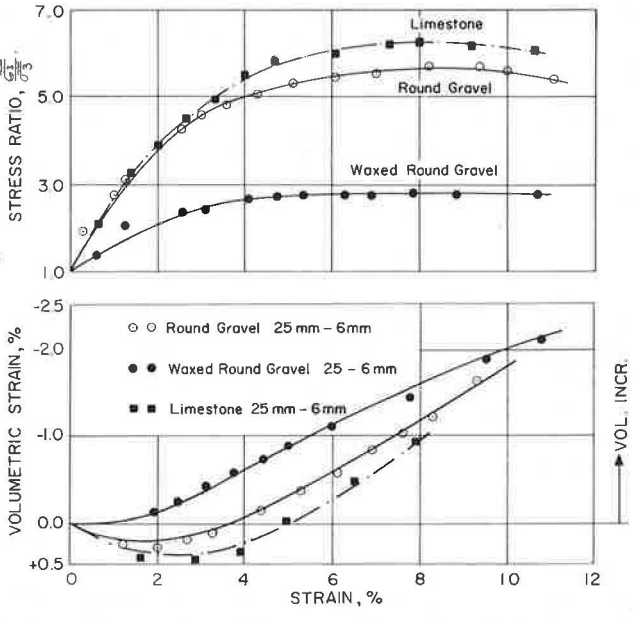

Figure 2. Drained triaxial test results: Stress ratio and volumetric strain related to axial strain, confining pressure 15 psi (100 kPa).

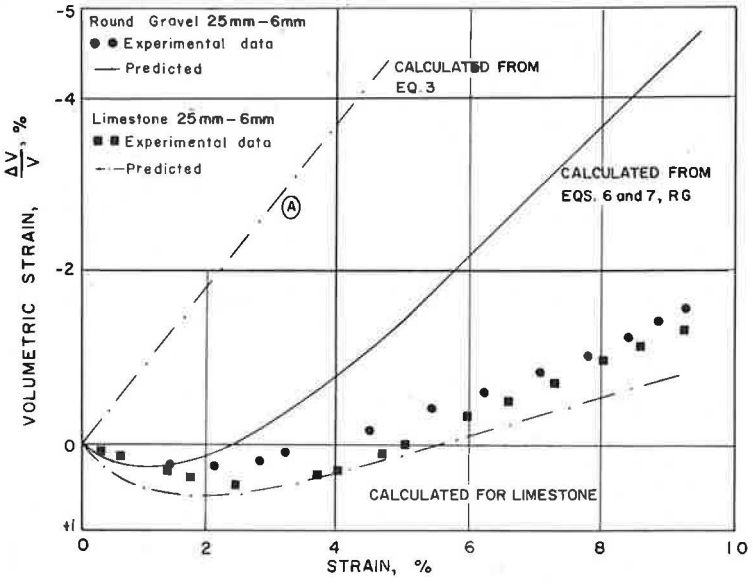

Figure 3. Volumetric strain of round gravel and limestone: Comparison of experimental and predicted values.

To clarify the effect of ϕ_μ on dilatancy, the stress-deformation-volumetric strain relations of round gravel with and without wax coating are predicted by Eqs. 6 and 7. In wax-coated gravel ϕ_μ is reduced from 28 deg to 22 deg, implying that the strength is substantially decreased, whereas the dilatancy is increased. Considering the energy dissipation during loading, both of these observations can be substantiated. The tentative conclusion, therefore, is that dilatancy of granular media increases with decreasing surface texture.

Strength and Volumetric Strain in Relation to Modulus of Particles

To study the stiffness characteristics of an aggregate theoretically, we may make use of the analysis of Deresiewicz (2). He derived the stress-strain relations for an aggregate of equal spheres (simple cubic lattice) subjected to triaxial loading. Because shear modulus for round gravel (29×10^6 kPa) is higher than that for limestone (15×10^6 kPa), the theory predicts that the round gravel is stiffer than the limestone (Fig. 4). The experimental curves in Figure 2, however, contradict the theoretical results. The fact that ϕ_μ and the grain concentration of limestone are greater than for round gravel partially explains and supports the experimental findings. These results are in general agreement with those of Morris (9), who reports that so-called tough and hard materials possess little, if any, strength advantage over relatively soft and friable materials, unless they differ in roughness.

Effect of Geometric Factors

The geometrical factor in soils is reflected in the grain size, shape, grain distribution, and density of packing.

Grain Size—The effect of grain size is studied by testing various mixes labeled A, B, C, and D in Figure 1. The results, as shown in the right side of Figure 5, indicate that ϕ_d remains constant regardless of d_{10}; however, the dilation component ϕ_δ increases with an increase in d_{10}.

By setting $\mu = 0$, Eq. 2 becomes

$$D_0 = \frac{1}{2\sqrt{2}\cos\beta}\left(2\sqrt{3}\,\sigma_3 R^2 + D_0 \cos\gamma\right) \tag{8}$$

where D_0 is the value given to the inclined force required to initiate failure when the sphere-to-sphere friction is zero. Equation 8 clearly demonstrates that D_0, which is the force required to dilate the sample, increases with the square of the radius of the constituent particles.

Effect of Roughness—Morris (9) proposed the concept of roughness, which includes the effects of both shape and texture of particles. The shape of the particles governs the number of contacts that will occur between adjacent particles, and the texture at the point of contact determines the strength or resistance to particles sliding over each other.

The effect of shape of the aggregate is investigated by testing two mixes prepared from the parent crushed limestone. The first mix consisted predominantly of "platey" particles ($r_v = 0.63$, where r is the shape factor) and the second of "chunky" or nearly cubical particles ($r_v = 0.72$). A comparison of the strengths (or ϕ_d) and the failure strains of three samples reveals that the peak strength is not materially changed, whereas the slope of the stress-strain diagram decreases with decrease in shape factor. This suggests that an aggregate of chunky particles is superior to one composed of platey particles, which is in agreement with others' results (8). The volumetric strain data confirm some previous results (7) that crushed gravels of elongated, platey particles will undergo a decrease in volume during failure in contrast to chunky materials, which will dilate during failure.

The effect of texture was discussed earlier, where it was shown that the texture influenced the strength more than the dilatancy characteristics. It is concluded that between the two factors, shape and texture, the former primarily controls the dilatancy characteristics whereas the latter influences the undrained shear strength.

Figure 4. Stress-strain relation for a simple cubic array of like spheres (radius 25 mm).

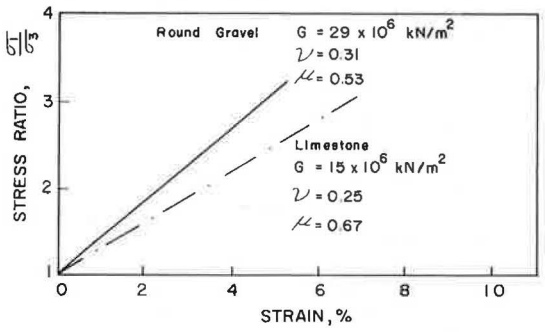

Figure 5. Components of ϕ for round gravel at various densities and different gradations: Three pairs of points on the left side are results from mix D compacted to three different porosities.

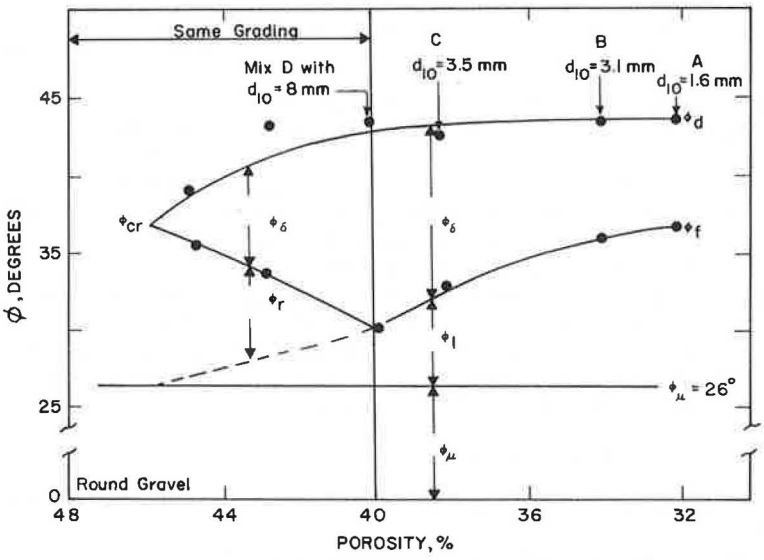

Porosity

The dilatancy component of shear strength, computed in accordance with the stress-dilatancy theory, is related to porosity. A minimum energy line is plotted for each test (10) and a value of ϕ_f is obtained from the best-fit curve for the plotted points by using

$$\bar{\sigma}_1 = \bar{\sigma}_3 (1 + K_F) \tan^2 \left(\frac{\pi}{4} + \frac{\phi_f}{2} \right) \quad (9)$$

in which $K_F = (\dot{dv}/v)/\dot{\epsilon}_1$ at failure, where $\dot{dv}/v$ = increment in volume change per unit volume, positive on expansion; $\dot{\epsilon}_1$ = maximum principal strain rate, positive on compression; and ϕ_f = that portion of ϕ_d with dilation removed.

The ϕ_f values on the left side of Figure 5 are obtained from mixes of different density having the same width of grading (mix D). In both materials ϕ_f increases with increase in porosity from a minimum value (which, according to Rowe, is equal to ϕ_μ) to ϕ_{cv} at the maximum porosity. We also note that $\phi_\delta (\phi_\delta = \phi_d - \phi_f)$ decreases with porosity; this relation reinforces the conjecture that, for a given mix of given gradation, looser packing lowers the energy spent in dilation.

Increasing the width of grading in a basic mixture (by adding more fines, mixes A, B, and C) results in decreased porosity. The results, as shown in Figure 5, show that, when the porosity is decreased, ϕ_d remains unchanged; however, ϕ_δ is somewhat reduced. For a graded sand Kirkpatrick (6) reported a decrease in the angle of shearing resistance with the decrease in porosity; he attributed this decrease, at least in part, to the reduction in dilatancy component.

The observation that ϕ_f increases with the decrease in porosity, however, contradicts Rowe's original hypothesis that, at the minimum porosity, ϕ_f tends to equal ϕ_μ. While clarifying certain aspects of stress-dilatancy theory, Horn (5) asserts that ϕ_μ should always be a few degrees smaller than ϕ_f. Accordingly, the statement may be advanced that the drained shear strength is constituted of the following four components rather than only three as proposed by Rowe (10): (a) strength arising from surface friction, ϕ_μ; (b) strength due to interlocking (which increases with the density of the mix), ϕ_i; (c) strength corresponding to the energy spent in remolding (which is zero in a dense mix), ϕ_r; and (d) strength equivalent to the energy spent in dilating the sample against the confining pressure, ϕ_δ. It may be noted that the present classification recognized an additional component, namely, the strength due to interlocking, which, according to the experimental results, increases with the decrease in porosity.

CONCLUSIONS

1. The main cause of strain in granular materials is relative movement (sliding and rolling) between particles.
2. The volumetric strain of crushed limestone, predicted according to the stress-dilatancy theory, is in agreement with the experimental data; in smooth gravel, however, the predicted value is larger than that of the observed data.
3. The dilatancy during failure increases with decreasing values of physical (solid) friction of the grains.
4. The strength and dilatancy of granular aggregates depend not on the stiffness of the constituent particles but on the shape and surface texture of the grains.
5. Crushed gravels of elongated (platey) particles undergo a decrease in volume in contrast to chunky subrounded aggregates, which tend to dilate at failure. A previous study (8) reports that all gravel materials contract at confining pressures of 50 psi and greater.
6. Dilatancy increases with increasing effective size (d_{10})—more so in the rounded natural gravel.
7. Increasing the coefficient of uniformity produces a negligible effect on ϕ_d; doing so, however, decreases the dilatancy component in both gravels.

REFERENCES

1. Bishop, A. W., and Henkel, D. J. The Measurement of Soil Properties in the Triaxial Test. Edward Arnold, London, 1957, p. 68.
2. Deresiewicz, H. Stress-Strain Relations for a Simple Model of a Granular Medium. Jour. Applied Mechanics, Trans. ASME, Sept. 1958, pp. 402-406.
3. Henkel, D. J., and Gilbert, G. C. The Effect of Rubber Membranes on the Measured Triaxial Compression Strength of Clay Samples. Geotechnique, London, Vol. 3, 1952, pp. 20-29.
4. Hirchfeld, R. C., and Poulos, S. J. High Pressure Triaxial Tests on a Compacted Sand and an Undisturbed Silt. ASTM Special Tech. Publ. 361, 1963, pp. 329-340.
5. Horn, M. R. The Behavior of an Assembly of Round, Rigid Cohesionless Particles. Proc. Royal Society, London, Series A, Vol. 286, 1965, pp. 62-97.
6. Kirkpatrick, W. M. Effect of Grain Size and Grading on the Shearing Behavior of Granular Materials. Proc., 6th International Conf. on Soil Mechanics and Foundation Engineering, Vol. 51, 1965, p. 273.
7. Koerner, R. M. Behavior of Single Mineral Soils in Triaxial Shear. Jour. Soil Mechanics and Foundations Div., ASCE, Vol. 96, No. SM4, July 1970, pp. 1373-1390.
8. Marachi, N. D., Chan, C. K., and Seed, H. B. Evaluation of Properties of Rockfill Materials. Jour. Soil Mechanics and Foundations Div., ASCE, Vol. 98, No. SM1, Jan. 1972, pp. 95-116.
9. Morris, H. C. Effect of Particle Shape and Texture on the Strength of Noncohesive Aggregates. ASTM Special Tech. Publ. 254, 1959, pp. 350-363.
10. Rowe, P. W. The Stress Dilatancy Relation for Static Equilibrium of an Assembly of Particles in Contact. Proc., Royal Society, London, Series A, Vol. 269, 1962, pp. 500-527.
11. Rowe, P. W. Stress-Dilatancy, Earth Pressures, and Slopes. Jour. Soil Mechanics and Foundations Div., ASCE, Vol. 89, No. SM3, May 1963, pp. 37-61.
12. Thurston, C. W., and Deresiewicz, H. Analysis of a Compression Test of a Model of a Granular Medium. Jour. Applied Mechanics, Trans. ASME, June 1959, pp. 251-258.
13. Yamaguchi, H. Strain Increments and Volume Change in the Plastic Flow of a Granular Material. Proc., 5th International Conf. on Soil Mechanics and Foundation Engineering, Vol. 1, 1961.

IDENTIFICATION OF PROBLEM LATERITE SOILS IN HIGHWAY ENGINEERING: A REVIEW

M. D. Gidigasu, Building and Road Research Institute, Kumasi, Ghana

Some laterite materials are known to be either inferior pavement aggregates or troublesome highway and earth dam construction materials. However, not all laterite soils belong to this group. A criterion for distinguishing problem laterite soils from non-problem ones for highway construction is proposed. Such a differentiation would be a considerable asset to highway engineers in determining the quality and suitability of doubtful laterite soils for highway and airfield construction. Laterite soils range in performance from excellent to poor, and in spite of considerable field and laboratory studies on these soils it is still not yet possible to predict accurately the behavior of all grades and genetic groups of laterite soils. From an engineering viewpoint, a criterion based on significant engineering characteristics, including such genetically inherent properties as sensitivity to drying and remolding, degree of potential swell and self-stabilization, and predominant clay minerals, may be more useful in predicting probable in situ behavior of laterite soils than the existing temperate-zone soil classification systems.

•STANDARD methods of identification of temperate-zone soils based mainly on particle size distribution and plasticity are applicable to most laterite soils. For example, the unified soils classification system has been found adaptable to some laterite soils when extended to include subclassifications for the durability characteristics of gravel and sand and for the plasticity characteristics of the clay and silt fractions of gravels and sands (20).

Indeed, the extended unified soil classification system may be applicable to all laterite soils "whose different modes of formation, color, mineralogical composition, etc., do not necessarily mean wide differences in engineering properties beyond the scope of presently used test methods and criteria" (120). The major difficulty in trying to develop a satisfactory identification system for laterite soils appears to evolve around the so-called problem laterite soils, which may not yield reproducible test results using standard laboratory test procedures and whose engineering behavior may not be accurately predicted on the basis of standard classification tests.

No criterion appears to be available for distinguishing problem laterite soils from non-problem ones. Such a system would be a considerable asset to soils engineers in determining the quality and suitability of doubtful laterite soils for construction purposes.

This review attempts to propose a criterion for separating problem and non-problem laterite soils for highway construction based on reported significant geotechnical properties. The term geotechnical properties is used here in a broad sense to include not only index and engineering properties but also such characteristics as sensitivity to drying and remolding, degree of potential swell and self-stabilization, and resistance to degradation during and after construction.

This is only a broad grouping that would serve as a basis from which, by expansion and amplification within the original framework, the more detailed and specific classification system required for various practical problems may be built up.

Publication of this paper sponsored by Committee on Soil and Rock Properties.

IDENTIFICATION BASED ON PEDOLOGICAL INFORMATION

Geotechnical studies on laterite soils (118) have revealed that similar combinations of soil-forming processes lead to soils of similar index and engineering properties. In surveys for highway materials and in finding sources of satisfactory fill material for embankment construction, the identification of localities in which pedogenic processes are similar has been found useful (19, 20, 22, 23). Since laterite soils have developed under the influence of pedogenic factors, these factors have been found useful in regional identification and classification of laterite soils for engineering purposes (47). Indeed, it has been shown (19, 118) that no system of classification nor any attempt to classify most tropically weathered soils can succeed if it is not based on an appreciation of tropical weathering processes. Because similar profiles do develop under similar weathering conditions, a useful means of regional description of laterite soils for highway construction would be to group and classify profiles at least as a first approximation on a regional and local basis according to the similarities or differences among the important soil-forming factors (49).

Depending on the degree of weathering (i.e., decomposition, laterization, and dessication), laterite materials occur in various textural forms ranging from practically unconsolidated soft clays breakable under finger pressure to hard pedogenic rocks. Empirical concepts of degree of hardness have been used (75), and such terms as "soft" and "hard" laterite rocks may be found in the literature, but such qualitative expressions without quantitative relation to any mechanical properties may be of limited value to engineers engaged in the use of laterite soils for construction. Because of the great variety of laterite materials along with the hardening or softening of these materials with changes in environmental conditions (97), it appears that any identification system based on purely morphological concepts is not likely to be of much use to the soils engineer. However, an engineering classification system based on degree of weathering and morphological characteristics has been proposed (68) for laterite soils. "It has been used now for some years with considerable success whereas the temperate climate classification has had to be discarded for tropical soils" (68).

A major limitation of the pedological classification system is that one material in this system may have a wide range of properties; the engineer desires a classification system based on significant geotechnical properties that fall within such small ranges that the material can be specified by its classification type. However, once geotechnical characteristics have been established for a pedological soil group, these data may always be applicable to soils formed under similar conditions.

IDENTIFICATION BASED ON CHEMICAL AND MINERALOGICAL CHARACTERISTICS

Fermor (39) was perhaps the first to propose a comprehensive chemical nomenclature for laterite soils. Martin and Doyne (76) proposed silica-alumina ratio for classification of laterite soils while others (60, 125) proposed silica-sesquioxide ratio; attempts were also made to relate chemical property to engineering behavior (84).

Lukens (73) summarized available data on the chemical composition of laterite soils and grouped these soils chemically. Some empirical correlations were found between the chemical composition of laterite aggregates and their strength properties. For example, Millard (79) reported a fairly good positive correlation between the iron oxide (Fe_2O_3) content and the strength, and Maignien (75) noted that ferruginous materials are stronger than aluminous ones. Apparently ferruginous laterite aggregates would be preferable to aluminous ones for base course construction because they are harder at the same degree of induration (75). However, chemical data are not always available; the determination of even the relatively simple silica sesquioxide ratio requires a chemical analysis not likely to be available to the soils engineer. Experience has also shown that this "ratio is by no means a unique indicator of index properties or engineering characteristics required by the engineer" (92). Moreover, available literature on laterite soils (75) would indicate that chemical analyses are often too crude to reveal the origin, nature, and composition of laterite soils.

The important minerals identified in laterite soils include goethite, hematite, limonite,

chlorite, halloysite (hydrated and dehydrated), kaolinite, and allophane (75). Free alumina was identified in the form of gibbsite, boehmite, and other amorphous forms, and combined silica is frequently present as clay, especially kaolinite or clays of the same group, such as halloysite, mainly in amorphous or subcrystalline forms. Montmorillonite and illite types of clays have not been identified in significant amounts.

Clay mineral analysis is not normally employed in the routine examination of soils for engineering purposes. However, in the engineering studies of laterite soils (35), consideration of the clay mineral present has been useful in a number of ways: (a) in the characterization of different groups of laterite soils having distinct engineering characteristics (32, 33, 34); (b) in the formulation of local engineering soils classifications, taking into account not only the soil but its environment, which affects both the nature of the soil and the engineering consideration; and (c) in the search for basic understanding of engineering properties of some laterite soils and interpretation of their test results (25, 30, 88, 114, 115).

Mineralogical composition of the clay fraction seems to be very important from an engineering point of view and can be used as a means of identification and classification. For example, laterite soils containing high percentages of hydrated halloysite, goethite, or gibbsite are known to be problem laterite soils; those containing montmorillonite and illite may have lower strengths, high construction pore pressure, high swelling potential, and other undesirable properties that laterite soils with the clay fraction consisting predominantly of kaolinite and chlorite do not have (33).

SIGNIFICANT GEOTECHNICAL CHARACTERISTICS OF LATERITE SOILS

Field performance of laterite soils (30, 74) may range from excellent to poor for engineering purposes. The problem is one of distinguishing the good ones from the poor ones. Difficulties in solving this problem are partly attributed to lack of definition and nomenclature of laterite soils and absence of an adequate system for their description coupled with lack of standardized testing procedures for evaluating them. However, considerable progress has been made in the identification and classification of laterite soils for engineering purposes (89, 118, 120), and it is now possible to predict the engineering behavior of some laterite soils based on their significant engineering properties (74).

The most important procedures for evaluating geotechnical properties of laterite soils are discussed in the following and the significant characteristics are identified as a basis for proposing an engineering criterion for identifying problem and nonproblem laterite soils based on experience of their engineering behavior.

Grain Size Distribution

Particle size distribution of laterite soils appears to be extremely varied and erratic, containing all sizes from clay through gravels to massive concretionary rocks. The vulnerability to degradation of the relatively weak structure of some concretionary laterite soils means that the grading can be affected by the pretreatment before test and by the testing procedures (89). Flocculation problems during hydrometer analysis are sometimes difficult to overcome, and variations of particle size distribution with methods of predrying, type of dispersing agent, and time of mixing or working have been reported (56, 114, 115).

Studies (26, 86, 114) have revealed that sodium hexametaphosphate is the most effective dispersion agent for most laterite materials. Apparently, the working or use of proper dispersing agents causes disaggregation of sesquioxide-bound structure into its original fine particles (88, 114).

In spite of these limitations the particle size distribution test can still be used for identification and classification of laterite soils provided the data obtained are used intelligently and with caution.

Atterberg Limits

Atterberg limits together with particle size distribution are generally used for classification of temperate-zone soils, and their engineering behavior may be inferred

based on information available on soils of similar classification. Correlation of this kind for some laterite soils has proved misleading because Atterberg limit tests may not yield reproducible results since they are influenced considerably by pretest preparations and testing procedures (56, 88, 114).

To overcome the limitation imposed by this difficulty, the laboratory vane test has been used to evaluate the plasticity of some laterite soils (84). Although no conclusions had been reached on the suitability of this test procedure because of the small number of soils studied and the lack of field correlation data, it seems that this approach may prove very useful in solving the greatest and perhaps the only objectionable handicap of the Atterberg limit test on remolded samples, since internal structure of the soil samples can be judged directly.

Troublesome laterite soils have been found to plot generally below the A line on the Casagrande chart, with liquid limits generally above 50 percent and plasticity index above 20 percent (Fig. 1).

Colloidal Activity

Colloidal activity of the clay-size fraction seems to be generally low for laterite soils. For example, the values lie between 0.4 and 1.0 for residual laterite soils and above 1.0 for the alluvial and tropical black clays (45). The relationships between clay mineralogy of some tropical clay soil types and the ranges of their colloidal activity values have been reported (38, 89). The various values quoted for different clay minerals are very low compared with results published by Skempton (111) for temperate-zone soils. It appears (47) that the low activity of laterite soils is due to the clay mineral impregnation and coatings by sesquioxides, with resultant reduction in specific surface of the clay minerals (115).

Because clay-size content and plasticity index vary with sample preparations and testing procedures, the application of colloidal activity for identification and classification of some laterite soils may be misleading. For example, colloidal activity of 0.5 may represent quartz-rich temperate-zone soil (111) whereas for laterite soil it may be for hydrated halloysitic clay, which is known to be very troublesome (114, 118). Obviously, to rely solely on "colloidal activity" for predicting the probable mineralogical composition of some laterite soils may be misleading.

Moisture, Density, and Void Ratio

Natural moisture content of laterite soils varies from as low as 3 percent for the laterite rocks (106) to over 200 percent for hydrated halloysitic and volcanic red clays (21, 43, 56, 114). The natural moisture contents for problem laterite soils are generally very high, being far above the plastic limit and in many cases beyond even the liquid limit, and yet in their natural, undisturbed state have characteristics of a solid rather than of a plastic or liquid mass (56). In situ dry densities of laterite soils range from as high as 130 to 160 lb/ft^3 (2082 to 2563 kg/m^3) for homogeneous laterite rocks (106) to as low as 20 to 60 lb/ft^3 (320 to 961 kg/m^3) for the volcanic red clays (56).

Void ratio has been used (44) for identification and classification of decomposed granite into dense (0.3-0.7), medium (0.7-1.1), and low (1.1-1.5). Moisture content, density, and void ratio are therefore significant properties for identification and classification of some laterite soils.

Linear Shrinkage

Ackroyd and Rhodes (3) and Easterbrook (37) have suggested the use of a linear shrinkage test for the selection of laterite gravels for unstabilized base and subbase construction. Studies on over 800 laterite soils in Nigeria established an upper linear shrinkage limit of 6 percent and 7 percent respectively for accepting sand clays and gravel-sand-clays for base course material. For the subbase material the respective values are 12 percent and 13 percent for sand clays and gravel-sand-clays (3). For laterite gravels for use in unstabilized base courses, a maximum linear shrinkage of 5 percent is proposed for Nigeria conditions. Zambia also specifies a maximum linear shrinkage of 3.3 percent for some gravel base materials.

Compaction Characteristics

Significant contributions have been made on the evaluation of compaction characteristics of laterite soils (55, 95). Wide variations of compaction characteristics of laterite soils are due to the heterogeneity, degree of weathering, sensitivity to molding moisture, variable strengths of the coarse particles, and effect of pretest preparations (38, 43, 45, 88, 95, 114, 118).

The effect of molding moisture on the compaction characteristics of laterite soils was investigated for soils varying in texture from red clays of volcanic origin (56, 88, 113) to gravelly soils (13, 44, 55).

Fruhauf (43), Tateishi (113), and Newill (88) have observed significant variations in moisture-density curves for some laterite soils in tests carried out from wet to dry and dry to wet. This has practical importance in construction: If at its natural state the soil has insufficient moisture, water is added and a relatively high maximum dry density is attainable. If on the other hand the residual moisture content exceeds that desired and the soil is dried before compaction, a lower dry density is obtained for the same compactive effort. Laterite gravels are known to give high CBR values when dry, but on absorption of water the strength drops abruptly (38). Investigations on typical laterite gravels revealed great sensitivity of CBR to changes in moisture content (38). For typical laterite gravels, heavy compactive effort may give a distinct CBR/moisture-content relationship with distinct maximum CBR values of about 100 and 200 percent and about 50 percent for modified AASHO and British Standard (light) compaction respectively. At a moisture content only a few percentage points higher than those corresponding to the optima for compaction, the CBR values may fall drastically to about 20 percent of original value.

The higher the compactive effort, the higher the degree of strength reduction with increase in moisture content (38). Another important factor is the strength of the concretionary particles (55). Laterite gravels generally contain concretionary particles that range from those that are very hard to those that are very soft. Weak concretionary particles do break down under rolling and traffic, with a resultant increase in the fines in the soils (8). On the other hand, hard concretionary particles are a useful source of blending materials for bituminous surface dressing in some countries (28). The influence of compaction on the breakdown of the concretionary particles of typical laterite gravels has been discussed by Hammond (55), who noted that the degree to which the material breaks down is a function of the strength of the concretionary particles, which in turn can be related to the iron oxide content and degree of dehydration (55). The higher the iron oxide content and the more dehydrated the concretionary particles, the harder they are (11). The effect of mica content on the compaction characteristics of soils has also been discussed by Tubey (117). It has been suggested that the amount of mica that can be tolerated in soils used for pavement construction depends on the purpose for which they are being used: i.e., as filling, as subgrades, or for making subbases and bases. From data on the effect of increasing mica content on compaction characteristics it appears (117) that not more than about 10 percent mica can generally be tolerated in fine-grained soils.

Strength and Mechanical Properties

Standard tests have been successfully used for assessing the strength and durability of laterite rocks and aggregates (82) and normal laboratory and field strength tests have been used for evaluating the strength and bearing capacity characteristics of unconsolidated laterite soils (71, 96, 98, 121). Shear parameters appear to be generally higher for undisturbed fine-grained laterite soils and are found to depend to a large extent on the type of parent rock, degree of weathering, and degree of saturation (63, 66, 67, 71, 72).

Laterite fine-grained soils that possess very low or no cohesion at full saturation may be suspect soils that should be thoroughly evaluated. The strength characteristics of soils in laterite profiles vary considerably with depth according to the influence of such factors as parent rock, depth of water table, topography, degrees of decomposition, laterization, and dessication as well as with mineralogical composition (98, 121). Field

evaluation of bearing capacity of laterite soils using penetration tests has been attempted (96) and found to be fairly reliable.

The degree of induration and hardness of laterite rocks has been studied and found to depend on amount of sesquioxide content, homogeneity, structure, and age (11, 75, 79, 83). Because of the petrological heterogeneity of laterite rocks and aggregates coupled with numerous factors that affect their strength, it has been found necessary to evaluate the relation between the physical and chemical properties and their mechanical characteristics for a better appreciation of their behavior in highway pavements (11, 82, 106).

EVALUATION OF ENGINEERING BEHAVIOR OF PROBLEM LATERITE SOILS

Sensitivity to Drying

Two factors appear to cause changes in the properties with drying: the tendency to form aggregations on drying and the loss of water in the hydrated minerals. The tendency to form aggregations on drying was perhaps first described by Hirashima (56) and later in more detail by Terzaghi (114).

In terms of grading, drying causes an increase in particle size such that much of the clay- and silt-sized materials agglomerate to the size of sand, with consequent modification of Atterberg limit values (124). The effect of drying on the moisture-density curves for some problem laterite materials has also been reported (88, 124). It was also found (88) that the specific gravity for the hydrated halloysitic Sasumua clay changed when the moisture content of the soil was reduced to below 15 percent, while that of the metahalloysitic Kabete clay did not show any variation in specific gravity values. The process of drying appears to transform unstable hydrated halloysite to the stable metahalloysite, and this is accompanied by loss of interlayer water, which affects the specific gravity values (88). Although it appears that the decrease in specific gravity with loss of interlayer moisture is only illusory (88), nevertheless it is apparent that the specific gravity test can be used to distinguish some problem laterite soils from non-problem ones.

The clay minerals most susceptible to changes in properties with drying appear to be hydrated halloysite, goethite, gibbsite, and allophane (42, 52, 88). When dealing with materials containing these it is useful (92) to determine the index properties on the samples at natural moisture content and again at various degrees of drying in order to evaluate the range of properties associated with the drying conditions that may prevail on site. Serious engineering and construction problems may arise through failure to recognize laterite soils whose properties may vary with degree of drying (56, 57, 114).

The degree of potential sensitivity to drying of laterite soils has been assessed using the so-called aggregation index test (113). Aggregation index is defined as the ratio of sand-equivalent test value of an oven-dried sample to that of the sample in its natural state. An aggregation index of 1 would indicate a non-problem laterite soil whereas higher values of, say, 2 and above would indicate a problem soil. Aggregation index is thus a significant property useful for distinguishing problem laterite soils from non-problem ones.

Dessication and Potential Self-Stabilization

Some laterite soils that, because of high plasticity and content of fines, would have been rejected on the basis of current specification as being unsuitable for base construction have been found to perform satisfactorily under field conditions (84). This is due to the phenomenon of self-stabilization. This phenomenon is attributed to the transformation of the hydrated sesquioxides and minerals to the dehydrated forms under dessicating field conditions (108).

Grant and Aitchison (53) have emphasized the need to distinguish hydrated and dehydrated laterite soils in order to ensure the use of appropriate testing procedures that will reflect the state of the iron oxide. If all the iron oxide in the soil is in a ferric state and there is no factor present to promote a reducing environment, then the soil is

essentially stable and no change can be expected; standard tests are then appropriate. If on the other hand all the iron oxide is not in the ferric state or conditions could exist that would promote a reducing environment allowing further mobilization of iron, changes in properties may occur, and standard tests become inappropriate.

The so-called petrification test was proposed (84) for assessing the probable degree of potential self-stabilization that may occur in a laterite soil. An undisturbed or remolded soil pat predried at about 60 C to constant weight is soaked in distilled water for 24 hours, after which the water content of the sample is determined; this is called absorption limit. The petrification degree is then determined as the ratio of shrinkage limit to absorption limit; the higher this value, the better the prospect of self-stabilization, notably in the surface layers of a pavement where drying is more marked and an improved behavior with successive dry periods is to be anticipated (84).

Structure and Sensitivity to Remolding

Some laterite soils in the natural state possess granular structure due to the abundance of sesquioxides that coat the pore walls, fill the voids, and bind the soil particles into bigger particles (4). The granular structure appears to be responsible for the desirable engineering properties displayed by some undisturbed laterite soils (115). However, the high bearing strength, low plasticity, and high permeability associated with undisturbed laterite soils are lost upon working the soil (i.e., mixing, compacting, or employing any type of extensive mechanical manipulation in the presence of water). The granular structure is apparently broken down and the soil becomes highly plastic, with low bearing capacity and poor drainage. Newill (88) and Townsend et al. (116) reported the effect of removing "free" iron oxide from laterite clays on the Atterberg limits and grading. The content of clay-size grains as well as the liquid limit were found to increase considerably after removing the "free" iron oxide from the material.

Progress in the field of compaction of "sensitive" laterite soils appears to lie in the search for suitable mixing and compaction methods that do not destroy the granular structure and yet yield sufficient density and strength (125). Experience at road construction sites has shown that light compaction plants with crude methods on "sensitive" laterite soils have yielded better pavements than compaction of the same soils using standard heavy compaction machinery and procedures (43).

Structure and the Significance of Potential Swell

Some hydrated laterite soils with Atterberg limits exceeding the values recommended in current specifications for subbase, base, and surfacing materials may behave satisfactorily in tropical roads (84). This fact has been ascribed to the low activity and especially the low potential swell of fines in laterite soils. The kneading of the fines during Atterberg limit tests apparently causes breakdown of the unique granular structure; with the consequent increase in specific surface, the fines tend to absorb far more water than would normally occur under field conditions. Since some laterite soils appear to be more sensitive to remolding than ordinary soils, they yield high Atterberg limit values and thus are rejected, although their behavior in the road would have been acceptable (84).

The overriding significance of Atterberg limits in accepting or rejecting subbase, base, or surfacing laterite materials may sometimes be misleading. The degree of potential swell was found to be more indicative or predictive of behavior of this group of laterite soils in pavements (18, 84), and studies were carried out to determine how far the existing specifications in terms of Atterberg limits can be safely exceeded based on allowable potential swell to ensure satisfactory field performance. Studies (86) have revealed that potential swell of 10 percent is critical for distinguishing good laterite soils from poor ones for pavement construction.

FIELD PERFORMANCE OF LATERITE SOILS IN HIGHWAY PAVEMENTS

Most laterite soils and gravels make good materials for subbase construction, being easy to obtain and to manipulate on the road surface and having naturally stable grad-

Figure 1. Plasticity characteristics of typical problem laterite soils.

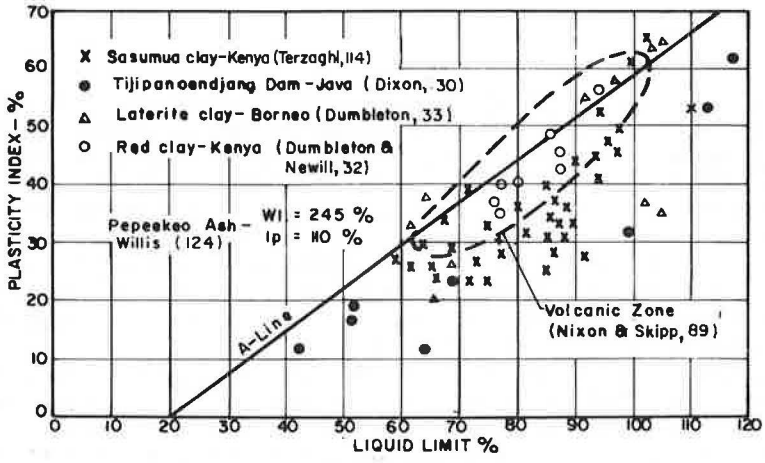

Figure 2. Grading characteristics of unsuitable and suitable laterite gravels for unstabilized base construction [after Remillon (96)].

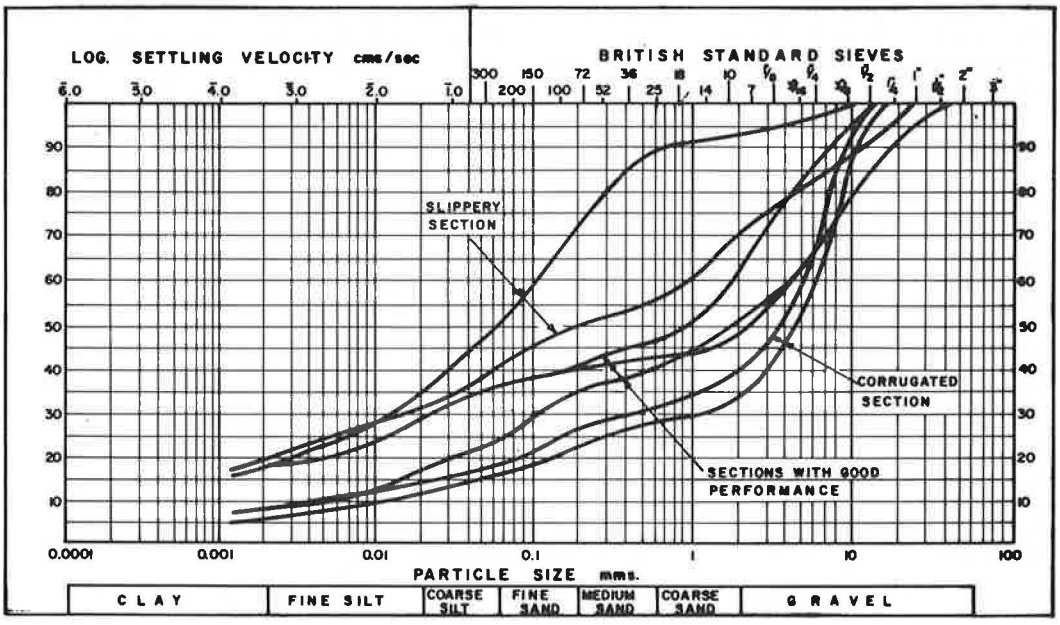

Figure 3. Recommended grading specifications of laterite gravels for unstabilized base construction [USAID (118)].

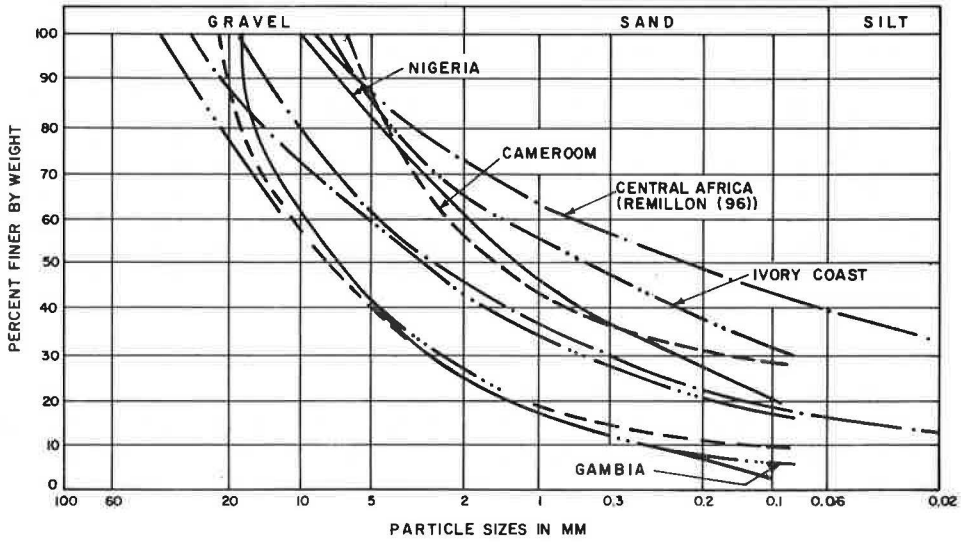

ings with appropriate fines to act as binders (2, 79). However, in most parts of the tropics there is only a limited choice of hard laterite base aggregates. Few varieties of laterite aggregates are also tough and strong enough to be used satisfactorily in surface dressing, and most of them become polished under the lightest traffic (79).

The most important requirement of good laterite gravels in terms of field performance is that they should be well graded, with high content of hard concretionary and quartz particles and adequate fines (79). For example, Remillon (96) has shown that poor grading can lead to undesirable failures (Fig. 2). Similar experience in many African countries has led to establishment of optimum grading envelopes of laterite gravels for unstabilized base construction (Fig. 3).

Weakly indurated gravels are poor base materials because they tend to break down during compaction and under repeated traffic loading. The situation may be worsened by the presence of water due both to its softening effect on the material and to the strength reduction it causes, and this condition leads to pavement distress and susceptibility to failure (8).

The major problems encountered on some laterite roads are the cracking of the open and surfaced pavement, stripping off of surfacing, and waviness of the pavement surface after a few years of use (74). These failures may be due to poor material selection, subgrade condition, or inadequate design, all of which may lead to reduction in soil strength with time (10). It appears that water plays a major role by entering the pavement structure, causing a progressive decrease in density and an increase in plasticity and possibly swell or shrinkage (8, 46). The performance pattern has also been found to depend on the nature of the soil system and on drainage facilities (22, 23). Failure has been found to vary over a wide range of ground conditions, from hilly to swampy and from well-drained to poorly drained and occasionally flooded areas (22). Twenty years of correlations between laboratory tests and the field performance records on laterite soils in South Africa under bituminous surfacings (31) have revealed that a sound basis for rating laterite gravels for base construction is given by Table 1. Experience on the use of laterite rocks and aggregates for pavement construction would suggest (11) that the bearing strengths of the materials are quite variable; the material may break down during compaction (8), rapidly losing its strength on wetting, and most of them are unacceptable as base material (82). Nanda and Krishnamachari (82) have shown that samples having impact, crushing, and abrasion values of up to 46, 47, and 48 percent respectively behave well as base course but poorly as a wearing course.

A rating system for West African laterite aggregates for pavement construction has been proposed (Table 2). There appears to be an urgent need to examine the behavior of laterite soils under road pavements, in particular the effect of wetting and drying and repeated loading on the strength characteristics of these soils (8).

GEOTECHNICAL IDENTIFICATION OF PROBLEM LATERITE SOILS

Most of the reported significant geotechnical characteristics of laterite soils for pavement construction have been reviewed and appear to reflect the effect of pedogenesis on the geotechnical characteristics of laterite soils. Table 3 is an attempt to relate some significant index and engineering properties to probable in situ behavior. The left side of the table lists a number of properties and gives average range of values for each property. These values can serve to sort out troublesome or problem laterite soils from the non-problem ones. Columns 4 to 8 list the commonest potential engineering problems that may be expected to occur in laterite soils having the physical and engineering properties shown. By carrying out tests for a particular laterite soil and running the values of the physical and engineering properties through the proposed classification chart in Table 3, one can readily determine whether the soil is potentially troublesome or not.

GENERAL CONCLUSIONS

At present it is difficult to develop a completely satisfactory criterion for identification of engineering behavior of all laterite soils because available data are imprecise and testing methods are not internationally standardized. However, it may be possible

Table 1. Rating of laterite soil for use under bituminous surfacing [see Dreyfus (31)].

Soil Properties	Field Performance Rating		
	Excellent	Average	Poor
Linear shrinkage, percent	0-4	4-6	Above 6
Plasticity index, percent	0-6	6-8	Above 12
Liquid limit, percent	14-21	22-30	Above 30
Expansion in CBR mold after saturation, percent	0-0.2	0.3-0.4	Above 0.4
Optimum moisture content, percent	—	8-10	—

Table 2. Rating of some West African laterite aggregates for pavement construction [after Bhatia and Hammond (11)].

Specific Gravity	Water Absorption After 24 Hours' Soaking (percent)	Aggregate Impact Value (percent)	Los Angeles Abrasion Value (percent)	Rating Based on Probable In Situ Behavior
>2.85	<4	<30	<40	Excellent
2.85-2.75	4-6	30-40	40-50	Good
2.75-2.58	6-8	40-50	50-60	Fair
<2.58	>8	>50	>60	Poor

Table 3. An engineering evaluation of laterite soils.

Geotechnical Properties			Probable Engineering Behavior and Field Performance					
	Average Range of Values							
Laboratory Tests (1)	Unfavorable (2)	Favorable (3)	Sensitivity to Drying (4)	Structure Sensitivity to Remolding (5)	Potential Self-Stabilization (6)	Field Compaction Problems (7)	Degradation Under Traffic and During Compaction (8)	References (9)
Aggregate impact value, percent	>50	<30					✓	(11)
Water absorption, percent	>8	<4					✓	(11)
Natural moisture content, percent	≈liquid limit	Below plastic limit	✓	✓		✓		(45) (56)
Linear shrinkage, percent	>6	<4				✓		(31)
Potential swell, percent	>11	<10			✓			(18) (84)
Predominant clay mineral	Montmorillonite; hydrated halloysite	Kaolinite, chlorite	✓	✓		✓		(33) (114)
Mica content, percent	>10	<10				✓		(117)
Aggregation index	>2	≈1	✓	✓				(113)

to sort out some problem laterite soils from the non-problem ones by means of a proposed chart (Table 3).

Certainly some laterite soils can be evaluated using standard soil testing procedures. The major difficulty in trying to develop a satisfactory procedure for assessing their engineering behavior appears to evolve around the so-called problem laterite soils that may not yield reproducible results by the standard test procedures. These soils present an engineering dilemma and are real problem soils. It seems that an international study by geotechnical laboratories in tropical countries is needed to produce a satisfactory engineering classification for laterite soils. Such a study has already been started through recent USAID programs in Asia and Africa (118, 120).

It is also urgently required that methods of evaluating laterite soils be standardized. The standard tests may be appropriate in certain cases, but in others new testing procedures may have to be evolved. Such a study may take several years but, in view of the fact that laterite soils constitute so much of the world's surface area and hence the foundation for so many future highways and airfields, it would be worthwhile.

ACKNOWLEDGMENTS

This literature study is part of a long-term study on the identification and evaluation of laterite soils for engineering purposes in progress at the Building and Road Research Institute, Ghana. The author wishes to acknowledge with sincere thanks the encouragement given by the Director and staff of the Soil Mechanics Division of the Institute. He is also grateful to the Editorial Committee and N. K. Kumapley, lecturer in soil mechanics at the University of Science and Technology, for reading through the manuscript and offering very useful suggestions.

REFERENCES

1. Ackroyd, L. W. Engineering Classification of Some Western Nigerian Gravels and Their Qualities in Road Making. Overseas Bulletin 10, British Road Research Laboratory, 1959, 32 pp.
2. Ackroyd, L. W. Notes on the Crushing Strength of Some Western Nigerian Concretionary Gravels and Their Selection for Use as Building Materials. Technical Paper 6, Ministry of Works, Ibadan, Nigeria, 1960.
3. Ackroyd, L. W., and Rhodes, F. G. Notes on Application of Linear Shrinkage Test to the Selection of Western Nigerian Gravel Soils. Technical Paper 5, Ministry of Works, Ibadan, Nigeria, 1960, 3 pp.
4. Alexander, L. T., and Cady, Y. G. Genesis and Hardening of Laterite in Soils. Technical Bull. 1282, U.S. Department of Agriculture, 1962, 90 pp.
5. Standard Specifications for Materials and Soil Aggregate Sub-Base: Base and Surface Courses—Part I. AASHO Designation M 147-65, 1966, pp. 49-50.
6. Tentative Specifications for Soil-Aggregate Sub-Base, Base and Surface Courses. ASTM Designations D 1241-55T, C 131-55, Pt. 3, 1965, pp. 1185-1190.
7. Aubert, G. Observations on Degradation of Soils and Laterite Crust Formation in Northeastern Dahomey. Proc. 4th International Congress on Soil Science, Amsterdam, 1950, pp. 127-128. (In French.)
8. Arulanandan, K. Classification, Engineering Properties and Behavior of Laterites. Proc. Specialty Session, Engineering Properties of Lateritic Soils, 7th International Conf. on Soil Mechanics and Foundation Engineering, Mexico City, Vol. 2, 1969, pp. 163-179.
9. Bawa, K. S. Laterite Soils and Their Engineering Characteristics. Proc. ASCE, Vol. 83, Paper 1428, 1957, pp. 1-15.
10. Bhatia, H. S. Personal communication, 1970.
11. Bhatia, H. S., and Hammond, A. A. Durability and Strength Properties of Laterite Aggregates of Ghana. Project Rept. 9, Building and Road Research Institute, Kumasi, Ghana, 1970, 15 pp.
12. Bhatia, H. S., and Yeboa, S. L. A Study on the Engineering Characteristics of Laterite Gravels of Ghana—II. Project Rept. SM 10, Building and Road Research Institute, Kumasi, Ghana, 1970, 20 pp.

13. Brand, E. W., and Hongsnoi, M. Effect of Method of Preparation on Compaction and Strength Characteristics of Lateritic Soils. Proc. Specialty Session, Engineering Properties of Lateritic Soils, 7th International Conf. on Soil Mechanics and Foundation Engineering, Mexico City, Vol. 1, 1969, pp. 107-116.
14. Methods of Sampling and Testing Mineral Aggregates, Sands and Fillers. British Standard 812, 1960.
15. Buchanan, F. A Journey From Madras Through the Countries of Mysore, Canara and Malabar. East Indian Company, London, Vol. 2, 1807, pp. 436-460.
16. Bulman, J. W. A Survey of Road Cuttings in Western Malaysia. Proc. South East Asian Regional Conference on Soil Engineering, Bangkok, 1968, pp. 289-300.
17. Ghana Building and Road Research Institute. Unpublished records, Soil Mechanics Division, 1964-1971.
18. De Castro, L. Swelling Test for the Study of Lateritic Soils. Proc. Specialty Session, Engineering Properties of Lateritic Soils, 7th International Conf. on Soil Mechanics and Foundation Engineering, Mexico City, Vol. 1, 1969, pp. 97-106.
19. Clare, K. E. Airfield Construction on Overseas Soils: Part I, Formation, Classification and Characteristics of Tropical Soils. Institution of Civil Engineers, London, Vol. 8, 1957, pp. 211-231.
20. Clare, K. E. Road Making Gravels and Soils in Central Africa. Overseas Bull. 12, British Road Research Laboratory, 1960, 43 pp.
21. Clare, K. E., and O'Reilly, M. P. Road Construction Over Tropical Red Clays. Proc. Conf. on Civil Engineering Problems Overseas, Institution of Civil Engineers, London, 1960, pp. 243-256.
22. Clare, K. E., and Beaven, P. J. Soils and Other Road Making Materials in Nigeria. Technical Paper 57, British Road Research Laboratory, 1962, 48 pp.
23. Clare, K. E., and Beaven, P. J. Road Making Materials in Northern Borneo. Technical Paper 68, British Road Research Laboratory, 1965, 78 pp.
24. Christophe, L. Les Laterites et Leur Utilisation Comme Materiaux de Construction. Revue Générale des Routes et des Aérodromes, Paris, Vol. 38, No. 212, 1949, pp. 38-40.
25. Coleman, J. D., Farrar, D. M., and March, A. D. The Moisture Characteristics, Composition and Structural Analysis of a Red Clay Soil From Nyeri, Kenya. Geotechnique, Vol. 14, No. 3, 1964, pp. 262-76.
26. De Graft-Johnson, J. W. S., and Irwin, M. J. A Laboratory Investigation of the Stabilisation With Portland Cement of Two Gravels From Ghana. British Road Research Laboratory, Research Note RN/3356, 9 pp., unpublished.
27. De Graft-Johnson, J. W. S., and Bhatia, H. S. Engineering Characteristics of Lateritic Soils,—General Report. Proc. Specialty Session on Engineering Properties of Lateritic Soils, 7th International Conf. on Soil Mechanics and Foundation Engineering Mexico City, Vol. 2, 1969, pp. 13-42.
28. De Graft-Johnson, J. W. S., Bhatia, H. S., and Gidigasu, M. D. The Engineering Properties of Laterite Soils. Special Session, 7th International Conf. on Soil Mechanics and Foundation Engineering, Mexico City, Vol. 1, 1969, pp. 117-128.
29. D'Hoore, J. Soils Map of Africa: Scale 1 to 5,000,000, and Explanatory Monograph. Commission for Technical Co-Operation in Africa, South of the Sahara, Publication 93, 1964, 205 pp.
30. Dixon, H. H. A Review of Test Results on Halloysitic Soils and Their Performance in the Field. Proc. 3rd Regional Conference for Africa on Soil Mechanics and Foundation Engineering, Salisbury, Rhodesia, Vol. 2, 1963, pp. 183-185.
31. Dreyfus, J. Laterites. Revue Général des Routes et des Aérodromes. Paris, Vol. 22, No. 245, 1952, pp. 88-100, discussion pp. 100-101.
32. Dumbleton, M. J., and Newill, D. A. A Study of the Properties of 19 Tropical Clay Soils and the Relation of These Properties With the Mineralogical Constitution of the Soils. British Road Research Laboratory, Laboratory Note LN/44, 1962, 14 pp., unpublished.
33. Dumbleton, M. J. The Clay Mineralogy of Some Soils From Northern Borneo Considered in Relation to Their Origin and Their Properties as Road Making Materials. British Road Research Laboratory, Laboratory Note LN/282/MJD, 1963, 18 pp., unpublished.

34. Dumbleton, M. J. Clay Mineralogy of Borneo Soils in Relation to Their Origin and Their Properties as Road Making Materials. Proc. 2nd Asian Regional Conf. on Soil Mechanics and Foundation Engineering, Tokyo, Vol. 2, 1963, pp. 63-69.
35. Dumbleton, M. J., and West, G. Some Factors Affecting the Relation Between Clay Minerals in Soils and Their Plasticity. Clay Minerals, 1966, Vol. 6, No. 3, pp. 179-193.
36. Dumbleton, M. J., West, G., and Newill, D. The Mode of Formation, Mineralogy and Properties of Some Jamaican Soils. Engineering Geology, Amsterdam, Vol. 1, No. 3, 1966, pp. 235-249.
37. Easterbrook, P. L. The Preliminary Selection of Road Base Material in Western Nigeria by Linear Shrinkage Test. Technical Paper 9, Ministry of Works, Ibadan, 1962, unpublished.
38. Evans, E. A. Laboratory Examination of the Properties of Fifteen Tropical Soils. British Road Research Laboratory, Research Note RN/3020/EAE, 1957, 20 pp., unpublished.
39. Fermor, L. L. What Is Laterite? Geological Magazine, Vol. 5, No. 8, 1911, pp. 454-462, 507-516, 556-566.
40. Florentin, J., et al. Studies of Some Physico-Mechanical Properties of Eluvial Laterite Soil Samples. Proc. 4th International Conf. on Soil Mechanics and Foundation Engineering, London, Vol. 1, 1957, pp. 28-31.
41. Frederickson, A. F. The Genetic Significance of Mineralogy. In Problems of Clay and Laterite Genesis. American Institute of Mining and Metallurgical Engineers, 1952, pp. 1-11.
42. Frost, R. J. Importance of Correct Pretest Preparation of Some Tropical Soils. Proc. First Southeast Asian Regional Conference on Soil Engineering, Bangkok, 1967, pp. 43-53.
43. Fruhauf, B. A Study of Lateritic Soils. HRB Proc., Vol. 24, 1946, pp. 579-593.
44. Gidigasu, M. D. The Formation and General Characteristics of Laterite Soils (Literature Review). Project Rept. SM 2, Building and Road Research Institute, Kumasi, Ghana, 1968, 44 pp.
45. Gidigasu, M. D. Highway Geotechnical Properties of Ghana Soils. State Technical Univ., Warsaw, PhD thesis, 1969.
46. Gidigasu, M. D. The Engineering Characteristics of Laterite Soils (Literature Review). Project Rept. 7, Building and Road Research Institute, Kumasi, Ghana, 1970, 31 pp.
47. Gidigasu, M. D. Parameters for Classification of Laterite Fine-Grained Soils of Ghana. Highway Research Record 374, 1971, pp. 57-79.
48. Gidigasu, M. D. Importance of Soil Genesis in the Engineering Classification of Ghana Soils. Engineering Geology, Amsterdam, Vol. 5, 1971, pp. 117-161.
49. Gidigasu, M. D., and Bhatia, H. S. Importance of Soil Profiles in the Engineering Studies of Laterite Soils. Proc. 5th African Regional Conference on Soil Mechanics and Foundation Engineering, Luanda, Vol. 1, 1971, pp. 255-260.
50. Gidigasu, M. D. A Contribution to the Study of the Physicochemical Implications of Tropical Weathering and Laterisation. Jour. Southeast Asian Society of Soil Engineering, Vol. 2, 1971, pp. 131-149.
51. Gidigasu, M. D. Mode of Formation and Geotechnical Characteristics of Laterite Soils of Ghana in Relation to Soil Forming Factors. Engineering Geology, Amsterdam, Vol. 6, No. 2, 1972, pp. 79-150.
52. Gradwell, M., and Birell, K. S. Physical Properties of Certain Volcanic Clays. New Zealand Journal of Science and Technology, Vol. 36, 1954, pp. 108-122.
53. Grant, K., and Aitchison, G. D. The Engineering Significance of Siltcrete and Ferricrete in Australia. Engineering Geology, Amsterdam, Vol. 4, 1970, pp. 93-120.
54. Hamilton, R. Microscopic Studies of Laterite Formation in Ghana. In Soil Micromorphology (Jongerius, A., ed.), Elsevier, Amsterdam, 1964, pp. 269-278.
55. Hammond, A. A. A Study of the Engineering Properties of Some Lateritic Gravels From Kumasi District. Project Rept. SM 5, Building and Road Research Institute, Kumasi, Ghana, 1970, 17 pp.
56. Hirashima, K. B. Highway Experience With Thixotropic Volcanic Clay. HRB Proc., Vol. 28, 1948, pp. 481-494.

57. Hirashima, K. B. Highway Construction Problems Involving Plastic Volcanic Ash. HRB Bull. 44, 1951, pp. 1-10.
58. Irwin, M. J. I. A Laboratory Investigation of the Properties of Five Soils From Uganda. British Road Research Laboratory, Laboratory Note RN/3343/MJI, unpublished.
59. Jennings, J. E. Heaving Foundations on Dessicated Clay Soils. Proc. First Regional Conference on Housing Research in Africa South of the Sahara, Pretoria, South Africa, 1952.
60. Joachin, A. W. R., and Kandiah, S. The Composition of Some Local Soils and Concretions. Tropical Agriculturist, Ceylon, No. 96, 1941, pp. 67-95.
61. Knight, B. H. Laterite as a Road Making Material. Contractors Record and Public Works Engineer, Vol. 5, No. 1, 1953, pp. 31-32.
62. Lacroix, A. Les Laterites de la Guinée et les Produits d'Alteration qui Leur Sont Associés. Nouv., Arch., Mus., 5 serie, Vol. 3, 1914, pp. 1-128.
63. Lamb, D. W. Decomposed Granite as Fill Material With Particular Reference to Earthdam Construction. Symposium on Hong Kong Soils, Hong Kong Joint Group, 1962, pp. 73-87.
64. Liang, T. Tropical Soils: Characteristics and Airphoto Interpretation. Cornell Univ. Rept. AFCRL 64-937, 1964, 163 pp.
65. Liautaud, G. Investigation of Safe Side Slopes in Ghana. Ingeroute Engineering Consultancy, Paris, 1970, unpublished rept.
66. Little, A. L. The Use of Tropically Weathered Soils in the Construction of Earthdams. Proc. 3rd Asian Regional Conf. on Soil Mechanics and Foundation Engineering, Haifa, Israel, 1968, Vol. 1, pp. 35-41.
67. Little, A. L. The Engineering Classification of Residual Tropical Soils. Proc. Specialty Session, 7th International Conf. on Soil Mechanics and Foundation Engineering, Mexico City, Vol. 1, 1969, pp. 1-19.
68. Little, A. L. Laterite. Proc. 3rd Asian Regional Conference on Soil Mechanics and Foundation Engineering, Haifa, Israel, Vol. 2, 1968, pp. 61-71.
69. Lohnes, R. A., Fish, R. O., and Demirel, T. Geotechnical Properties of Selected Puerto Rican Soils in Relation to Climate and Parent Rock. Geological Society of America Bull., Vol. 82, pp. 2617-2624.
70. Loughnan, F. E. Chemical Weathering of the Silicate Minerals. American Elsevier, New York, 1969, 154 pp.
71. Lumb, P. The Properties of Decomposed Granite. Geotechnique, London, Vol. 12, No. 3, 1952, pp. 226-243.
72. Lumb, P. Effect of Rainstorms on Slope Stability. Proc. Symposium on Hong Kong Soils, Hong Kong Joint Group, 1962, pp. 74-87.
73. Lukens, J. E. Chemical Properties of Tropical Soils. Cornell University, 1964, unpublished rept.
74. Lundgren, R. Field Performance of Lateritic Soils. General Rept., Proc. Specialty Session on Engineering Properties of Lateritic Soils, 7th International Conf. on Soil Mechanics and Foundation Engineering, Mexico City, Vol. 2, 1969, pp. 45-57.
75. Maignien, R. Review of Research on Laterites. Natural Resources Research IV, UNESCO, Paris, 1966, 148 pp.
76. Martin, F. J., and Doyne, H. C. Laterite Soils in Sierra Leone. Jour. Agricultural Science, Vol. 17, 1927, pp. 530-546.
77. Van der Merwe, D. H. The Prediction of Heave From the Plasticity Index and the Percentage Clay Fraction. The Civil Engineer in South Africa, Pretoria, Vol. 6, No. 6, 1964, pp. 103-107.
78. Meyer, M. P. Comparison of Engineering Properties of Selected Temperate and Tropical Surface Soils. Geological Society of America Bull., Abstract for 1967, Special Paper 115, 148 pp.
79. Millard, R. S. Road Building in the Tropics. Jour. Applied Chemistry, London, Vol. 12, 1962, pp. 342-357.
80. Mohr, E. C. J., and Van Baren, F. A. Tropical Soils. Interscience Publishers, New York, 1954, 498 pp.

81. Moh, Z. C., and Mazhar, F. M. The Effects of Methods of Preparation on Index Properties of Lateritic Soils. Proc. Specialty Session on Engineering Properties of Lateritic Soils, 7th International Conf. on Soil Mechanics and Foundation Engineering, Mexico City, Vol. 1, 1969, pp. 23-35.
82. Nanda, R. L., and Krishnamachari, R. Study of Soft Aggregates From Different Parts of India With a View to Their Use in Road Construction, II—Laterites. Central Road Research Institute of India, 1958, 32 pp.
83. Nascimento, U., et al. Laterites of Portuguese Overseas Territories. National Civil Engineering Laboratory, Lisbon, Memo. 141, 1959. (In Portuguese.)
84. Nascimento, U., de Castro, E., and Rodrigues, M. Swelling and Petrification of Lateritic Soils. National Civil Engineering Laboratory, Lisbon, Technical Paper 215, 1964, 19 pp.
85. Nascimento, U., et al. Identification of Petrification in Soils. Proc. 6th International Conf. on Soil Mechanics and Foundation Engineering, Montreal, Vol. 1, 1965, pp. 80-81.
86. Portuguese Studies on Engineering Properties of Lateritic Soils. Proc. Specialty Session, Engineering Properties of Lateritic Soils, 7th International Conf. on Soil Mechanics and Foundation Engineering, Mexico City, Vol. 1, 1969, pp. 85-96.
87. Newill, D. An Investigation of Linear Shrinkage Test as Applied to Tropical Soils and Its Relation to Plasticity. British Road Research Laboratory, Laboratory Note RN/4106/DN, 1961, 6 pp., unpublished.
88. Newill, D. A Laboratory Investigation of Two Red Clays From Kenya. Geotechnique, London, Vol. 2, 1961, pp. 308-318.
89. Nixon, L. K., and Skipp, B. O. Airfield Construction on Overseas Soils: Part 5—Laterite. Proc. Institution of Civil Engineers, London, Vol. 8, 1957.
90. Novais-Ferreira, H., and Correia, J. A. The Hardness of Laterite Concretions and Its Influence on the Performance of Soil Mechanics Tests. Proc. 6th International Conf. on Soil Mechanics and Foundation Engineering, Montreal, Vol. 1, 1965, pp. 82-86.
91. Novais-Ferreira, H., and Miereles, J. M. F. The Influence of Temperature of Humidification on Geotechnical Properties of Lateritic Soils. Proc. Specialty Session on Engineering Properties of Laterite Soils, 7th International Conf. on Soil Mechanics and Foundation Engineering, Mexico City, Vol. 1, 1969, pp. 65-74.
92. Peck, R. B. Engineering Implications of Tropical Weathering and Laterisation. Lecture at Seminar on Laterite and Other Problem Soils of Africa. Univ. of Science and Technology, Ghana, Jan. 27, 1971, unpublished.
93. Pendelton, R. L. On the Use of the Term Laterite. American Soil Survey Bull. 17, 1966, pp. 102-108.
94. Persons, B. S. Laterite: Genesis, Location, Use. Plenum Press, New York, 1970, 103 pp.
95. Quinones, P. J. Compaction Characteristics of Tropically Weathered Soils. Univ. of Illinois at Urbana-Champaign, PhD thesis, 1963.
96. Remillon, A. Stabilization of Laterite Soils. HRB Bull. 108, 1955, pp. 96-101.
97. Rosevear, R. D. Soil Changes in Enugu Plantation. Farm and Forest, Vol. 5, 1942.
98. Ruddock, E. C. Residual Soils of the Kumasi District. Geotechnique, London, Vol. 17, 1967, pp. 359-377.
99. Ruddock, E. C. Properties and Positions in Laterite Ground: Some Statistical Relationships. Proc. Specialty Session, Engineering Properties of Lateritic Soils, 7th International Conf. on Soil Mechanics and Foundation Engineering, Mexico City, Vol. 1, 1969, pp. 11-21.
100. Russan, K., and Dumbleton, M. J. The Nature and Properties of the Sub-Grade Soil at Melbourne Airport. Proc. 2nd Conf., Australian Road Research Board, Melbourne, Vol. 2, 1964, pp. 869-879.
101. Salas, J. A. J. Note on a Halloysitic Red Clay From Fernando Po Island. Proc. 3rd Regional Conf. on Africa Soil Mechanics and Foundation Engineering, Salisbury, Rhodesia, 1963, Vol. 1, pp. 85-88.
102. Dos Santos, M. P. P., and de Castro, M. Soil Erosion in Roads. Proc. 6th International Conf. on Soil Mechanics and Foundation Engineering, Montreal, Vol. 1, 1965, pp. 116-120.

103. Schoefield, A. N. Lime Stabilisation of a Nodular Clayey Pea-Laterite in Nyasaland. British Road Research Laboratory, Overseas Bull. 3, 1957.
104. Schuster, J. A. Mechanical Durability of Lateritic Gravels From Southeast Asia: Suggested Tests and Test Standards for Highway Uses. Jour. Australian Road Research Board, Melbourne, Vol. 4, No. 405, 1970, pp. 32-44.
105. Seed, H. B., Woodward, R. J., and Lundgren, R. Prediction of Swelling Potential for Compacted Clays. Jour. Soil Mechanics and Foundations Division, ASCE, Vol. 88, No. SM 3, 1962.
106. Shergold, F. A. Physical Tests on Three Samples of Laterite Rock. British Road Research Laboratory, Laboratory Note RN/578/FAS, 1945, unpublished.
107. Shergold, F. A., and Hosking, J. R. The Ten Per Cent Test for Evaluating the Strength of Roadstone and Road Base Materials. British Road Research Laboratory, Laboratory Note RN/3192/FAS.JRH, 1958, unpublished.
108. Sherman, G. D., Kanchiro, Y., and Matsusaka, Y. The Role of Dehydration in the Development of Laterite. Pacific Science, Vol. 7, 1953, pp. 438-446.
109. Sherman, G. D. The Genesis and Morphology of the Alumina Rich Laterite Clays. In Problems of Clay and Laterite Genesis. American Institute of Mining and Metallurgical Engineers, 1952, p. 154.
110. Sherwood, P. T. Classification Tests on African Red Clays and Keuper Marl. Quarterly Journal of Engineering Geology, Geological Society, London, Vol. 1, No. 1, 1967, pp. 47-55.
111. Skempton, A. W. The Colloidal Activity of Clays. Proc. 3rd International Conf. on Soil Mechanics and Foundation Engineering, Zurich, Vol. 1, 1953, pp. 57-62.
112. The Coarse and Fine Durability Test. Division of Highways, California Department of Public Works, Sacramento, Proc. 229-C.
113. Tateishi, H. Basic Engineering Characteristics of High Moisture Tropical Soils. Proc. WASHO Conf., Honolulu, 1967.
114. Terzaghi, K. Design and Performance of Sasumua Dam. Proc. Institution of Civil Engineers, London, Vol. 9, 1958, pp. 369-395.
115. Townsend, F. C., Manke, G. P., and Parcher, J. V. Effect of Remolding on the Properties of a Lateritic Soil. Highway Research Record 284, 1969, pp. 76-84.
116. Townsend, F. C., Manke, G. P. and Parcher, J. V. The Influence of Sesquioxides on Lateritic Soil Properties. Highway Research Record 374, 1971, pp. 80-92.
117. Tubey, L. W. A Laboratory Investigation to Determine the Effect of Mica on the Properties of Soils and Stabilised Soils. British Road Research Laboratory, Note RN/4077/LWT, 1961, unpublished.
118. Laterite and Lateritic Soils and Other Problem Soils of Africa. U.S. Agency for International Development, 1971, 289 pp.
119. Uppal, H. L., and Singh, B. A Study of Soft Aggregates of Different Parts of India With a View to Their Use in Low Cost Road Construction—I, Rajasthan. Jour. Indian Roads Congress, Vol. 21, No. 3, 1957, pp. 433-457.
120. Vallerga, B. A., Shuster, J. A., Love, A. L., and Van Til, C. J. Engineering Study of Laterite and Lateritic Soils in Connection With Construction of Roads, Highways and Airfields. U.S. Agency for International Development, 1969, 165 pp.
121. Vergas, M. Some Engineering Properties of Residual Clay Soils Occurring in Southern Brazil. Proc. 3rd International Conf. on Soil Mechanics and Foundation Engineering, Zurich, Vol. 1, 1953, pp. 67-71.
122. Walther, J. Laterite in West Australia. Zeits. Dtsch. Geol. Ges., Vol. 67B, 1915, pp. 113-140.
123. West, G., and Dumbleton, M. J. The Mineralogy of Tropical Weathering Illustrated by Some West Malaysian Soils. Quarterly Jour. Engineering Geology, London, Dec. 1970.
124. Willis, E. A. Discussion of "A Study of Lateritic Soils" by Fruhauf, B., HRB Proc., Vol. 26, 1947, pp. 589-590.
125. Winterkorn, H. F., and Chandrasekharan, E. C. Laterite Soils and Their Stabilization. HRB Bull. 44, 1951, pp. 10-29.
126. Yeboa, S. L., and Hornsby Odoi, A. G. The Effect of Pretreatment on the Atterberg Limits of Lateritic Soils. Building and Road Research Institute, Kumasi, Ghana, Project Rept. SM 4, 1969, 34 pp.

SPONSORSHIP OF THIS RECORD

GROUP 2—DESIGN AND CONSTRUCTION OF TRANSPORTATION FACILITIES
W. B. Drake, Kentucky Department of Transportation, chairman

SOIL MECHANICS SECTION
John A. Deacon, University of Kentucky, chairman

Committee on Subsurface Drainage
George W. Ring III, Federal Highway Administration, chairman
Mike Bealey, Paul J. Brudy, Charles C. Calhoun, Jr., Harry R. Cedergren, Kenneth F. Ferrari, David S. Gedney, W. R. Lovering, Alfred W. Maner, Glen L. Martin, Lyndon H. Moore, William B. Nern, Carl I. Olsen, Travis W. Smith, W. T. Spencer, R. S. Standley

SOIL AND ROCK PROPERTIES AND GEOLOGY SECTION
L. F. Erickson, Idaho Department of Highways, chairman

Committee on Exploration and Classification of Earth Materials
Robert L. Schuster, University of Idaho, chairman
Robert C. Deen, Albin D. Hirsch, William P. Hofmann, Robert B. Johnson, Ralph W. Kiefer, Robert D. Krebs, Clyde N. Laughter, R. M. Mattox, Donald E. McCormack, Olin W. Mintzer, R. Woodward Moore, Arnold C. Orvedal, David L. Royster, A. Rutka, William W. Shisler, Preston C. Smith, Ernest G. Stoeckeler, Walter H. Zimpfer

Committee on Soil and Rock Properties
T. H. Wu, Ohio State University, chairman
William F. Brumund, Richard W. Christensen, George B. Clark, Charles L. Emery, James P. Gould, Ernest Jonas, Charles C. Ladd, G. A. Leonards, Victor Milligan, Gerald P. Raymond, Hassan A. Sultan, David J. Varnes, Harvey E. Wahls, John L. Walkinshaw

Committee on Physicochemical Phenomena in Soils
Joakim G. Laguros, University of Oklahoma, chairman
Kandiah Arulanandan, Gerald H. Brandt, Turgut Demirel, Sidney Diamond, Donald H. Gray, Mo Chih Li, James K. Mitchell, Charles A. Moore, Harold W. Olsen, Gilbert L. Roderick, Dwight Abram Sangrey, Hans F. Winterkorn

Committee on Frost Action
Arthur L. Straub, Clarkson College of Technology, chairman
Wilbur J. Dunphy, Jr., L. F. Erickson, E. R. Greek, Wilbur M. Haas, Frank B. Hennion, Glenn E. Johns, Alfreds R. Jumikis, Miles S. Kersten, Clyde N. Laughter, George W. McAlpin, Marvin D. Oosterbaan, R. G. Packard, Edward Penner, Harold R. Peyton, A. Rutka, Wayne G. Williams